STUDIES IN DRYING : THROUGH-CIRCULATION AND ROTARY SYSTEMS

A thesis presented by

Arthur Craig Gowan, B.Sc.

in fulfilment of the requirements of the degree of Doctor of Philosophy of the University of Glasgow.

Department of Pure and Applied Chemistry,
University of Strathclyde.

August, 1969.

ProQuest Number: 11011937

All rights reserved

INFORMATION TO ALL USERS
The quality of this reproduction is dependent upon the quality of the copy submitted.

In the unlikely event that the author did not send a complete manuscript
and there are missing pages, these will be noted. Also, if material had to be removed,
a note will indicate the deletion.

ProQuest 11011937

Published by ProQuest LLC (2018). Copyright of the Dissertation is held by the Author.

All rights reserved.
This work is protected against unauthorized copying under Title 17, United States Code
Microform Edition © ProQuest LLC.

ProQuest LLC.
789 East Eisenhower Parkway
P.O. Box 1346
Ann Arbor, MI 48106 – 1346

CONTENTS

PART III

ROTARY DRYING

ACKNOWLEDGMENTS

The author wishes to thank Professor P.D. Ritchie, B.Sc., Ph.D., F.R.I.C., F.P.I., M.I.Chem.E., F.R.S.E. for providing facilities for this research. The author is also indebted to Dr. T.J. Mitchell, Ph.D., A.R.C.S.T., F.R.I.C., A.M.I.Chem.E. who supervised the research, and to Dr. D. Smith, A.R.C.S.T., for his advice on the statistical aspects of the work.

Thanks are also due to the staff of the departmental workshop for their assistance in the construction and maintenance of the experimental plant.

To the Science Research Council goes the author's gratitude for the Research Studentship which made this investigation possible.

SUMMARY

For the accurate design of a system in which a transfer process such as drying is taking place, the effects of the dominant variables in the system must either be determined experimentally or predicted from reliable empirical or theoretical correlations. Reliable predictions may be made when the transfer process is occurring under steady state conditions, as in the constant rate period of drying. When the transfer rate varies and depends on the system being investigated as in the falling rate period of drying, the effect of the controlling factors should be determined experimentally.

In the present work, drying tests have been conducted using two systems which are distinguished by the type of design procedure necessary for each system.

The two series of drying tests were designed:

(1) to permit the prediction of heat and mass transfer rates during the constant rate period of drying of spheroidal Celite pellets arranged in a packed bed

(2) to apply the "factorial" method of experimentation to the drying of barley in a rotary dryer.

1. Packed Bed Tests.

Tests have been carried out to determine the effect of air flow, air temperature, depth of pellet bed and size of pellet on the constant drying rate of Celite pellets arranged in a packed bed. The ranges of the factors studied were:

Air flow	300 - 875 lb/h ft^2 dryer area
Air temperature	35 - 60°C
Bed depth	1 - 2 in
Size of pellet	0·312 - 0·500 in diameter

From the drying rates, heat and mass transfer coefficients and j factors have been computed to develop transfer relationships which have compared favourably with those of previous workers. The general correlations derived from the results were:

$$j_h = 0{\cdot}900 \; Re^{-0{\cdot}35}$$

$$j_d = 0{\cdot}678 \; Re^{-0{\cdot}34}$$

The average deviation of the experimental values from the above expressions was 6%.

A shape factor f, which may be used in conjunction with a general correlation derived by Gupta and Thodos[35], has been evaluated for the Celite pellets, by substituting the test data in the general correlation of Gupta and Thodos.

Table 1

Values of ξ

Particle Shape	
Speroidal Pellets	0·872
Spheres	1·000
Regular Cylinders	0·865
Cubes	0·825
Partition Rings	1·24
Raschig Rings	1·34
Berl Saddles	1·36

The values of ξ given in Table 1 show that the average value of the spheroidal pellets lies between the values given by Gupta and Thodos for cylindrical and spherical particles.

A comparison of the shape of the spheroidal pellets with regular and irregular cylindrical particles has indicated that the experimental shape factor for the pellets conforms with the pattern set by the shape factors for the cylindrical and spherical particles.

2. Rotary Dryer Tests.

In most dryer systems, including the rotary dryer, the effects of the dominant factors in the system must be determined experimentally before the dryer can be designed accurately. These tests are usually conducted by varying each factor in turn while the rest are kept constant at arbitrarily fixed levels. This "Classical" method of experimentation of studying each factor in turn assumes that each factor acts independently of the other factors. This is frequently untrue, and interactions may occur between the effects of the two or more variables.

Such interactions may be detected by using the "Factorial" method of experimentation in which each factor is studied over a range of values of the other factors. This method is applied in the present work, to the drying of barley in a rotary dryer. The factors studied were air flow, air temperature, dryer rotational speed and the feed rate of the barley. The approximate ranges over which the factors were studied were:

Air flow	600 - 800 lb/h ft^2 dryer area
Air temperature	100 - 110^oC
Dryer speed	8 - 13 rev/min
Feed rate	3·0 - 5·8 lb B.D.S./h

A two level factorial experiment, consisting of 32 drying tests covering all combinations of the various factor levels, was carried out. The drying behaviour of the material in the dryer was characterised by the variation in the moisture content of the material as it progressed along the dryer. The moisture content variation was found to have a linear profile, the slope being designated as the moisture content profile coefficient, b_r. A statistical analysis of the coefficients indicated that the effect of each factor was dependent on the value of the other three factors. This infers that the mechanism of drying in a rotary dryer is very complicated and emphasises the necessity for experimental drying tests to be performed over a wide range of operating conditions before an attempt is made to predict the drying behaviour of a material in a rotary dryer.

A study of the material hold-up values and retention times obtained in the tests indicated that they conformed to the mechanism proposed by Saeman and Mitchell[65] for the transport of material through a rotary dryer.

PROGRAMME OF WORK

When this work started, it had been intended to devote the whole time to the application of the factorial method of experimentation to the rotary drying system. However, the results of preliminary tests described in Part III of the thesis indicated that complex interactions existed between the effects of various factors and prevented a lucid interpretation of the results. Although these interactions may have been caused by the small scale of the dryer, there was not sufficient time available for the design and construction of a larger dryer.

Consequently, the research work was transferred to a through-circulation dryer which already existed in the department and a study was undertaken to evaluate the heat and mass transfer characteristics of spheroidal pellets arranged in a packed bed. This work is described in Part II of the thesis.

PART I

1. GENERAL INTRODUCTION

The unit operation of drying consists of the removal of a liquid (usually water) from a soild by thermal means. This general definition of drying distinguishes it from mechanical methods of dewatering solids such as filtration and centrifuging. Drying differs from evaporation in the type of equipment used and also in the amount of water removed, evaporation processes removing greater quantities. In addition, drying generally involves the removal of water at a temperature below its boiling point whereas evaporation usually means the removal of water by boiling a solution.

Drying of a material may be required in a process for one or more of the following reasons:

(1) to facilitate handling of the material in further stages of the process

(2) to increase the capacity of other equipment in the process

(3) to permit satisfactory use of the final product

(4) to preserve a product during storage

(5) to increase the value and usefulness of waste or by-products

(6) to reduce transport costs.

Many types of industrial dryers may be distinguished by the method of sypplying heat to dry the material and of removing water vapour from the surface of the material.

Dryers may be classified according to whether the heat is supplied directly or indirectly and may be operated as batch or continuous units.

The selection of a dryer for a given application depends mainly on the kind of material to be dried. Slurries are usually dried in drum, spray or flash dryers while granular materials are dried in rotary, through-circulation or tray dryers. The suitability of a dryer is influenced by the handling properties of the material and by the usefulness and saleability of the dried material. The operating conditions of a dryer are controlled by the temperature which the material can stand without decomposition and by the liability of the material to dusting during drying.

For the accurate design of a dryer, the effects of the controlling factors must be determined either from pilot plant tests or from reliable correlations. In most instances, the complexity of the drying action necessitates a programme of small-scale experiments from which the drying rate of the material in the full-scale dryer may be estimated precisely. This is particularly so, when the drying rate is dependent on the moisture content of the material and is governed by the movement of moisture within the material. However, reliable predictions may be made when the drying rate of the material is constant and controlled by the conditions in the drying medium.

This thesis describes two sets of drying experiments designed to produce information which may be used by each of the dryer design procedures outlined above.

In Part II, the drying of Celite pellets during the constant rate period in a through-circulation dryer is discussed in heat and mass transfer terms and the development of a shape factor, which compares the drying characteristics of the pellets with other particle shapes, is also described.

Part III of the thesis discusses the limitations of the normal classical method of experimentation and describes the application of the factorial method of experimentation to the drying of barley in a rotary dryer.

2. THEORY OF DRYING

When a material, saturated with water, is exposed to a stream of hot air, drying generally occurs for a time at a constant rate after which the drying rate falls off continuously until drying is complete.

2.1 Constant Drying Rate Period.

Drying takes place by diffusion of vapour from the saturated surface of the material through an air film into the hot airstream. The movement of moisture within the material is sufficiently rapid to maintain a saturated condition on the surface and the rate of drying is controlled by the rate of heat transfer to the evaporating surface. This heat transfer rate is balanced by the rate of mass transferred from saturated surface so that the temperature of the surface remains constant. As the saturated surface behaves essentially as a free water surface, the mechanism of moisture removal is equivalent to the evaporation from a water surface and is dependent only on the air conditions. However, different materials dry at slightly different rates because of the differences in the amount of surface area exposed to the air-stream.

Although the surface temperature remains constant during this period of drying, its level depends on the type of heat transfer occurring. If convection is the only mode of heat transfer, the surface temperature approaches the wet bulb temperature of the air-stream. However, if heat is also transferred by conduction and radiation, the surface temperature exceeds the wet bulb temperature and higher rates of transfer and drying are obtained.

The relationship between the drying and heat and mass transfer may be described as:

$$N = \frac{h\,A(t_a - t_s)}{L_h} \qquad .....(2.1)$$

$$= k\,A(p_s - p_a) \qquad .....(2.2)$$

where
- N = drying rate (lb/h)
- h = heat transfer coefficient (Chu/h ft^2 ^oC)
- A = drying surface available (ft^2)
- t_a = air temperature (^oC)
- t_s = surface temperature (^oC)
- L_h = latent heat of water at t_s (Chu/lb)
- k = mass transfer coefficient (lb/h ft^2 unit partial pressure difference)
- p_s = vapour pressure of water on material surface (atm)
- p_a = partial pressure of water vapour in air stream (atm)

2.2 Falling Rate Period of Drying.

As the drying of a material progresses, a critical moisture content is reached when the rate of moisture movement within the material does not maintain saturated conditions on the surface and the drying rate consequently decreases. During this stage of drying, the area of the saturated surface diminishes and the drying rate is sometimes a linear function of the moisture content of the material. Eventually, however, the surface of the material is completely unsaturated and evaporation takes place within the material, the vapour reaching the surface by diffusion through the material.

Consequently, during the falling rate period, the drying rate is governed by the rate of internal moisture movement and depends not only on the air conditions but also on the mechanism by which the internal moisture is transferred to the surface.

Several controlling mechanisms have been postulated to explain the movement of internal moisture; the more significant ones are outlined below.

2.2.1 Diffusion Theory.

Diffusion of moisture may be produced by a concentration gradient between the depths and surface of the material. Under these conditions, the rate of moisture movement may be described by the following expression, which is analogous to the Fourier heat conduction equation:

$$\frac{W - W_e}{W_c - W_e} = \frac{8}{\pi^2}\left[e^{-D_l \theta (\pi/2d)^2} + \frac{1}{9} e^{-9D_l \theta (\pi/2d)^2} + \frac{1}{25} e^{-25D_l \theta (\pi/2d)^2} \right] \quad ..(2.3$$

where W = moisture content of materials (lb/lb B.D.S.)

W_c = critical moisture content (lb/lb B.D.S.)

W_e = equilibrium moisture content (lb/lb B.D.S.)

D_ℓ = diffusivity of liquid (ft^2/h)

θ = time from start of falling rate period (h)

d = one-half the thickness of layer through which diffusion occurs (ft)

This method of moisture transport is probably limited to solid systems such as soap, gelatin and glue and to the removal of bound water in the drying of materials such as paper, textiles and wood.

2.2.2 Capillary Theory.

In porous or granular solids, moisture may move from a region of high to low concentration by means of capillary forces acting on the water in the network of interconnecting pores and channels in the interior of the solid.

As drying proceeds, the water surface recedes into the pores and channels forming menisci which establish the capillary forces by the interfacial tension between the water and solid.

This type of moisture movement occurs in coarse granular materials such as clays, paint pigments and sand.

PART II

DRYING IN A PACKED BED

3. INTRODUCTION

In the chemical industry, numerous processes such as catalyst regeneration, adsorption, drying, solution and many exchange processes involve heat and mass transfer between solid particles arranged in fixed beds and fluid streams. The importance of the evaluation of heat and mass transfer rates in fixed beds to their design and successful operation is generally recognised and widely discussed.

Development in this field of chemical engineering has been based primarily on the empirical treatment of pertinent factors during steady state conditions in which resistance to heat and mass transfer resides in one phase only. This phenomenon offers a means of describing the characteristics of a system in terms of transfer coefficients, j factors and heights of transfer unit (H.T.U.)

One of the important factors in the packed bed is the shape of individual particles in the bed. Most of the previous experimenters investigated systems of either spherical or cylindrical particles which are comparatively regular in shape. However, the use of other shaped particles is increasing and knowledge of the effect of particle shape on heat and mass transfer rates in a packed bed is becoming more necessary.

In this work, the through-circulation drying of spheroidal particles, described in detail in Section 5.2, is studied with a view to incorporating a shape factor for this type of particles in general equations derived by previous workers.

3.1 Heat and Mass Transfer Theory.

Although the current theories of heat and mass transfer have been developed from both empirical and theoretical considerations, they are all based on the fact that the rate of heat and mass transfer between a moving fluid and boundary surface depends both on the molecular transport of the fluid and on the dynamic characteristics of the flow.

The development of heat and mass transfer relationships from basic principals is described in standard text books[1,2,3] and is only briefly summarised here. Firstly, however, the general theories postulated for mass transfer, are outlined.

3.1.1 The Two Film Theory.

The basis of most theoretical equations is the "two film" theory due to Whitman[4], who postulated that a laminar film existed on each side of a phase boundary and that, assuming equilibrium at the interface, the only resistance to mass transfer resided in these films. It was assumed that Fick's first law applied, i.e. the rate of mass transfer is proportional to the concentration difference and the molecular diffusivity, and inversely proportional to the film thickness.

From this, the rate at which one component A of a gaseous mixture A and B is transferred across a phase boundary may be written as:

$$N_A = \frac{D_{AB}}{Z_f} (y - y_i) \qquad .....(3.1)$$

where N_A = mass transfer rate of diffusing component A (lb mol/h ft^2)

D_{AB} = diffusivity of A through B (ft/h)

Z = thickness of laminar film (ft)

y = concentration of diffusing component in bulk gas phase (lb mol/ft^3)

and y_i = concentration of diffusing component in gas film at phase boundary (lb mol/ft^3)

This may also be expressed as:

$$N_A = k_c (y - y_i) \qquad .....(3.2)$$

where k_c = the gas film transfer coefficient (ft/h)

If the concentration of the diffusing gas is defined in terms of its partial pressure, equation (3.2) becomes:

$$N_A = k_p (p_a - p_i) \qquad .....(3.3)$$

where p_a = partial pressure of diffusing component in bulk of gas phase (atm)

p_i = partial pressure of diffusing component at interface (atm)

and k_p = mass transfer coefficient (lb mol/h ft^2 atm)

An analogous expression may be derived to describe the flow of heat from a fluid to a boundary surface. This may be written as:

$$q = h_g \ (t_a - t_s) \qquad .....(3.4)$$

where q = rate of heat transfer (Chu/h ft^2)

h_g = heat transfer coefficient (Chu/h ft^2 ^oC)

t_a = temperature of the bulk fluid (^oC)

t_s = temperature of the boundary surface (^oC)

3.1.2 The Penetration Theory.

The two film theory of Whitman predicts that the rate of mass transfer should be directly proportional to the diffusivity. Several workers[5,6,7] found that gas film transfer coefficients, measured in wetted wall columns, varied with the diffusivity raised to a power ranging from 0·4 to 0·5. Studies of liquid controlled mass transfer also showed that the liquid phase mass transfer coefficient k was not directly proportional to the diffusivity, D_v[8]. Calderbank and Moo-Young[9] proposed $k_1 \propto D_V^{0\cdot5}$.

The penetration theory, first postulated by Higbie[10] to describe mass transfer in gas absorption, predicts that the mass transfer coefficient is proportional to the square root of the diffusivity. This model proposes that the laminar liquid film is systematically renewed and that each element of liquid surface is exposed to the gas for the same limited period of time. According to the theory, the relation between the mass transfer coefficient and diffusivity is:

$$k_1 \propto \sqrt{\frac{D_V}{\theta}}$$

where θ = the period of exposure.

The conventional picture of a laminar boundary layer was refuted by Danckwerts[11] who suggested that turbulence extends to the liquid surface and that the period of gas liquid contact during which molecular transfer takes place, is dependent on the rate of renewal of the surface. The relation between the mass transfer coefficient and diffusivity becomes:

$$k_1 \propto \sqrt{D_V S}$$

where S = the rate of surface renewal.

Kishinevskii[12] proposed that during the period of contact, the absorbed gas molecules move into the volume of the liquid mainly by turbulent or convective diffusion while molecular diffusion plays a secondary part.

The importance of ascertaining the hydrodynamic conditions for the computation of mass transfer coefficients was emphasised by Kishinevskii and Mochalova[13] who pointed out that while molecular diffusion is predominant under the gentler conditions of bubbling, eddy diffusion becomes of increasing importance in other regimes.

Although experimental data conforms more with the penetration theory than the two-film theory, Danckwerts[14] has shown that neither is completely valid for a packed column but Hanratty[15] found that at high values of the Schmidt number, results fitted the penetration theory.

This latter fact is in accordance with a model, postulated by Toor and Marchello[16], which conformed with the penetration theory for short periods of contact and with the film theory for long contact periods.

In a novel interpretation of mass transfer in packed beds, Carberry[17] postulated that the mass transfer coefficient is proportional to the Schmidt number raised to the power 0·67. This agrees with the experimental data from a wide range of various packed bed systems and moreover it leads to the same general framework of dimensionless groups as the conventional mass transfer theory. These groups are now discussed.

3.2 Heat and Mass Transfer Factors.

The procedure of describing a transfer process in terms of a transfer coefficient has the disadvantage of requiring a number of units for the definition of the coefficient. However, the incorporation of the coefficients in dimensionless factors facilitates the application of data from one system to another.

The prediction of heat and mass transfer characteristics from the dynamic properties of a system has led to the derivation of dimensionless j factors which have been universally employed to describe and correlate the transfer properties of the system.

In order to compute heat transfer data from the established friction factor correlation for pressure drop in flow through pipes, Chilton and Colburn[18,19] introduced the j_h factor defined as:

$$j_h = \frac{h}{C_p u \rho} Pr^{0.67} \qquad \ldots.(3.5)$$

where h = heat transfer coefficient (Chu/h ft^2 °C)

C_p = specific heat of fluid (Chu/lb)

ρ = density of fluid (lb/ft^3)

u = velocity of fluid (ft/h)

Pr = Prandtl number (dimensionless)

By applying a similar analogy to mass transfer, Chilton and Colburn[19] proposed the mass transfer factor j_d, which they expressed in the form:

$$j_d = \frac{k\ P_{Bm}}{uP} Sc^{0.67}$$

where k = mass transfer coefficient (lb/h ft^2 atm)

P_{Bm} = logarithmic ratio of the partial pressure of the inert component (atm)

P = total pressure (atm)

Sc = Schmidt number (dimensionless)

Experimental studies in various systems have been performed to substantiate the direct analogy between heat and mass transfer. In 1943, the analogy was applied to a packed bed by Gamson <u>et al.</u>[20], who studied the steady state evaporation of water from the surface of particles in a bed into a stream of air passing through the bed. They concluded that a direct correspondence exists between heat and mass transfer in a packed bed and obtained a value of 1·076 for the ratio j_h/j_d.

Much information has since been reported on the flow of fluids through beds of particles with values of the ratio ranging from 0·86 to 1·51 [21,22]. However, Gupta and Thodos[23] proposed that for a direct analogy between heat and mass transfer, the following conditions should be fulfilled:

(1) the physical properties of the system should remain constant

(2) the rate of mass transfer should be very small, since for high rates of mass transfer, the velocity profile across the gas film becomes distorted and the mass transfer coefficient is dependent on the rate of mass transfer.

(3) there should be no chemical reaction

(4) there should be no viscous dissipation

(5) radiant energy should be neither emitted nor absorbed

(6) there should be no pressure, thermal or forced diffusion.

3.2.1 Application of j Factors to a Packed Bed.

The j_h factor was used by Chilton and Colburn to describe the heat transferred by convection to a fluid flowing through a pipe by an expression of the form:

$$j_h = a\,Re^b \qquad \text{....(3.7)}$$

where Re = Reynolds number (dimensionless)

$= \dfrac{d_p G}{\mu}$

d_p = characteristic dimension of system (ft)

G = mass velocity of fluid (lb/h ft^2)

μ = viscosity of fluid (lb/h ft)

and a and b are empirical constants.

A similar relationship may be applied to packed bed systems in which heat and mass are being transferred provided that steady state conditions exist in the bed and that the only resistance to mass transfer resides in the fluid phase. These stipulations are met in systems such as the drying of particles during the constant rate of drying and the solution and sublimation of particles into a fluid.

This method of describing heat and mass transfer was introduced to packed bed systems by Gamson et al.[20] who studied the evaporation of water from the surfaces of spherical and cylindrical particles into an air stream. Since then, correlations with j factors have been derived for a wide range of packed bed systems and have been used in the present work to describe heat and mass transfer in the drying of Celite pellets in a through-circulation dryer.

3.3 Effect of Process Variable on j Factors.

The variables influencing heat and mass transfer in a packed bed may be classified as follows:

(a) operating variables e.g. gas or liquid rate, temperature, pressure

(b) properties of the bed e.g. shape and size of particles, depth and porosity of bed

(c) fluid properties e.g. viscosity, density, diffusivity.

The effects of the most important variables are outlined below.

Fluid Rate.

Although an increase in fluid velocity produces higher transfer rates, the values of the j factors are reduced. It has been found, however, that the extent by which the factors are affected is decreased when the fluid rate is increased, [23,24,25,26,27] and also when particles other than spheres or cylinders are used in the bed[25].

Temperature and Pressure.

The effects of temperature and pressure on the j factors are relayed through their effects on the properties of the fluid.

Particle Shape.

The shape of the particles appears to be ineffective provided that the particles are approximately spherical or symmetrical. However, in systems of irregularly shaped particles, the values of the j factors are reduced by the inaccessibility of parts of the particle surface to the fluid stream[25]. Values are also reduced if the surface of the particles is very smooth[28].

Particle Size.

Although the effect of the size of the particles is generally accounted for by the characteristic dimension of the Reynolds number in equation (3.7), additional effects, reducing the value of the j factors, have been experienced for systems of particles with diameter less than 0·125 in[29,30,31].

Bed Depth.

If the proper driving force is used in the computation of the heat and mass transfer coefficients, the depth of the bed has no effect on the transfer factors [32,33,34].

Voidage of Bed.

The j factors are reduced by increasing the voidage of the bed and have been shown to be inversely proportional to the voidage[35].

Fluid Properties.

The effects of the physical properties of the fluid i.e. density, diffusivity, heat capacity, thermal conductivity and viscosity are relayed through the dimensionless Prandtl and Schmidt numbers used in the calculations of the j factors. It is generally accepted that the Schmidt number raised to the power 0·67 should be used when calculating j_d although the power 0·58 has also been recommended[26].

4. PREDICTION OF TRANSFER FACTORS.

The application of equation (3.7) to a packed bed system requires a definition of the characteristic dimension and the fluid velocity for that system. Studies of packed beds containing irregularly shaped particles have utilised several varied forms of the characteristic dimension d_p. For beds of spherical particles, d_p is simply the diameter of one particle, while for other shapes of particle, d_p is usually defined as the diameter of a sphere having the same surface area as the particle.

i.e. $$d_p = \sqrt{\frac{A_p}{\pi}} \qquad .....(4.1)$$

$$= 0.567\sqrt{A_p} \qquad .....(4.2)$$

where A_p = surface area of particle (ft)

This concept is difficult to visualise for irregular commercial packings such as Raschig rings and Berl saddles. To overcome this, Taecker and Hougen[25] suggested that $\sqrt{A_p}$ alone be used as the characteristic dimension and this was subsequently used by Gupta and Thodos[35] in their development of a general relationship applicable to all shapes of particles.

The hydraulic diameter, defined as $D_p\varepsilon/(1 - \varepsilon)$ where D_p is the particle diameter and ε is the voidage of the bed, has also been employed as the characteristic dimension[26,27]. In these studies, the superficial fluid velocity was replaced by the interstitial velocity, u/ε, thus defining Re as $\frac{D_p G}{\mu(1-\varepsilon)}$.

However, Gupta and Thodos[35] pointed out that this form of Re is only of limited application since it cannot be used to describe the behaviour of single particles for which $\varepsilon = 1$.

In the present work, the Reynolds number is defined as $\frac{\sqrt{A_p}\,G}{\mu}$, which was introduced by Taecker and Hougen and used by Gupta and Thodos in their general correlation.

4.1 Prediction of j Factors for Gas - Solid Systems.

One of the earliest studies of gas-solid systems was carried out by Gamson *et al.*[20] (1943) who studied the evaporation of water from the surface of spherical and cylindrical Celite particles in a packed bed into an airstream flowing through the bed. In their tests, which were conducted in beds 12 in square and 1 to 2·5 in in depth, air inlet temperature ranged from 80 to 160^{o}F and the air mass velocity from 400 to 2,300 lb/h ft^2. Their results were presented by the correlations:

for $\left[\frac{D_p G}{\mu}\right] > 350$,

$$j_h = 1{\cdot}064\left[\frac{D_p G}{\mu}\right]^{-0{\cdot}41} \quad \ldots\ldots(4.3)$$

$$j_d = 0{\cdot}989\left[\frac{D_p G}{\mu}\right]^{-0{\cdot}41} \quad \ldots\ldots(4.4)$$

and for $\left[\frac{D_p G}{\mu}\right] < 40$,

$$j_h = 18{\cdot}1\left[\frac{D_p G}{\mu}\right]^{-1} \quad \ldots\ldots(4.5)$$

$$j_d = 16{\cdot}8\left[\frac{D_p G}{\mu}\right]^{-1} \quad \ldots\ldots(4.6)$$

Additional data for low Reynolds numbers were obtained by Wilke and Hougen[39] who derived the following expression for $\left[\frac{D_p G}{\mu}\right] < 350$:

$$j_d = 1{\cdot}82 \left[\frac{D_p G}{\mu}\right]^{-0{\cdot}51} \qquad \ldots\ldots(4.7)$$

In a more recent study of the evaporation of water from beds of similarly shaped particles ranging from 1 in to 5 in in depth, Bradshaw and Myers[33] found that the transfer coefficients and factors were independent of the depth of the bed provided that axial mixing is accounted for in the computation of the transfer driving force; otherwise, the coefficients were found to decrease as the bed depth increased. They considered the logarithmic driving force to be satisfactory for determining coefficients when the ratio of inlet driving force to outlet driving force is less than 6. Their results were described by the equation:

$$j_d = 2{\cdot}25 \left[\frac{D_p G}{\mu(1-\epsilon)}\right]^{-0{\cdot}50} \qquad \ldots\ldots(4.8)$$

Similar observations were made by Bradshaw and Bennet[32] on the sublimation of naphthalene pellets arranged in a packed bed into an airstream. The following expressions were derived from the results of tests conducted with beds of 5 in to 10 in deep:

$$j_d = 0{\cdot}506 \left[\frac{D_p G}{\mu}\right]^{-0{\cdot}293} \qquad \ldots\ldots(4.9)$$

$$j_d = 0{\cdot}606 \left[\frac{D_p G}{\mu}\right]^{-0{\cdot}309} \qquad \ldots\ldots(4.10)$$

In equation (4.10), the values of j_d were derived from coefficients which were corrected for axial diffusion. Axial mixing may be reduced by inserting inert particles in the inlet section of the bed, thereby minimising the bed entrance effects[23].

The influence which the accessibility of the particle surface for heat and mass transfer exerts on the exchange process has been investigated in beds of irregularly shaped particles. In a study of the evaporation of water from beds of Raschig rings, partition rings and Berl saddles, Taecker and Hougen[25] found that the inaccessibility of the inner surface of the rings caused the values of j_h for the rings to be about 19% lower than the values previously established by Gamson[20] for spherical and cylindrical particles. The results for the rings were expressed as:

$$j_h = 1{\cdot}148 \left[\frac{\sqrt{A_p}\,G}{\mu}\right]^{-0{\cdot}41} \qquad \text{.....(4.11)}$$

The corresponding equation for the Berl saddles was:

$$j_h = 0{\cdot}920 \left[\frac{\sqrt{A_p}\,G}{\mu}\right]^{-0{\cdot}34} \qquad \text{.....(4.12)}$$

The ratio $j_h/j_d = 1{\cdot}076$, calculated from the data of Gamson[20], was used by Taecker to compute the corresponding correlations for j_d.

Similar studies were carried out by Shulman and De Gouff[40] who were, however, primarily interested in the effect of diffusivity and interfacial area on mass transfer in packed columns.

In a comprehensive study of gas phase mass transfer in packed columns using napthalene packings, Shulman et al.[41,42,43,44] found that mass transfer rates could be predicted from a general correlation provided that the surface temperature of packings is used to evaluate the proper driving force.

Although it is generally assumed that, for the evaporation of water from particles, the surface ttmperature of the particles is equal to the wet-bulb temperature of the air, Bradshaw and Myers[23] found that the temperatures are only identical if the air velocity exceeds 4 ft/s. Similar observations were made by De Acetis and Thodos[22] who studied the evaporation of water from the surface of Celite spheres randomly interspersed with solid spheres to produce an extended bed arrangement. They found that the introduction of inactive spheres did not affect the transfer characteristics of the bed but that the particle surface temperature only equals the wet-bulb temperature of the air at high air velocities. This probably accounts for their j_h/j_d value of 1·51 which is abnormally high. Their results were described by the equations:

$$j_h = \frac{1 \cdot 10}{\left[\frac{D_p G}{\mu}\right]^{0 \cdot 41} - 0 \cdot 15} \qquad .....(4.13)$$

$$j_d = \frac{0{\cdot}725}{\left[\frac{D_pG}{\mu}\right]^{0{\cdot}41} - 0{\cdot}15} \qquad \ldots\ldots(4.14)$$

In an extension of this study, McConnachie and Thodos[38] determined j factors for distended beds of spherical particles which were separated and held in place by short lengths of fine rigid wire. Similar expressions, given below for packed and distended beds were obtained when the transfer factors were correlated with the modified Reynolds number $\frac{D_pG}{\mu(1-\varepsilon)}$:

$$j_h = \frac{1{\cdot}192}{\left[\frac{D_pG}{\mu(1-\varepsilon)}\right]^{0{\cdot}41} - 1{\cdot}52} \qquad \ldots\ldots(4.15)$$

$$j_d = \frac{1{\cdot}192}{\left[\frac{D_pG}{\mu(1-\varepsilon)}\right]^{0{\cdot}41} - 1{\cdot}52} \qquad \ldots\ldots(4.16)$$

This agreed with the work of Chu, Kalil and Wetteroth[36] who studied the sublimation of naphthalene from the surface of cylindrical and spherical particles in fixed and fluidised beds. Their results were correlated by:

$$j_d = 1{\cdot}77 \left[\frac{D_pG}{\mu(1-\varepsilon)}\right]^{-0{\cdot}44} \qquad \ldots\ldots(4.17)$$

Using the results of McConnachie[38], Gupta and Thodos[23] re-examined the effect of bed voidage on the transfer factors and found that if the j factors are correlated with the conventional Reynolds number $\frac{D_pG}{\mu}$, they decrease as the void fraction increases and that the product εj is constant. Data from heat and mass transfer studies in fixed and fluidised beds of spherical beds reported in the literature, were re-correlated in terms of this product to give the expressions:

$$\epsilon j_h = 0{\cdot}018 + \frac{0{\cdot}929}{\left[\frac{D_p G}{\mu}\right]^{0{\cdot}58} - 0{\cdot}483} \qquad .....(4.18)$$

$$\epsilon j_d = 0{\cdot}01 + \frac{0{\cdot}863}{\left[\frac{D_p G}{\mu}\right]^{0{\cdot}58} - 0{\cdot}483} \qquad .....(4.19)$$

4.2 Prediction of j_d Factors for Liquid-Solid Systems.

Relationships, similar in form to those describing gas-solid transfer systems, have been used satisfactorily to correlate mass transfer data from liquid-solid packed bed systems in which the sole resistance to mass transfer resided in the liquid phase. This similarity is somewhat striking in view of the very high Schmidt numbers occurring in liquid systems and furthermore, it stresses the applicability of the j factors to describe the transfer properties of packed beds.

One of the first reported studies using liquid systems was conducted by Hobson and Thodos[46] who measured the rate of transfer of methyl ethyl ketone and isobutyl alcohol from the surface of spherical particles arranged in a packed bed into a stream of water. Steady state coefficients were computed by extrapolating the concentration of alcohol in the exit stream back to zero time and assuming that the surface was completely wetted. Their results were represented by the equation:

$$j_d = 0{\cdot}537 \left[\frac{D_p L}{\mu}\right]^{-0{\cdot}57} \quad .....(4.20)$$

The following generalised equation, correlating also the data of Gamson et al.[20] and Wilke and Hougen[39] was recommended by Hobson and Thodos.

$$\log j_d = 0{\cdot}7683 - 0{\cdot}9175 \log\left[\frac{D_p L}{\mu}\right] + 0{\cdot}0817 \log\left[\frac{D_p L}{\mu}\right]^2 \quad .....(4.21)$$

Further work in liquid-solid systems was carried out by McCune and Wilhelm[24] who measured the rate of solution of 2-naphthol flakes and spheres into a stream of water. They concluded that the mass transfer characteristics of fixed beds and single particles at rest are similar, provided that due consideration is given for the average velocity around individual particles. Their results were represented by the equation:

$$\text{for } \left[\frac{D_p L}{\mu}\right] < 120, \qquad j_d = 1{\cdot}625 \left[\frac{D_p L}{\mu}\right]^{-0{\cdot}507} \quad ...(4.22)$$

$$\text{and for } \left[\frac{D_p L}{\mu}\right] > 120, \qquad j_d = 0{\cdot}687 \left[\frac{D_p L}{\mu}\right]^{-0{\cdot}327} \quad .....(4.23)$$

Similar studies were conducted by Gaffney and Drew[26] who investigated the solution of salicylic acid pellets into a stream of benzene and succinic acid pellets into streams of acetone and n-butyl alcohol. Although their results were originally expressed in terms of heights of a transfer unit, the same were later re-arranged by Ergun[37] in the form of the conventional j factors to give the equations:

for $\left[\frac{D_pL}{\mu\varepsilon}\right] < 200$, $\quad j_d' = 1{\cdot}97 \left[\frac{D_pL}{\mu\varepsilon}\right]^{-0613}$ .....(4.14)

and for $\left[\frac{D_pL}{\mu\varepsilon}\right] > 200$, $\quad j_d' = 0{\cdot}290 \left[\frac{D_pL}{\mu\varepsilon}\right]^{-0{\cdot}254}$ .....(4.25)

(in j_d', the Schmidt number is raised to the power 0·58)

Results have also been reported for the solution of benzoic acid pellets into water[47] and into water and propylene glycol solution[34]. The data, collected by Evans and Gerald[47], were obtained for values of $\left[\frac{D_pL}{\mu}\right]$ less than 80 and were correlated by the equation:

$$j_d = 1{\cdot}48 \left[\frac{D_pL}{\mu}\right]^{-0{\cdot}52} \quad .....(4.26)$$

In the investigations of Wilson and Geankoplis [34], a wider range of Reynolds numbers was studied and the following equations were derived:

for $\left[\frac{D_pL}{\mu}\right] < 55$, $\quad j_d = 1{\cdot}09 \left[\frac{D_pL}{\mu}\right]^{-0{\cdot}52}$ .....(4.27)

and for $55 < \left[\frac{D_pL}{\mu}\right] < 1{,}500$, $\quad j_d = 0{\cdot}250 \left[\frac{D_pL}{\mu}\right]^{-0{\cdot}31}$ .....(4.28)

4.3 Prediction of j_h Factors for Electrically Heated Packed Beds.

j_h Factors have also been used to describe the steady state transfer of heat from metallic particles arranged in a packed bed into an air stream, the heat being generated either by passing an electric current through the particles[49] or by surrounding the particles with a high frequency induction coil[50].

From a comprehensive study of heat transfer from beds of spheres, cubes and cylinders, Glaser and Thodos[49] concluded that the value of the j_h factor, evaluated from the average of the local heat transfer coefficients was influenced by the shape and size of the particles. Their results were presented in terms of a j_{ho} factor which was calculated by extrapolating a plot of j_h against the ratio $\sqrt{A_p}/D_c$ (D_c being the bed diameter) to a value of $\sqrt{A_p}/D_c$ equal to zero. The values of j_{ho} were correlated by the equation:

$$j_{ho} = \frac{0.535}{\left[\frac{\sqrt{A_p}G}{\mu(1-\varepsilon)\varphi}\right]^{0.35} - 1.6} \quad .....(4.29)$$

where φ = fraction of surface taking part in transfer process.

Baumeister and Bennet[50] found that the average test transfer coefficient was dependent on the ratio of tube to particle diameter, for a given Reynolds number. The effect was quite significant for ratios less than 18 but diminished as the ratio increased. Their results were described by the equation.

$$j_h = 1.09\left[\frac{D_pG}{\mu}\right]^{-0.32} \quad .....(4.30)$$

4.4 Prediction of j Factors for Single Particles.

Several studies [21,51,52,53] have shown that the heat and mass transfer properties of a single particle in a fluid stream are similar to those of a packed bed under the same conditions and that expressions, relating the j factors to the Reynolds number may be used also to describe them.

4.5 General Correlation of Heat and Mass Transfer Results in a Packed Bed.

The increasing use of irregularly shaped particles in industrial packed bed systems, has created a need for a general heat and mass transfer relationship, from which the behaviour of any particle system may be reliably predicted.

In several investigations[20,36,39,40], the selection of a proper equivalent diameter or characteristic dimension in the Reynolds number has enabled the results from systems consisting of regular geometrical configurations to be correlated satisfactorily. However, difficulty is encountered in establishing an equivalent diameter for commercial packings in which a portion of the surface area is inaccessible and not used in the transfer process.

To circumvent this problem, Gupta and Thodos[35] introduced an area availability factor, f, which they defined as the ratio of the surface of particle available to transfer to the surface area of sphere having the same volume as the particle. As a result, f is not necessarily a constant for a particular packing since it also depends on the state of aggregation of the bed.

Gupta and Thodos evaluated values of f from results published in the literature by dividing the relationship for each particle shape by f such that the new correlation coincided with that for spherical particles. Good agreement was obtained between the values of f and those calculated from a consideration of the geometrical orientations in the bed.

The general expressions derived by Gupta and Thodos contain the Reynolds number introduced by Taecker and Hougen[25] and are given below:

$$\frac{\varepsilon j_d}{f} = \frac{0{\cdot}300}{\left[\frac{\sqrt{A_p}\,G}{\mu}\right]^{0{\cdot}35} - 1{\cdot}90} \qquad \ldots\ldots(4.31)$$

$$\frac{\varepsilon j_h}{f} = \frac{0{\cdot}322}{\left[\frac{\sqrt{A_p}\,G}{\mu}\right]^{0{\cdot}35} - 1{\cdot}90} \qquad \ldots\ldots(4.32)$$

4.6 Shape Factors.

Although Gupta and Thodos based their shape factor on the area available for transfer in their attempt to correlate heat and mass transfer data for packed beds of spheres, cylinders, Raschig rings and Berl saddles, a considerable amount of work has previously been carried out on the use of shape factors to correlate fluid flow through packed beds.

In any system, however, the numerical value of the shape factor depends on the characteristic dimension or equivalent diameter chosen to represent the particles in the bed. One of the earliest characteristic dimensions used was called the "nominal diameter" and was defined as the diameter of the sphere having the same volume as the particle. Similar to this were the "degrees of sphericity and circularity" adopted by Wadell[89] who found that a measure of sphericity or circularity could be obtained by dividing the nominal diameter by the diameter of the smallest sphere circumscribing the particle.

The sphericity factor, defined as the ratio of surface area of the equivalent volume sphere A_s, to the surface area of the particle itself A_p, was introduced as a shape factor by Leva[90] in his analysis of flow through packed and fluidised beds of regular geometrical particles.

i.e. shape factor $$f_a = \frac{A_s}{A_p}$$

For irregularly shaped granular particles Leva[91] suggested the alternative factor $f_a = \frac{V_p^{2/3}}{0 \cdot 205 A_p}$

where V_p = Volume of particle.

In his sedimentation studies, Dallavalle[92] derived another characteristic dimension which he called the "effective diameter" and defined as the diameter of a sphere which takes the same length of time to fall between two fixed points in a medium as does the irregular particle. The "effective diameter" is influenced, however, not only by the density and size of the particle but also by its configuration and surface condition.

In similar studies, Heywood[93,94,95] introduced a shape factor in order to calculate the terminal velocities of irregularly shaped particles. As the size of such particles is frequently determined by microscopical methods, Heywood used the mean projected diameter d_m as the characteristic dimension of the particle and defined his shape factor φ_m by the equation:

$$\text{volume of particle} = \varphi_m \times d_m^3$$

It is apparent, however, that the value of φ_m which Heywood found to vary from $\pi/6$ for spheres to $0 \cdot 1$ or less for very flat particles, is a measure of the degree of flatness of the particle.

Shape factors based on the same form of equation but on different characteristic dimensions to those of Heywood were developed by Dallavalle[92] using the work of Green[96] and Martin[97] who showed that for irregularly shaped particles having a statistical diameter d_s and volume V_p, the ratio V_p/d_s^3 was constant, the constant f_v, being termed the "volumetric shape factor". A corresponding "surface shape factor" f_s was derived by Dallavalle[92].

Fair and Hatch[98] showed that the ratio f_s/f_v gives a useful measure of particle shape as it ranges from 6·0 for spheres to 7·0 for sharp particles. Values of 6·1 and 6·4 were obtained for rounded and worn particles respectively.

Although the shape factors of Wadell, Heywood and Dallavalle are useful for comparing the performance of individual particles, they have limitations when applied to packed beds in which the porosity and form of packing affect the performance of the particles.

In a study of the porosity effect, Blake[99] treated a random packed bed as a bundle of parallel capillaries and applied a mean hydraulic radius equal to ε/S, where ε is the porosity and S is the particle surface per unit volume of bed, to the fluid flow correlations of Schiller[100]. This treatment led to the introduction of a factor, k, which combined the effects of flow path and particle shape on the flow of a fluid through a packed bed.

An identical factor was derived independently by Kozeny[10 who assumed that the pore space was equivalent to a bundle of parallel capillaries with a common hydraulic radius and a cross-sectional shape representative of the average shape of a pore cross-section. By considering the tortuous path followed by the fluid as it passed through the bed, Kozeny suggested that the factor k consisted of a tortuosity factor and a second factor associated with the shape of the particle.

Several studies [102,103,104] using beds of spheres have reported values of k ranging from 4·1 to 5·5 with no apparent trend with either size or porosity. However, for flat sided particles, Coulson[105] and Wyllie[106] both found that the value of k depended on the porosity of the bed. This appeared to have been caused by the flat sided particles tending to give planes instead of points of contact and emphasises the importance of determining accurately the amount of particle surface area actually being used in the operation when assessing the performance of a packed bed.

The effect of shape on packing depends on the procedure by which the bed is formed. Evans and Millman[107] and Orr[108] reported that in beds formed by simple deposition, spherical particles pack to higher densities than irregular ones. However, irregular particles pack more closely than spherical ones if the bed is subjected to vibration or compaction at moderate pressures. This factor together with other dominant factors influencing the packing of particles is discussed comprehensively in a recent text by Gray[109].

It is apparent, therefore, that in randomly packed beds of irregular particles, it is very difficult to determine precisely the porosity of the bed and the particle surface area taking an active part in the operation of the bed. In these circumstances, the properties of the bed are determined empirically.

Consequently, in the present work in which randomly packed beds of tabloid pellets are used, the empirical shape factor, introduced by Gupta and Thodos[35] to represent the particle surface area taking part in the process, is used to compare the performance of the tabloid pellets with spherical and cylindrical particles.

5. EXPERIMENTAL APPARATUS AND PROCEDURE

5.1 Description of Through-Circulation Dryer.

The dryer, used in the tests and shown in Figures 5.1 and 5.2 and Plate No. 5.1, consisted essentially of a drying chamber in which a steady stream of air at a desired temperature passed upwards through of a bed of wet material held in a basket with a wire mesh bottom. The progress of drying was followed by removing the basket from the dryer at intervals and weighing it.

The air flow, which was supplied by a forced draught fan driven by a variable speed 0·5 hp motor, was metered through a 3 in diameter orifice plate in a 5 in diameter pipe on the suction side of the fan, the orifice tappings being connected to a differential pressure gauge on the control panel. A "Stardrive" control unit fitted to the motor enabled air flows from 300 to 900 lb air/ft^2 basket area h to be achieved in the test section.

The air was heated as it passed through a chamber containing twenty-one 1 kW electric bar heaters which were wired to give eight 2 kW heaters, one 1 kW heater and two 0·5 kW heaters; one of the 0·5 kW heaters was controlled by a thermistor-relay system which could maintain a given temperature within $\pm$0·25°C.

The humidity of the air could be raised by injecting low pressure steam through jets in a copper tube

FIG 5.1

THROUGH - CIRCULATION DRYER

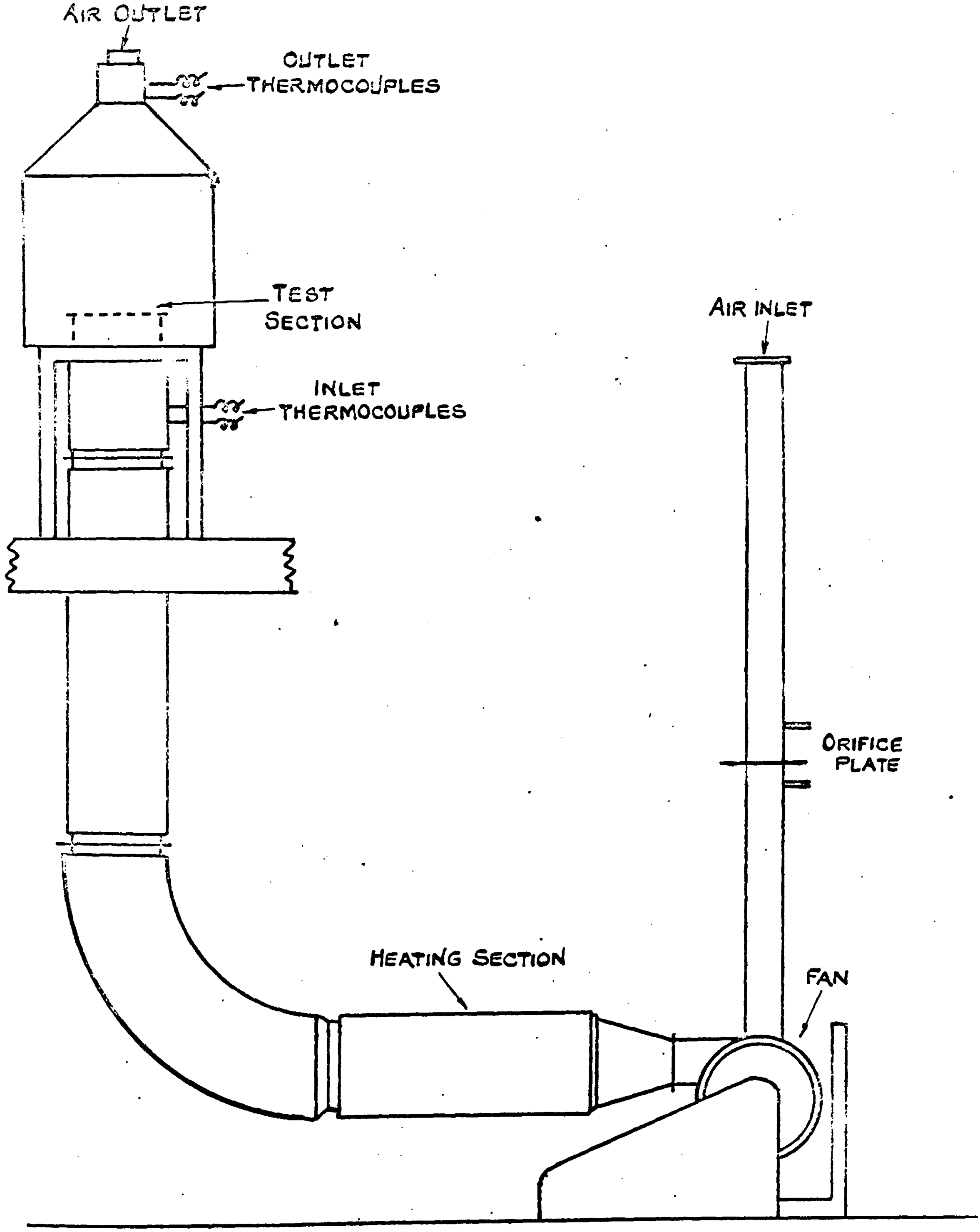

FIG 5.2.

DETAILS OF TEST SECTION AND BASKET OF THROUGH CIRCULATION DRYER.

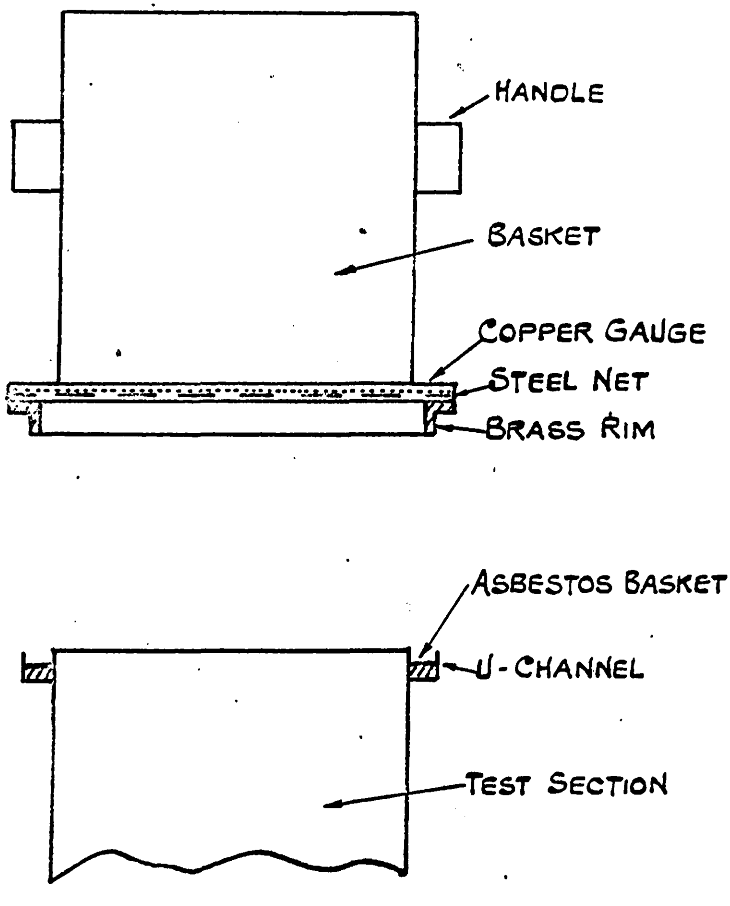

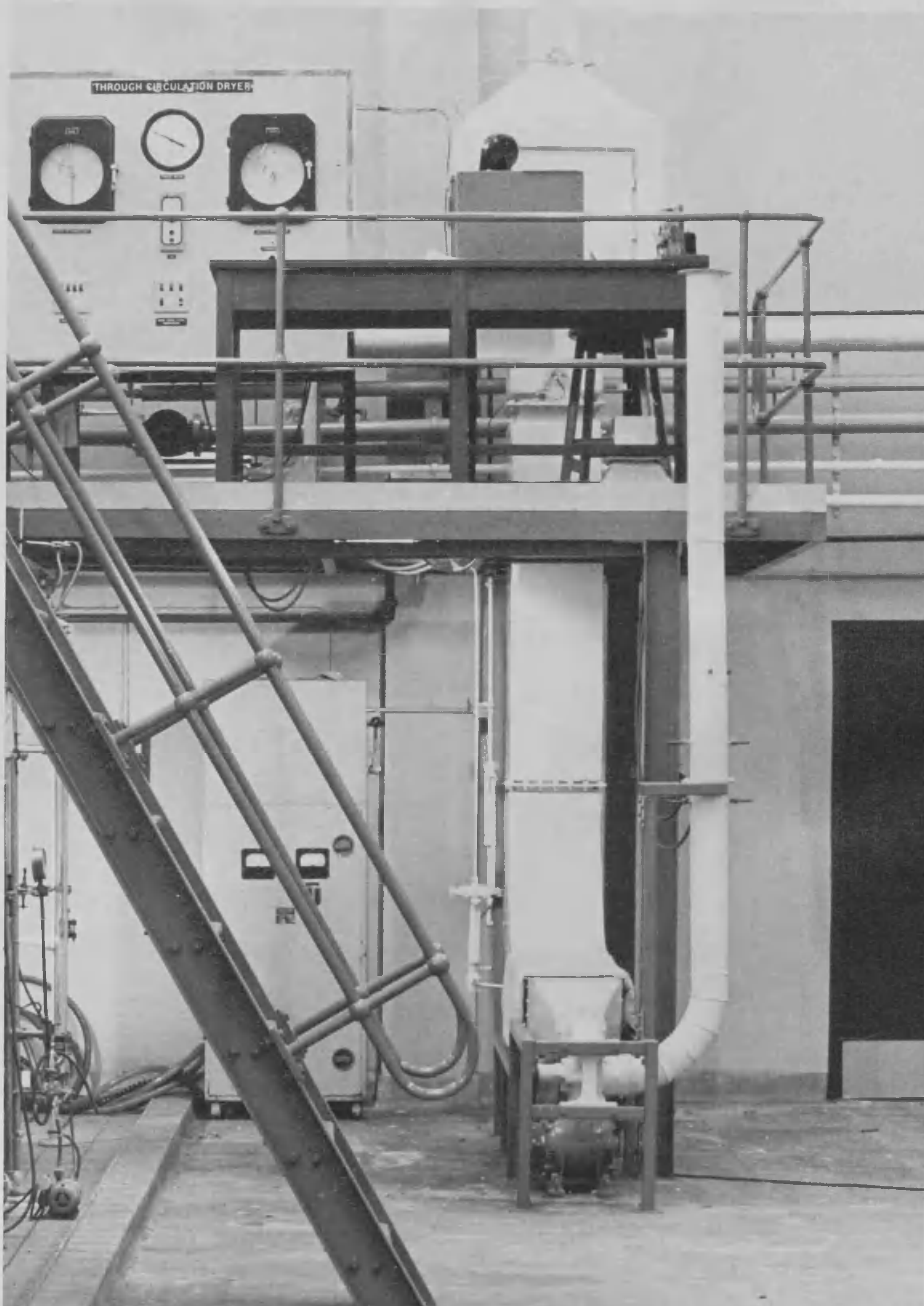

PLATE 5.1

extending across the dryer duct. This facility of the dryer was not used in the present investigation as the required humidity control could not be attained.

The long rising section of the dryer enabled disturbances in the air flow, caused by obstructions such as heater bars, injection pipe etc., to even-out before the air stream reached the test section. The wire mesh on the base of the test basket also helped to give uniform air flow through the bed of material.

The humidity of the air entering the test section corresponded to atmospheric humidity and was measured by a psychrometer situated at the mouth of the inlet air duct. The psychrometer consisted of a small fan which sucked air along a glass tube containing wet and dry bulb thermometers. The temperature and humidity of the air leaving the test section were measured in the outlet duct by dry and wet copper-constantan thermocouples, wired to a Honeywell temperature recorder, which also recorded the temperature, measured by another copper-constantan thermocouple, of the hot air entering the test section. The calibration of the recorder was checked periodically by measuring the outlet humidity of the air with the psychrometer.

During a drying test, the wet material was contained in a 12 in square aluminium basket with 12 in sides and a bottom of copper gauze supported by 0·25 in mesh steel net.

The basket sat on top of the test section.

The air ducts consisted of welded galvanised steel insulated with 1 in lay of magnesia lagging. The heating chamber was 0·375 in thick "Sindanyo" asbestos-cement insulating board lagged with asbestos pads.

The fan controls, differential pressure gauge, heater switches, and the temperature control unit were mounted on a central control panel.

3.2 Description of Celite Pellets.

The pellets, used in the drying tests, consisted mainly of Celite which is used widely in the chemical industry as a filter aid and a mineral filler. The highly porous character of Celite makes it very absorbent and ideal as test material.

Celite consists essentially of pure amorphous diatomaceous silica with small amounts of aluminium, iron, calcium and magnesium, usually combined as silicates. The Celite was obtained from John Walker & Company, Sugar Refiners, Greenock.

The pellets were prepared by compressing a mixture of 75% Celite and 25% ethyl cellulose N22 in a rotary Manesty tableting machine. The diameter of the pellets was determined by the punches and dies used in the machine and their thickness by the compressibility of the machine.

The dimensions of the various sizes of the pellets, used in the tests, are given in Table 5.1 and were the average dimensions of 100 pellets of each type. The pellets are shown in Plates 5.2 and 5.3.

Table 5.1

Dimension of Pellets.

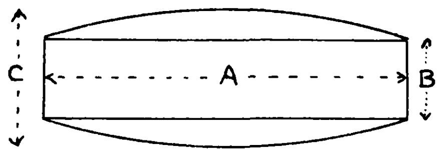

Series	A in	B in	C in	Surface area of 1 tablet in^2	Volume of 1 tablet in^3	Bone dry weight of 1 tablet gm	Voidage of bed ε
1	0·406	0·075	0·161	0·366	0·0154	0·324	0·442
2	0·500	0·093	0·238	0·555	0·284	0·470	0·458
3	0·312	0·054	0·125	0·217	0·00714	0·154	0·450
4	0·406	0·102	0·210	0·436	0·0220	0·298	0·467

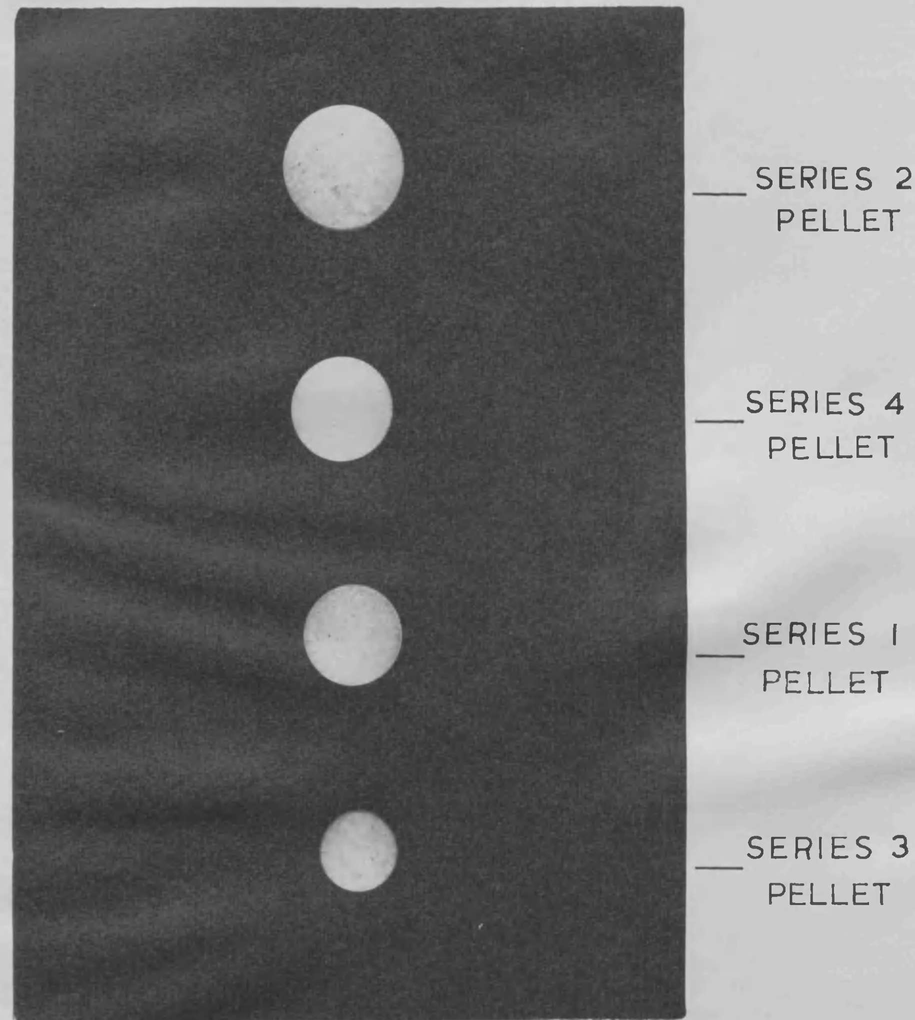
SERIES 2 PELLET
SERIES 4 PELLET
SERIES 1 PELLET
SERIES 3 PELLET

PLATE 5.2

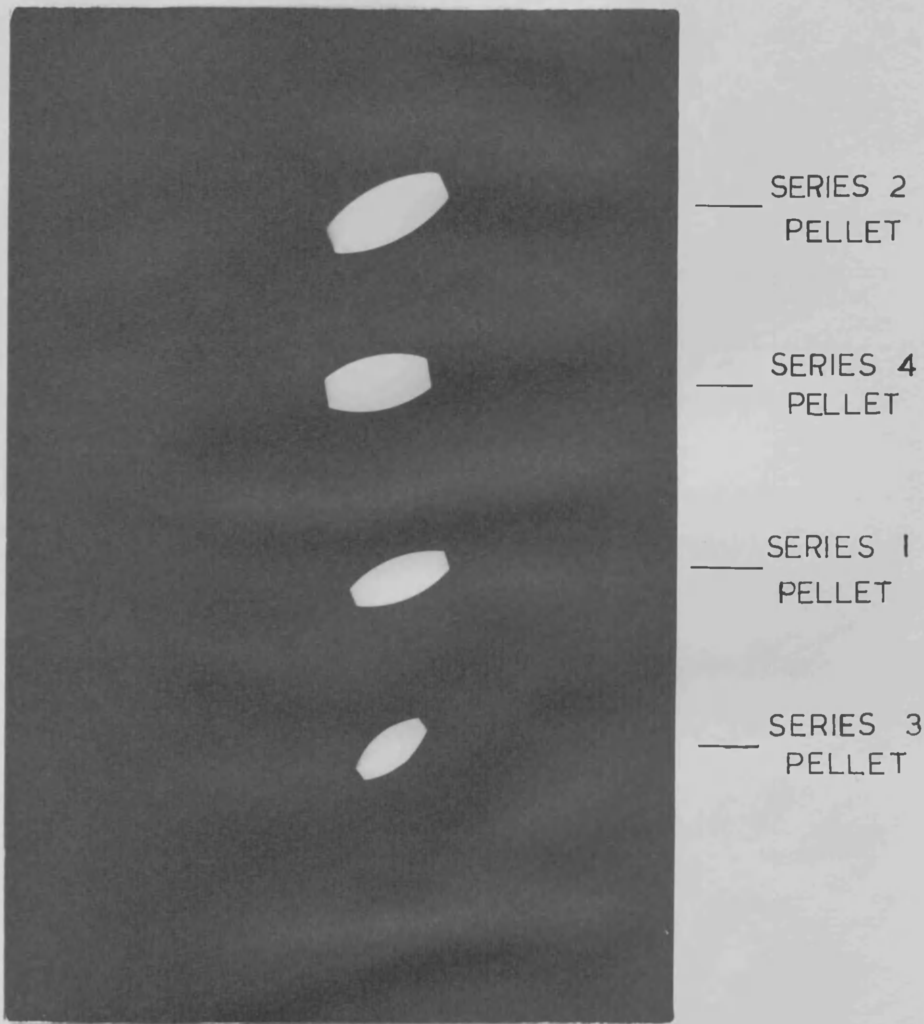
SERIES 2
PELLET
SERIES 4
PELLET
SERIES 1
PELLET
SERIES 3
PELLET

PLATE 5.3

The calculation of the surface area and the volume of a pellet is given in Appendix V together with the method of computing the bed voidage.

5.3 Experimental Procedure.

The dryer was energised by switching on the air fan and the desired air flow was set by adjusting the fan speed. Sufficient heaters were switched on to heat the air stream to just below the required temperature and the automatically controlled heater was set to make the final temperature adjustment.

While the dryer was heating up, the basket was filled to the required depth with pellets, and immersed in a tank of distilled water for thirty minutes. When the pellets were saturated, the basket was allowed to drain for ten minutes, dried with a cloth and weighed. As soon as the air conditions in the dryer had stabilised the basket was placed in the dryer and the drying test commenced.

The progress of drying was followed by removing the basket at regular intervals and weighing it to determine the loss in moisture due to drying. The time intervals were dependent on the conditions in the chamber, varying from one minute during very fast drying conditions to five minutes during slow drying conditions. Drying was continued until the moisture content of the pellets was estimated to be less than 0·05 lb water/lb B.D.S.

The weight of bone dry solid (B.D.S.) in the basket was evaluated by sampling the bed of pellets at the end of a test and determining the moisture content of the samples by drying overnight in an oven with a temperature of 100°C.

3.4 Presentation of the Results of a Drying Test.

A specimen of the data collected in a drying test is given in Appendix I.

The weight of bone dry solid (B.D.S.)in the bed of pellets used in the test was determined from its final weight and residual moisture content. The weight of water in the bed and hence its moisture content, w (lb water/lb B.D.S.) was calculated by subtracting the weight of B.D.S., w_s, from the total weight of material.

The drying curve for the experimental conditions was drawn by plotting w against drying time (min). The constant drying rate N_c', (lb water/lb B.D.S. h) was calculated from the linear portion of the drying curve. The constant drying rate N_c, (lb water/h), obtained by multiplying N_c' by W_s, was used in the evaluation of the transfer coefficients and j factors.

6. RESULTS

6.1 Series 1 Pellets.

The dimensions and physical properties of the pellets are given in Table 5.1 on page 34.

Drying tests were carried out in the 12 in square basket using the following values of bed loading, W_B(lb B.D.S./ft^2 dryer area) and inlet air temperature t(^oC).

Table 6.1

Values of W_B and t for Series 1 Pellets.

W_B	t
3·80 (1 in layer)	35 42·5 50 60
5·70 (1·5 in layer)	42·5 50 60
7·58 (2 in layer)	42·5 50 60

At each level of W_B and t, tests were performed using the following values of G(lb/h ft^2 dryer area):

300 : 390 : 450 : 535 : 630 : 720 : 785 : 875

Duplicate tests were performed with the 1 in layer and a temperature of 50°C to determine whether the drying characteristics of the pellets altered with use.

6.1.1 Constant Drying Rates.

Values of N'_c were calculated as described in Section 5.4 and are given in Table 6.2 for the 1 in bed of pellets and in Table 6.3 for the 1·5 in and 2 in pellet beds.

Table 6.2

Values of N'_c for 1 in Bed of Series 1 Pellets.

G	t				
	35	42·5	50	50 (Duplicated)	60
300	0·418	0·560	0·695	0·632	0·845
390	0·529	0·679	0·822	0·803	1·058
450	0·618	0·774	0·921	0·884	1·232
535	0·687	0·956	1·122	1·042	1·375
630	0·805	1·058	1·310	1·232	1·664
720	0·892	1·169	1·421	1·405	1·873
785	1·027	1·263	1·562	1·518	2·052
875	1·106	1·405	1·736	1·72	2·164

Table 6.3

Values of N_c' for 1·5 in and 2 in Beds of Series 1 Pellets.

G	t					
	42·5		50		60	
	1·5 in bed	2 in bed	1·5 in bed	2 in bed	1·5 in bed	2 in bed
300	0·375	0·295	0·465	0·358	0·605	0·468
390	0·446	0·379	0·579	0·379	0·746	0·600
450	0·588	0·422	0·681	0·512	0·842	0·679
535	0·684	0·502	0·779	0·612	1·021	0·829
630	0·776	0·553	0·948	0·741	1·158	0·948
720	0·812	0·655	1·052	0·809	1·331	1·066
785	0·886	0·702	1·148	0·884	1·432	1·209
875	1·003	0·789	1·263	0·963	1·580	1·311

The duration of the constant drying rate period varied from 30 min under slow drying conditions i.e. obtained in the deep bed with low air rates and temperatures, to 5 min under fast drying conditions experienced in the 1 in bed with high air rates and temperatures.

The drying rates, obtained with the used pellets, were on average 6% higher than the rates with the fresh pellets, but were achieved with air of slightly lower humidity, the inlet driving force being 3% greater. Consequently the alteration in the drying characteristics of the pellets with use was considered to be negligible.

The drying rates conformed with established drying theory in that they increased with the rate and temperature of the air but decreased as the pellet bed deepened.

The drying characteristics of the pellets were investigated further by determining the effect of the air flow rate on the constant drying rate of the pellets.

<u>Variation of N'_c with G.</u>

The relationship between N'_c and G may be expressed in the form:

$$N'_c = a_1 \quad G^{b_1} \qquad .....(6.1)$$

The constants a_1 and b_1 may be determined either graphically by measuring the gradient and the intercept on the abscissae of the plot of log N'_c against log G, or statistically by subjecting values of log N'_c and log G to a regression analysis as described in Appendix VII. Because of its greater accuracy, the latter method was used and values of a_1 and b_1 for the different combinations of bed depth, Δ(in), and air temperature, are given in Table 6.4.

Table 6.4

Values of a_1 and b_1 for Series 1 Pellets.

Z	t	a_1	b_1
1	35	0·00244	0·90
	42·5	0·00412	0·86
	50	0·00307	0·93
	50	0·00447	0·88
	60	0·00485	0·90
			av. 0·90
1·5	42·5	0·00362	0·91
	50	0·00206	0·95
	60	0·00328	0·91
			av. 0·92
2	42·5	0·00169	0·91
	50	0·00160	0·95
	60	0·00184	0·97
			av. 0·94

The results, shown graphically in Fig. 6.1, reveal that the value of b_1 was independent of temperature but increased as the bed depth increased from an average of 0·90 at the 1 in bed depth to an average of 0·94 at the 2 in bed depth. Since the constant a_1 is calculated from the corresponding value of b_1, the values of a_1 have therefore little significance.

FIG 6.1

EFFECT OF AIR RATE ON CONSTANT DRYING RATE FOR SERIES I PELLETS.

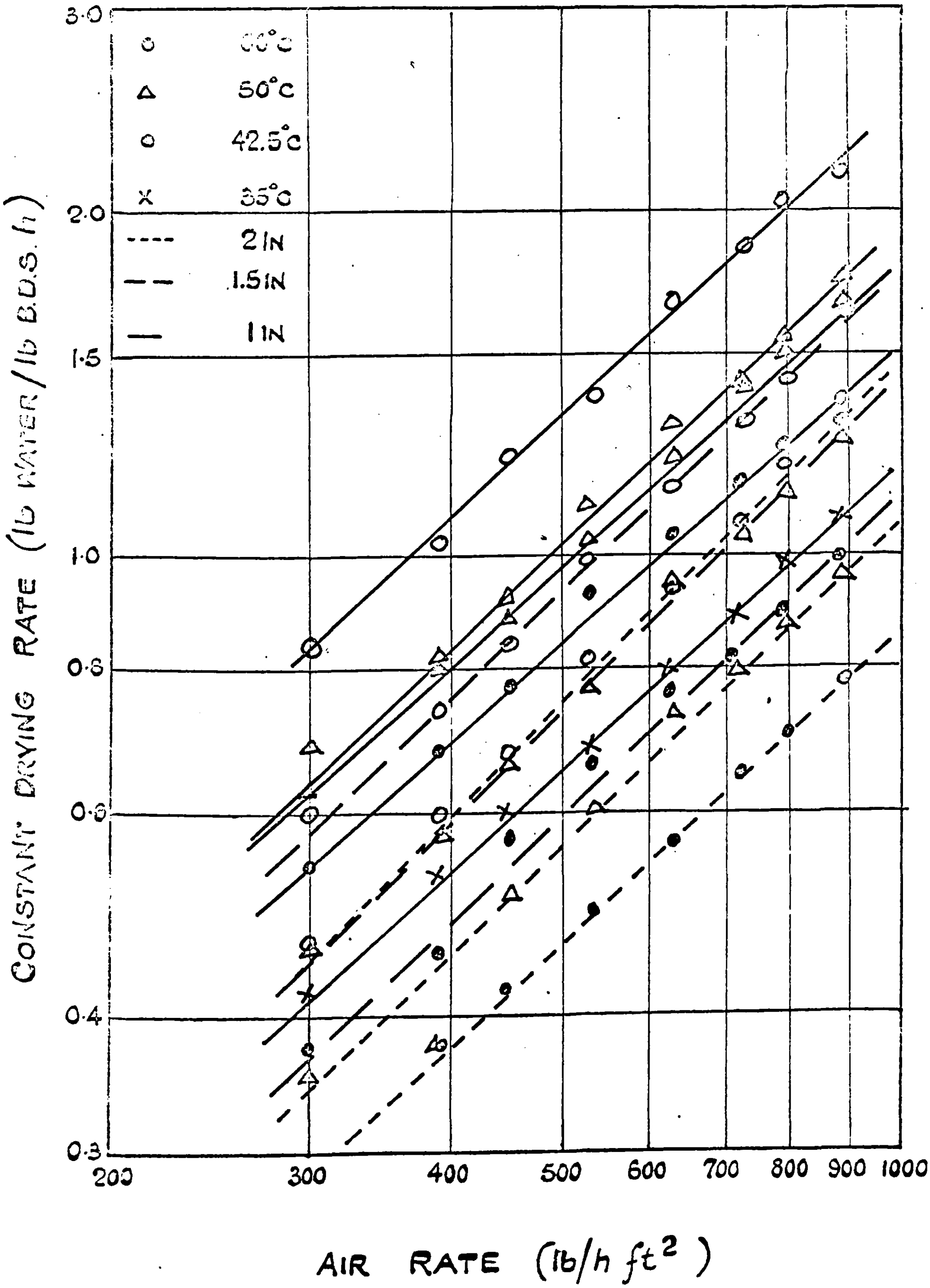

6.1.2 Heat and Mass Transfer Coefficients.

The heat transfer coefficient, h_g, (Chu/h ft^2 deg C), and mass transfer coefficient, k_g, (lb/h ft^2 unit humidity driving force), were calculated for each of the test conditions as described in Appendix II.

h_g

The values of h_g, given in Table 6.5 for the 1 in bed tests and in Table 6.6 for the 1·5 in and 2 in bed tests, indicate that the coefficients were independent of the air temperature, increased with the air rate but decreased as the bed depth increased.

Table 6.5

Values of h_g for 1 in Bed of Series 1 Pellets.

G	t				
	35	42·5	50	50	50
300	10·8	9·83	8·94	11·4	9·80
390	12·4	10·7	11·1	11·4	11·6
450	14·6	12·5	11·6	12·2	13·4
535	15·7	15·9	13·3	14·8	14·0
630	17·5	16·8	15·7	17·6	17·4
720	18·9	17·2	17·6	18·3	19·0
785	22·2	18·6	18·8	19·8	20·6
875	23·8	20·8	21·5	22·3	20·9

Table 6.6

Values of h_g for 1·5 in and 2 in Beds of Series 1 Pellets.

G	1·5 in bed			2 in bed		
	t			t		
	42·5	50	60	42·5	50	60
300	7·25	7·26	7·39	5·68	5·96	6·80
390	7·96	8·32	8·94	7·29	7·15	8·40
450	10·3	10·1	4·67	7·52	7·54	9·61
535	10·8	10·8	11·9	9·06	8·90	11·8
630	12·4	14·3	12·9	9·07	10·2	13·0
720	14·1	14·7	14·3	11·3	11·7	13·6
785	15·3	15·9	15·6	12·4	12·5	17·0
875	17·0	17·3	16·8	13·7	13·7	18·1

Variation of h_g with G.

Since h_g was independent of t, all the values of h_g at each bed depth were grouped together for analysis. As with the constant drying rate data, the effect of G on h_g is most efficiently described by an expression of the form:

$$h_g = a_2 G^{b_2} \qquad \text{.....(6.2)}$$

The values of the constants a_2 and b_2 were determined for each bed depth by subjecting the values of h_g at each bed depth to a regression analysis, as described in Appendix VII. The results of the analyses are given in Table 6.7.

Table 6.7

Values of a_2 and b_2 for Series 1 Pellets.

Z	a_2	b_2
1	0·139	0·75
1·5	0·064	0·83
2	0·048	0·85

The analyses indicated that the value of b_2 increased from 0·75 for the 1 in bed to 0·85 for the 2 in bed and consequently an interaction existed between the air rate and bed depth.

Variation of h_g with Z.

The reduction in the value of the transfer coefficient as the bed depth increased has been reported in previous studies [32,33,34]. Some of these workers, Bradshaw and Myers[33], considered the possibility of an error in the driving force and discovered that the profile of a curve, constructed for the log mean driving force in a deep bed using the inlet and outlet temps, was different from the curve drawn through measured outlet temperatures of beds at intermediate heights, the values of the log mean curve being high. Bradshaw and Myers modified their values by applying a correction factor consisting of the ratio of the area under the log mean curve for each bed height to the area under the curve drawn through the measured outlet temperatures. The modified coefficients were independent of bed depth.

In the present work, the possibility of an error in the driving forces for the 1·5 in and 2 in beds was investigated by drawing curves as described above. Two such curves for test conditions are shown in Fig. 6.2.

It was found that, in every case, the log mean curve lay above the curve drawn through the measured outlet temperatures at intermediate bed depths and consequently since the area under such a curve is a measure of the corresponding driving force, the log mean driving force was greater than the actual driving force. This discrepancy in the driving forces in the deeper beds produced a reduction in the heat transfer coefficient for these beds.

The values of h_g at the 1·5 in and 2 in beds given in Table 6.6 were corrected for bed depth effect by dividing them by the ratio of the areas under the log mean and actual driving force curves. As this factor was compiled from experimental conditions and not based on theoretical assumptions, its value did not remain constant but varied for each individual drying test. The method, by which the correction factor was computed and applied, is described in Appendix III.

Table 6.8 gives the values of h_g' for the 1·5 in and 2 in beds which have been modified for bed depth effect.

FIG 6.2

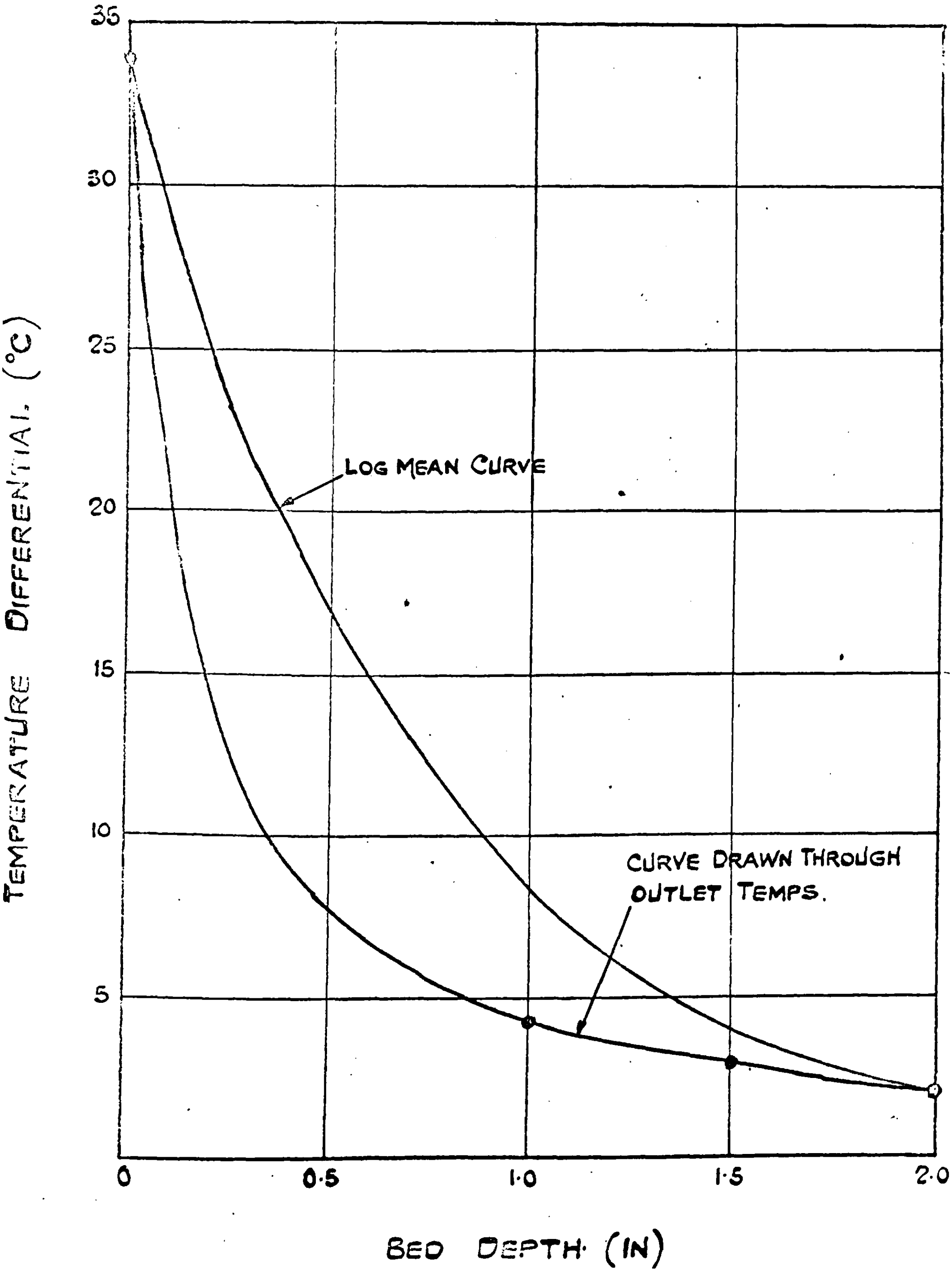

35
30
25
20
15
10
5
0
0.5
1.0
1.5
2.0
LOG MEAN CURVE
CURVE DRAWN THROUGH OUTLET TEMPS.
TEMPERATURE DIFFERENTIAL (°C)
BED DEPTH (IN)

Table 6.8

Values of h'_g for 1·5 in and 2 in Beds of Series 1 Pellets.

G	1·5 in bed			2 in bed		
	t			t		
	42·5	50	60	42·5	50	60
300	11·0	10·5	11·8	8·61	10·1	11·5
390	11·4	11·9	12·4	9·96	11·6	12·3
450	13·4	12·8	14·5	11·5	11·5	13·9
535	16·4	14·7	15·0	14·8	13·3	15·4
630	17·7	16·9	18·4	15·2	16·9	17·7
720	18·2	19·2	20·1	15·9	17·6	19·0
785	17·6	19·9	21·6	16·7	19·1	21·5
875	21·3	23·3	22·0	18·4	21·6	20·8

The values of h'_g for the 1·5 in and 2 in beds were also subjected to a regression analysis to investigate their variation with G. Values of a_2 and b_2 calculated in the analysis are given in Table 6.9.

Table 6.9

Results of Regression Analysis for Values of h'_g.

Z	a_2	b_2
1·5	0·230	0·67
2	0·185	0·69

Although it appeared that the values of h'_g obtained in the 1·5 in and 2 in beds and the values of h_g for the 1 in beds were similar and independent of the bed depth, the effect of bed depth on these coefficients was examined by determining whether the values of b_2 for each bed depth varied significantly and by comparing the average values of the coefficients at each bed depth.

The possibility of differences existing among the values of b_2 was tested by subjecting the values of h_g and h'_g to an Analysis of Variance as described in AppendixVIII. The results of the analysis, given in Table 6.10, show that there was no significant difference in the values of b_2.

Table 6.10

Analysis of Variance for Testing Differences in Values of b_2 for Series 1 Pellets.

Source of Variance	Degrees of Freedom	Sum of Squares	Mean Sum of Squares
Combined Regression	1	1·004794	1·004794
Difference of Regression	2	0·002028	0·001014
Combined Residual	82	0·083133	0·001014
Total with groups	85	1·089955	

F ratio = 1·0

Values of F for significane at 5% level of probability = 3·1

The average values of the coefficients for each bed depth were very similar being 15·3 Chu/h ft^2 ^oC for the 1 in bed, 15·9 Chu/h ft^2 ^oC for the 1·5 in bed and 14·7 Chu/h ft^2 ^oC for the 2 in bed.

Consequently, the values of h_g for the 1 in beds and h'_g for the 1·5 in bed and 2 in bed were considered to be independent of the pellet bed and were grouped together and correlated with the values of G to give the expression shown in Fig. 6.3 of :

$$h'_g = 0 \cdot 1756 \, G^{0 \cdot 71}$$

$\underline{k_g}$

The values of the mass transfer coefficient, k_g, calculated from the 1 in bed tests are given in Table 6.11, while the coefficients obtained in the 1·5 in and 2 in beds are given in Table 6.12.

FIG 6.3

EFFECT OF AIR RATE ON HEAT TRANSFER COEFFICIENT FOR SERIES I PELLETS

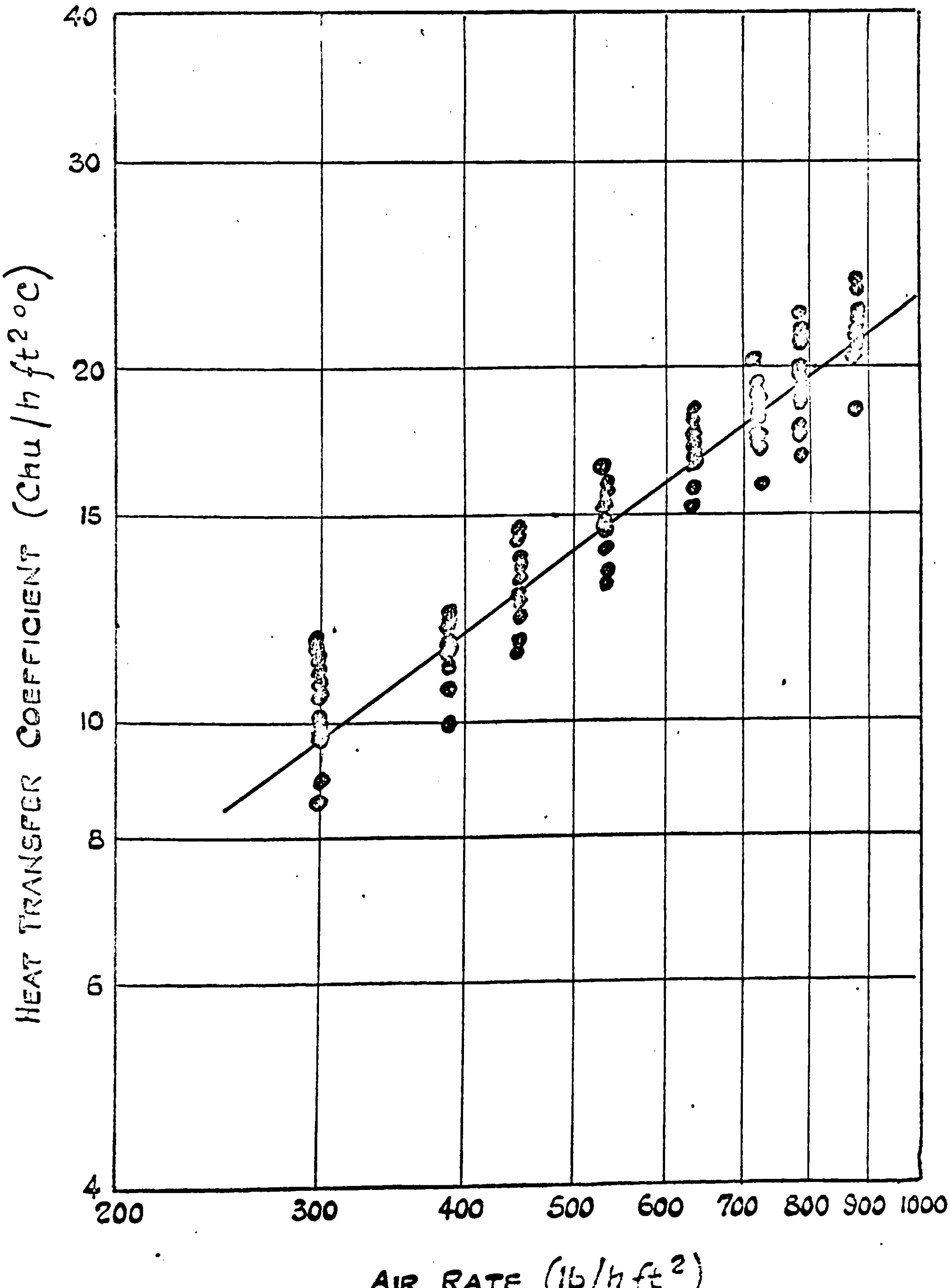

Table 6.11

Values of k_g for 1 in Bed of Series 1 Pellets.

G	t				
	35	42·5	50	50	60
300	41·6	36·8	33·9	44·9	36·9
390	48·5	40·7	42·1	43·8	43·9
450	55·9	47·4	44·4	46·8	51·7
535	60·4	60·6	50·4	58·8	53·5
630	67·2	62·7	59·6	68·9	66·8
720	70·8	66·4	68·8	71·4	72·8
785	87·1	70·1	72·5	77·5	79·0
875	91·0	78·9	81·5	86·8	80·1

Table 6.12

Values of k_g for 1·5 in and 2 in beds of Series 1 Pellets.

G	1.5 in			2 in		
	t			t		
	42·5	50	60	42·5	50	60
300	27·6	27·8	29·3	21·7	23·0	25·8
390	30·6	32·2	34·5	28·1	27·5	32·0
450	40·1	39·0	37·1	29·0	29·3	36·6
535	44·1	41·7	46·1	34·7	34·1	45·4
630	47·4	54·5	49·7	35·2	39·4	50·3
720	54·2	56·3	57·5	43·4	45·0	52·3
785	59·4	61·7	59·6	45·7	48·3	64·4
875	65·8	66·6	64·3	52·3	53·3	64·3

In this type of transfer system, heat and mass are being simultaneously exchanged between the air and the pellets, so that the value of k_g is related to the corresponding value of h_g and the behaviour of k_g closely follows that of h_g. Consequently, it was found that the value of the ratio of the coefficients h_g/k_g was approximately constant for each drying test , the average value being 0·260, and the values of k_g behaved similarly to those of h_g in that they were independent of the air temperature, increased with the air rate and decreased as the bed depth increased.

Variation of k_g with G.

As with the heat transfer coefficient, the variation of the mass transfer coefficient with air flow rate was investigated by correlating the data in the form:

$$k_g = a_3 \, G^{b_3} \qquad \text{.....(6.3)}$$

The values of a_3 and b_3 for each bed depth, computed from the regression analyses, are given in Table 6.13.

Table 6.13

Values of a_3 and b_3 for Series 1 Pellets.

Z	a_3	b_3
1	0·528	0·75
1·5	0·260	0·82
2	0·190	0·84

The analyses indicated that the value of b_3 depended on the bed depth i.e. an interaction existed between G and Z.

<u>Variation of k_g with Z.</u>

Because the driving forces present in a simultaneous heat and mass transfer system are related to each other, the error in the driving force responsible for the reduction in the values of h_g in the deeper beds is also present in the driving forces used in the calculation of k_g for the deeper beds. Since the ratio of h_g/k_g was independent of the bed depth, it may be assumed that the errors in the driving forces used in the computation of k_g for the 1·5 in and 2 in beds will be identical to those in the driving forces for the corresponding h_g values. Consequently the values of k_g in the 1·5 in and 2 in beds may be modified for the error in the driving force by applying the same correction factor as was used for the modification of the corresponding value of h_g. Table 6.14 gives the values of k_g' which have been modified for bed depth effect.

Table 6.14

Values of k_g' for Series 1 Pellets.

G	1.5 in bed			2 in bed		
	t			t		
	42.5	50	60	42.5	50	60
300	41.1	40.0	45.1	32.9	38.9	43.7
390	44.0	46.1	47.7	38.5	44.8	46.1
450	52.1	49.4	55.4	44.5	44.8	53.1
535	66.9	56.7	58.3	57.7	51.0	57.6
630	67.5	64.7	70.5	59.3	65.4	68.4
720	70.1	73.8	77.4	61.4	68.0	73.0
785	75.3	77.0	82.5	63.8	73.8	81.8
875	81.7	89.3	84.2	70.5	83.9	78.7

The modified coefficients were correlated with the air rate to give the following expressions:

For the 1.5 in bed $k_g' = 0.771\ G^{0.69}$

and for the 2 in bed $k_g' = 0.694\ G^{0.70}$

Since the values of h_g for the 1 in bed tests and of h_g for the 1.5 in and 2 in bed tests were found to be independent of the depth of the pellet bed, the corresponding values of k_g and k_g' were also assumed to be independent of the bed depth. Hence the mass transfer coefficients were grouped together and correlated with the air rate to give the following relationship which is shown in Fig. 6.4:

$$k_g' = 0.621\ G^{0.72}$$

FIG 6.4

EFFECT OF AIR RATE ON MASS TRANSFER COEFFICIENT FOR SERIES I PELLETS

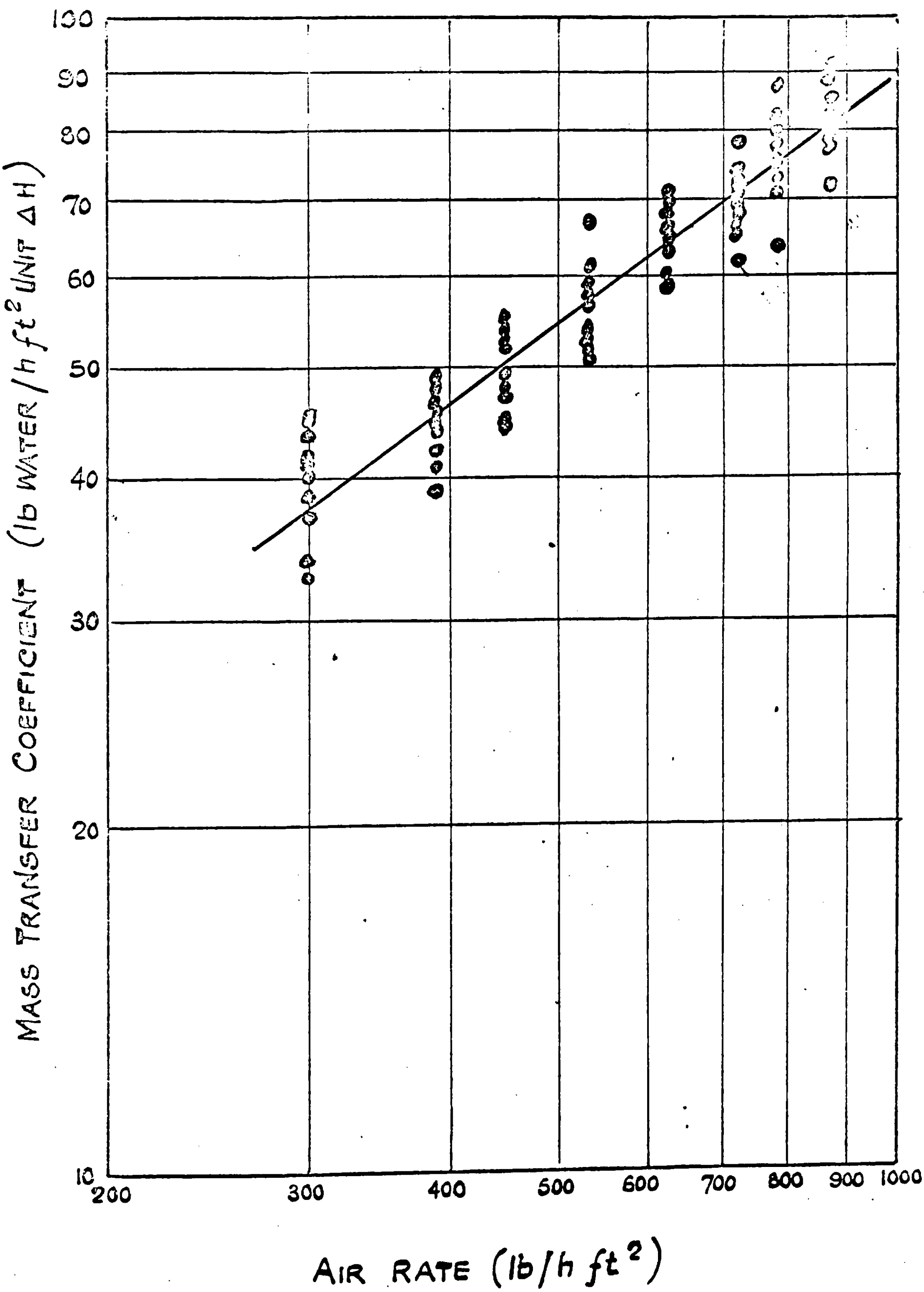

6.1.3 Heat and Mass Transfer Factors.

The j_h and j_d factors were derived from the corresponding heat and mass transfer coefficients as described in Appendix II.

j_h Factor.

The value of j_h calculated from the 1 in bed tests are given in Table 6.15 while the j_h factors from 1·5 in and 2 in bed tests are shown in Table 6.16.

Table 6.15

Values of j_h for 1 in Bed of Series 1 Pellets.

	t				
	35	42·5	50	50	60
300	0·1227	0·1120	0·1019	0·1298	0·116
390	0·1088	0·0941	0·0973	0·0997	0·1017
450	0·1111	0·0953	0·0890	0·0934	0·1024
535	0·0995	0·1010	0·0939	0·0939	0·0891
630	0·0950	0·0916	0·0851	0·0956	0·0946
720	0·0898	0·0818	0·0838	0·0870	0·0905
785	0·0965	0·0810	0·0819	0·0862	0·0896
875	0·0931	0·0812	0·0840	0·0872	0·0818

Table 6.16

Values of j_h for 1·5 in and 2 in Beds of Series 1 Pellets.

G	1·5 in bed			2 in bed		
	t			t		
	42·5	50	60	42·5	50	60
300	0·0978	0·1195	0·1346	0·0783	0·1147	0·1307
390	0·1000	0·1042	0·1083	0·0873	0·1021	0·1080
450	0·1026	0·0976	0·1105	0·0878	0·0890	0·1062
535	0·1044	0·0934	0·0949	0·0939	0·0845	0·0954
630	0·0960	0·0917	0·0999	0·0829	0·0919	0·0961
720	0·0866	0·0914	0·0957	0·0758	0·0837	0·0902
765	0·0763	0·0862	0·0938	0·0725	0·0829	0·0933
875	0·0830	0·0909	0·0861	0·0721	0·0845	0·0813

The values of j_h conformed to the pattern followed by the corresponding heat transfer coefficients in that they were independent of the depth of the pellet bed and the air inlet temperature. However, the factors decreased as the air rate increased whereas the coefficients increased with the air rate.

The general heat transfer relationship for the Series 1 pellets was derived by correlating the values of j_h, for each drying test with the value of the Reynolds number, Re, for that test as described in Appendix VII. The method of computing the Reynolds number is given in Appendix IV.

The following expression, which is shown in Fig. 6.5, was obtained:

FIG 6.5

EFFECT OF REYNOLDS NO. ON HEAT TRANSFER FACTOR FOR SERIES 1 PELLETS.

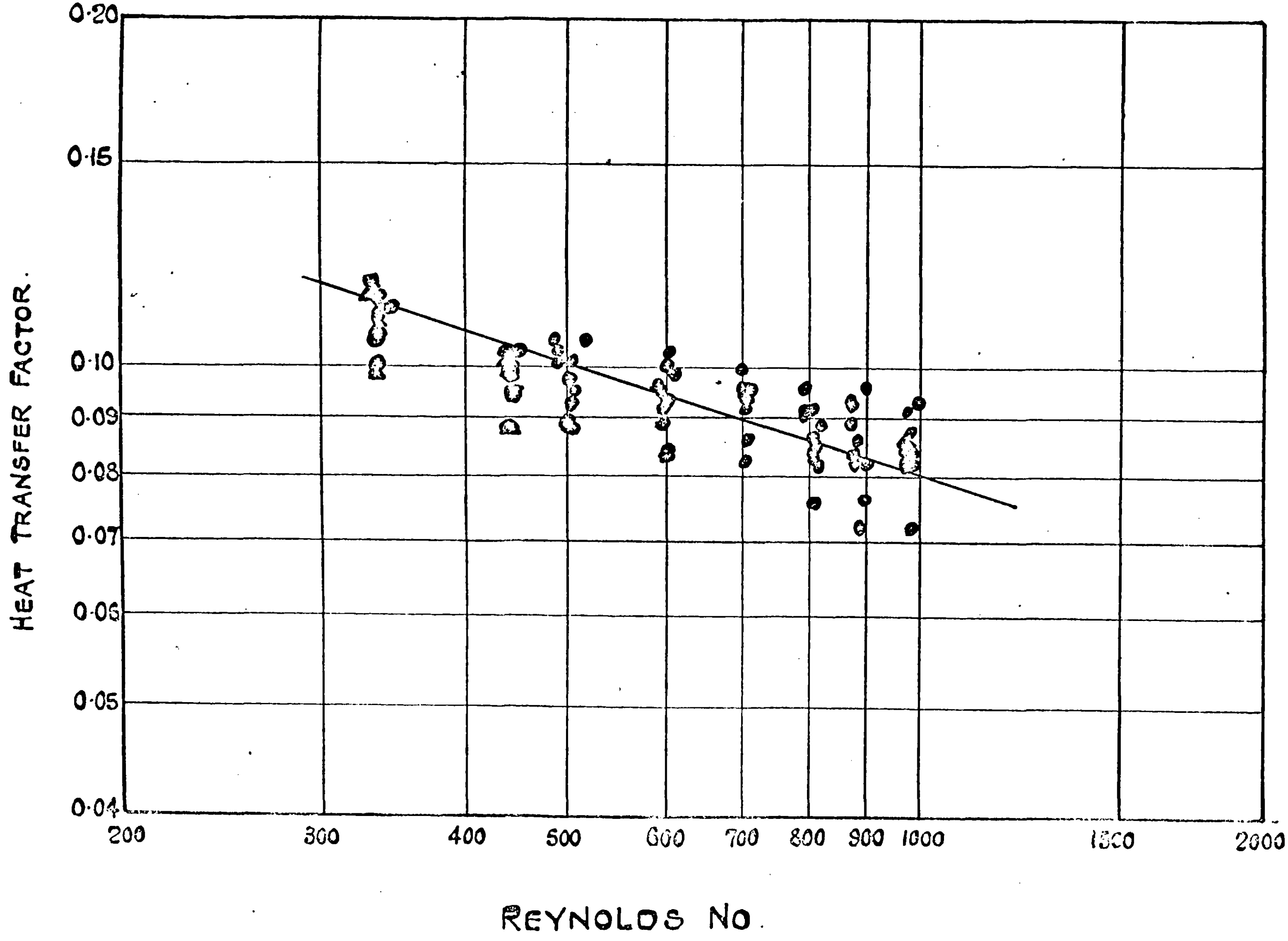

$$j_h = 0{\cdot}729\ Re^{-0{\cdot}32}$$

The average deviation of the experimental values of j_h from this equation was 6·2%.

j_d Factor.

It can be seen from Tables 6.17 and 6.18 that the values of j_d followed the same pattern as the corresponding values of j_h. It was found that the ratio of j_h/j_d varied from 1·17 to 1·29, the average value being 1·25.

Table 6.17

Values of j_d for 1 in Bed of Series 1 Pellets.

G	t				
	35	42·5	50	50	60
300	0·0991	0·0876	0·0808	0·1070	0·0881
390	0·0888	0·0746	0·0772	0·0803	0·0803
450	0·0891	0·0756	0·0710	0·0747	0·0825
535	0·0805	0·0807	0·0672	0·0785	0·0715
630	0·0752	0·0712	0·0678	0·0784	0·0760
720	0·0704	0·0660	0·0684	0·0710	0·0725
785	0·0790	0·0636	0·0659	0·0705	0·0718
875	0·0743	0·0652	0·0667	0·0709	0·0655

Table 6.18

Values of j_d for the 1.5 in and 2 in Beds of Series 1 Pellets.

G	1.5 in beds			2 in beds		
	t			t		
	42.5	50	60	42.5	50	60
300	0.0978	0.0955	0.1075	0.0783	0.0928	0.1042
390	0.0805	0.0846	0.0875	0.0705	0.0822	0.0845
450	0.0813	0.0789	0.0885	0.0709	0.0716	0.0848
535	0.0891	0.0756	0.0778	0.0769	0.0681	0.0769
630	0.0766	0.0736	0.0802	0.0673	0.0743	0.0778
720	0.0696	0.0734	0.0770	0.0610	0.0676	0.0726
785	0.0683	0.0700	0.0750	0.0579	0.0671	0.0743
875	0.0667	0.0730	0.0688	0.0575	0.0686	0.0643

The general mass transfer relationship for the Series 1 pellets was obtained by correlating the values of j_d with Re as described on page 55 to give the expression:

$$j_d = 0.490 \; Re^{-0.29}$$

The experimental values of j_d deviated on average by 6.1% from the above correlation. The correlation is shown in Fig. 6.6.

FIG 6.6

EFFECT OF REYNOLDS NO ON MASS TRANSFER FACTOR FOR SERIES I PELLETS.

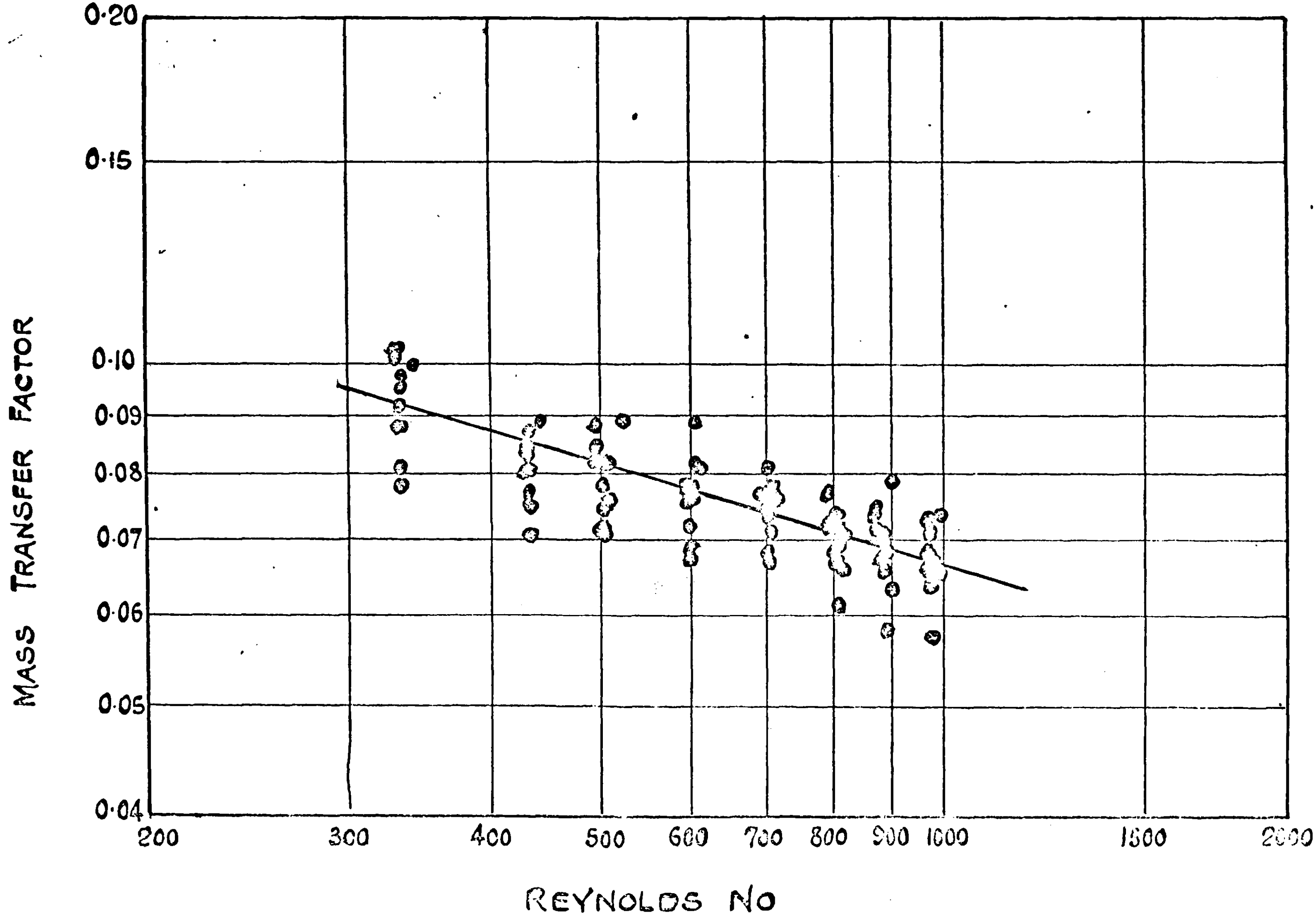

6.2 Series 2 Pellets.

The dimensions and physical properties of the pellets are given in Table 5.1 on page 34.

Drying tests were conducted in the 12 in square basket using the following conditions of w_B and t:

Table 6.19

Values of W_B and t for Series 2 Pellets.

W_B	t
3·2 (1 in layer)	35 42·5 50 60
6·4 (2 in layer)	50 60

At each level of W_B and t, tests were carried out using the values of G given in Section 6.1 on page 38.

The effect of repeated use of the pellets on their drying characteristics was determined by performing duplicate tests in the 1 in bed using an air temperature of 50°C.

6.2.1 Constant Drying Rates.

Values of N_c', derived according to the procedure described in Section 5.4 are given for the 1 in bed tests in Table 6.20 while Table 6.21 contains the values of N_c' from the 2 in bed tests. In these tests, inlet temperatures were restricted to 50°C and 60°C as the air leaving the bed approached saturation at the lower temperature levels.

In the 1 in bed tests, drying occurred so rapidly when using the highest air rate and temperature that the value of N'_c could not be determined accurately. The length of the constant drying rate period in the other tests varied from approximately 3 minutes to 30 minutes.

As the corresponding values of N'_c obtained in the duplicate series of tests were very similar it was considered that the drying characteristics of the pellets did not alter with use.

The drying rates showed the same characteristics as Series 1 pellets and conformed with the accepted drying theories

Table 6.20

Values of N'_c for 1 in Bed of Series 2 Pellets.

G	t				
	35	42.5	50	50	60
300	0.435	0.550	0.754	0.718	1.000
390	0.494	0.674	0.925	0.843	1.109
450	0.622	0.781	1.038	0.976	1.305
535	0.678	0.895	1.153	1.146	1.562
630	0.844	1.000	1.385	1.323	1.746
720	0.932	1.137	1.537	1.528	1.980
785	0.938	1.199	1.599	1.670	2.132
875	1.066	1.330	1.828	1.767	

Variation of N'_c with G.

The effect of G on N'_c was expressed in the form of equation 6.1 and determined by the procedure described in section 6.1.1. The values of the constants a_1 and b_1 given in Table 6.22 show that the exponent of G, b_1, was independent of the air temperature but increased with the bed depth. Hence, an interaction exists between the effects of G and Z on N'_c, which are shown in Fig. 6.7.

Table 6.21

Values of N'_c for 2 in Beds of Series 2 Pellets.

G	t	
	50	60
300	0.395	0.530
390	0.539	0.670
450	0.587	0.733
535	0.687	0.888
630	0.758	1.007
720	0.906	1.092
785	0.996	1.269
875	1.142	1.000

FIG 6.7

EFFECT OF AIR RATE ON CONSTANT DRYING RATE FOR SERIES 2 PELLETS

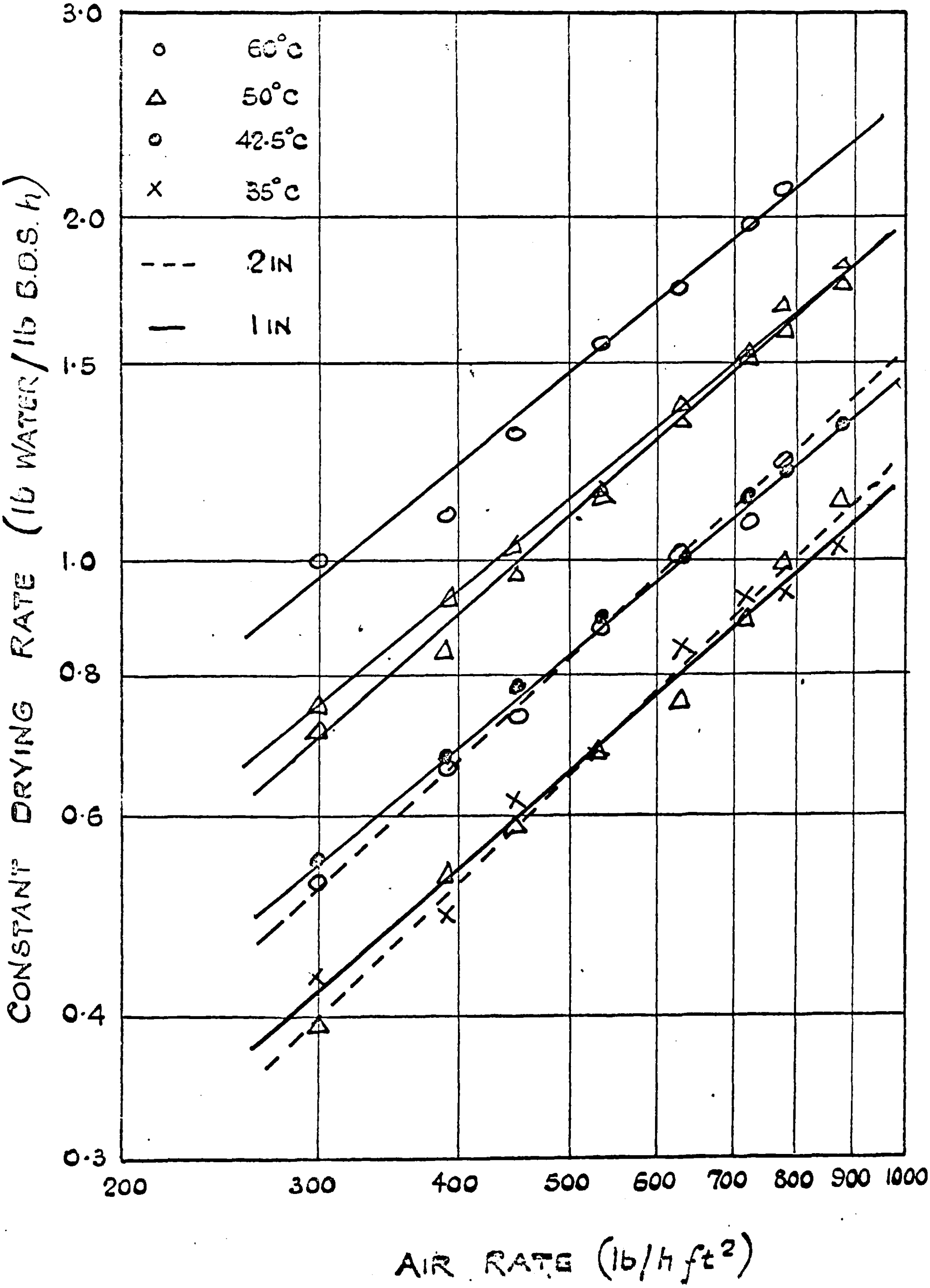

Table 6.22

Values of a_1 and b_1 for Series 2 Pellets.

Z	t	a_1	b_1
	35	0·00300	0·87
	42·5	0·00520	0·82
1	50	0·00755	0·81
	50	0·00482	0·87
	60	0·00898	0·82
			av. 0·84
2	50	0·00170	0·94
	60	0·00325	0·90
			av. 0·92

6.2.2 Heat and Mass Transfer Coefficients.

The calculation of the heat and mass transfer coefficients from the data collected in the drying tests is described in Appendix II.

It can be seen from the values of h_g, given in Table 6.23, for the 1 in bed tests and in Table 6.24 for the 2 in bed tests, that the coefficients showed the same characteristics as those of the Series 1 pellets in that they were independent of t, increased with G but decreased as Z increased.

Table 6.23

Values of h_g for 1 in Bed of Series 2 Pellets.

G	t				
	35	42·5	50	50	60
300	10·4	9·4	10·6	10·6	11·4
390	10·5	10·4	12·0	10·6	10·5
450	13·4	12·0	13·0	12·5	12·9
535	14·0	13·8	13·7	14·2	15·1
630	16·7	14·5	16·6	15·6	16·0
720	17·4	16·2	17·7	17·6	18·6
785	18·1	17·0	18·3	20·2	19·0
875	20·7	18·6	21·4	20·8	

Table 6.24

Values of h_g for 2 in Bed of Series 2 Pellets.

G	t	
	50	60
300	6·57	7·29
390	9·42	8·35
450	9·81	8·51
535	11·2	10·6
630	11·1	11·1
720	13·7	10·9
785	15·4	13·9
875	17·0	15·1

Variation of h_g with G.

The effect of air rate on the coefficients was determined as described in Section 6.1.2. The values of constants a_2 and b_2 of Equation (6.2) are given in Table 6.25 and show that the effect of G on h_g depended on the level of Z.

Table 6.25

Values of a_2 and b_2 for Series 2 Pellets.

Z	a_2	b_2
1	0·232	0·66
2	0·108	0·73

Variation of h_g with Z.

As mentioned in Section 6.1.2, the reductions in the values of h_g in the 2 in bed tests were produced by errors in the driving forces used in the calculations of the coefficients. The values of h_g, which were modified for the bed depth effect as described in Appendix III, are given in Table 6.26.

Table 6.26

Values of h'_g Modified for Bed Depth.

G	t	
	50	60
300	10·6	11·1
390	11·3	10·7
450	12·9	12·2
535	14·1	14·7
630	15·6	14·4
720	16·6	15·8
785	18·4	17·5
875	20·5	

The modified coefficients were related to the air rate by the equation:

$$h'_g = 0{\cdot}394\ G^{0{\cdot}57}$$

Although the values of h'_g appeared to be similar to those of h_g obtained in the 1 in bed tests, an analysis of variance was carried out to find out if a difference existed between the regressions relating the air rate and coefficients at each bed depth. The results of the analysis given in Table 6.27 indicate that there was no significant difference between the values of b_2. Furthermore, the mean values of the coefficients for the 1 in and 2 in bed depths were almost identical being 14·9 Chu/h ft^2 ^oC and 15·1 Chu/h ft^2 ^oC respectively. Hence the coefficients were independent of the bed depth and may therefore be grouped together to give the general expression:

$$h'_g = 0{\cdot}264\ G^{0{\cdot}64}$$

The correlation is shown in Fig. 6.8.

FIG 6.8

EFFECT OF AIR RATE ON HEAT TRANSFER COEFFICIENT FOR SERIES 2 PELLETS.

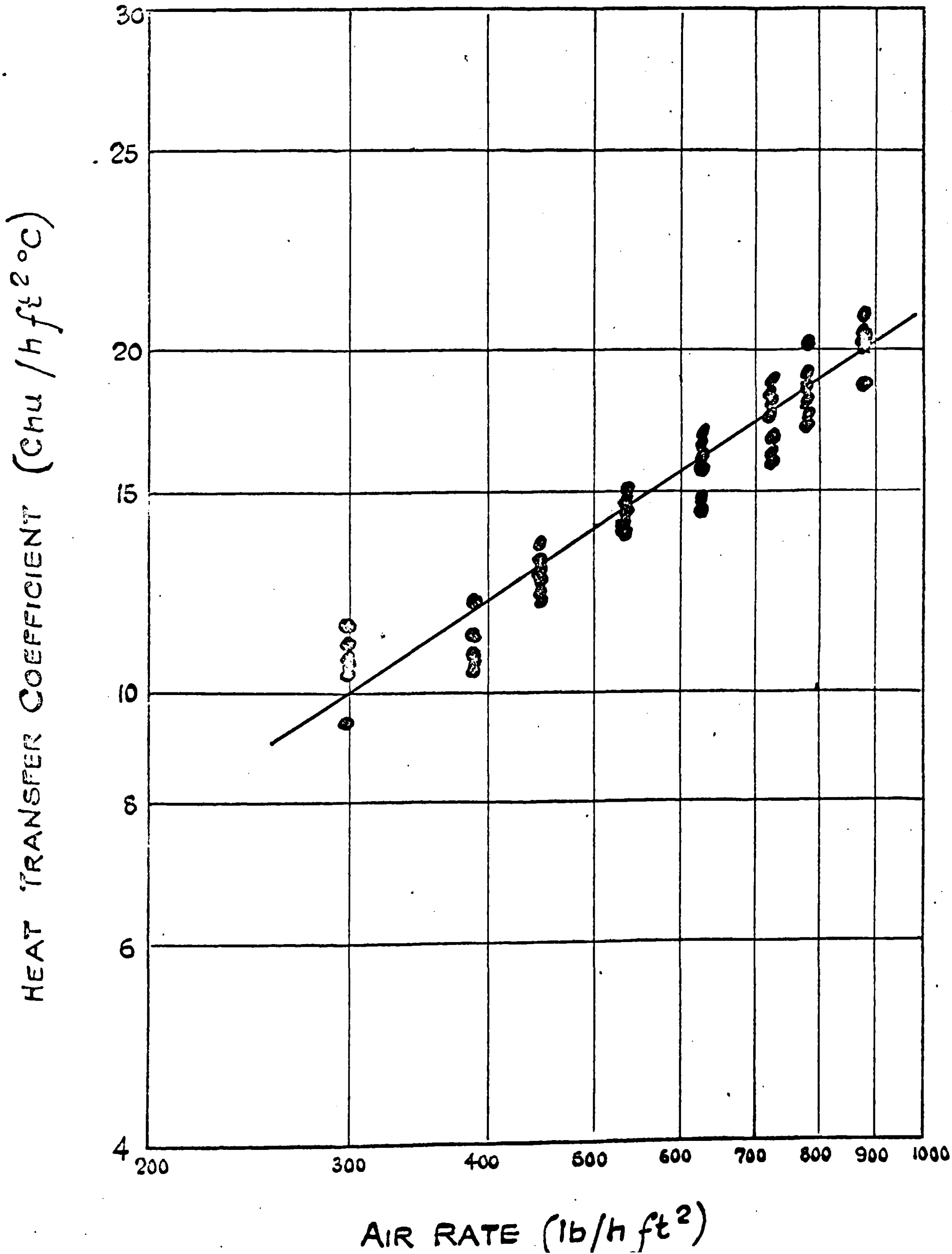

Table 6.27

Analysis of Variance for Testing Differences in Value of b_2 for Series 2 Pellets.

Source of Variance	Degrees of Freedom	Sum of Squares	Mean Sum of Squares
Combined Regression	1	0·475801	0·475801
Difference of Regression	1	0·001570	0·001570
Combined Residual	50	0·037359	0·000747
Total within groups	52	0·514730	

F ratio = 2·10

Value of F for significance at 5% level of probability = 4·0

$\underline{k_g}$

Values of k_g calculated from the tests with the Series 2 pellets are given in Table 6.28 and 6.29.

Table 6.28

Values of k_g for the 1 in Bed of Series 2 Pellets.

G	t				
	35	42.5	50	50	60
300	39·8	35·8	41·1	39·8	44·3
390	39·9	39·7	46·2	41·1	40·4
450	51·6	45·0	49·8	46·5	48·6
535	52·1	53·5	52·8	54·6	57·9
630	62·5	55·3	64·0	60·2	61·5
720	71·3	62·4	68·2	68·0	70·8
785	69·6	64·6	69·9	78·4	73·3
875	80·9	71·0	81·8	81·7	

Table 6.29

Values of k_g for the 2 in Bed of Series 2 Pellets.

G	t	
	50	60
300	25·1	27·9
390	38·0	32·9
450	35·8	32·3
535	42·8	40·6
630	42·5	42·8
720	52·2	41·5
785	59·0	53·2
875	63·6	57·3

A comparison of the values of h_g and k_g for the Series 2 pellets showed that k_g exhibited the same characteristics as h_g and that the ratio of h_g/k_g for each set of conditions was approximately constant, the average value being 0·260.

Effect of G on k_g.

The mass transfer coefficients calculated from the 1 in bed tests were correlated by the equation:

$$k_g = 0{\cdot}817\ G^{0{\cdot}67}$$

while those from the 2 in bed tests were correlated by the equation:

$$k_g = 0{\cdot}364\ G^{0{\cdot}75}$$

Effect of G on k_g.

The values of k_g for the 2 in bed tests, corrected for the bed depth effect by applying the same factor as was used in the modification of the corresponding values of h_g are given in Table 6.30 and were correlated with G by the equation:

$$k'_g = 1.57\ G^{0.56}$$

Table 6.30

Values of k'_g for the Series 2 Pellets.

G	t	
	50	60
300	40·7	42·6
390	44·0	41·3
450	49·0	47·5
535	53·7	56·2
630	59·5	55·2
720	63·3	59·0
785	70·0	67·2
875	79·5	

Since the values of h_g for the 1 in bed tests and h'_g for the 2 in bed tests were independent of bed depth, it may be assumed that the corresponding values of k_g and k'_g will behave similarly. Hence, these coefficients were grouped together and correlated with G to give the following relationship which is shown in Fig. 6.9:

$$k'_g = 0{\cdot}982\ G^{0{\cdot}64}$$

6.2.3 Heat and Mass Transfer Factors.

The values of j_h and j_d were derived as described in Appendix II.

j_h Factor.

Values of j_h are given in Table 6.31 for the 1 in bed tests and in Table 6.32 for the 2 in bed tests. The factors for the 2 in bed were calculated from the modified coefficients.

The j_h factors were independent of the bed depth and air inlet temperature but decreased as the air rate increased.

Table 6.31

Values of j_h for the 1 in Bed of Series 2 Pellets.

G	t				
	35	42·5	50	50	60
300	0·1181	0·1075	0·1211	0·120[illegible]	0·1301
390	0·0919	0·0913	0·1058	0·0916	0·0916
450	0·1025	0·0912	0·0988	0·0956	0·0981
535	0·0885	0·0875	0·0866	0·0900	0·0958
630	0·0905	0·0790	0·0904	0·0848	0·0868
720	0·0829	0·0771	0·0843	0·0838	0·0882
785	0·0784	0·0737	0·0795	0·0875	0·0827
875	0·0809	0·0726	0·0837	0·0813	

FIG 6.9

EFFECT OF AIR RATE ON MASS TRANSFER COEFFICIENT FOR SERIES 2 PELLETS

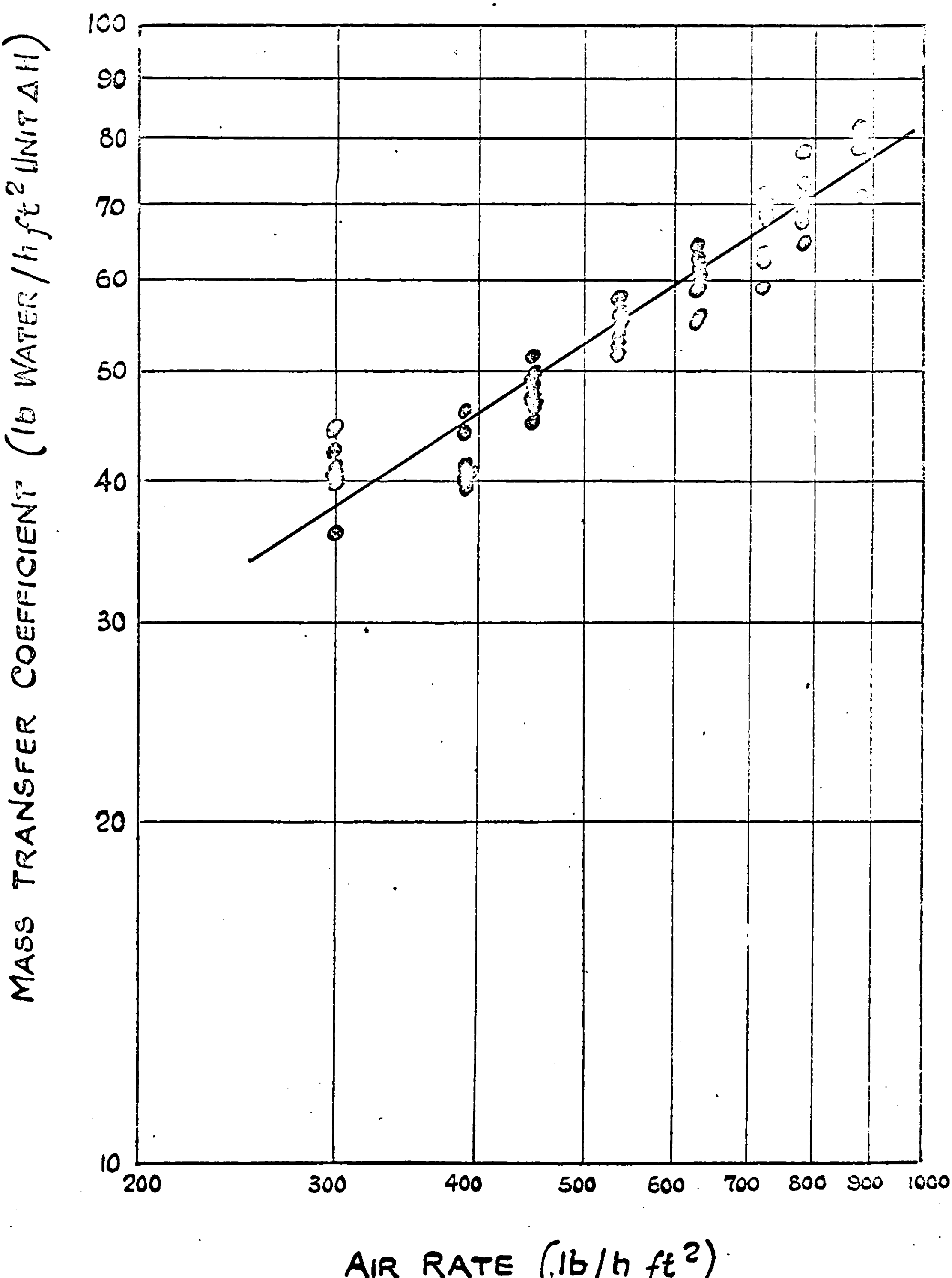

Table 6.32

Values of j_h for the 2 in Bed of Series 2 Pellets.

G	t	
	50	60
300	0·1211	0·1264
390	0·0944	0·0937
450	0·0983	0·0934
535	0·0892	0·0935
630	0·0847	0·0782
720	0·0792	0·0750
785	0·0799	0·0761
875	0·0802	

The general heat transfer relationship for this Series of pellets was obtained by correlating the values of j_h against the Reynolds number as described in Section 6.1.3. The resulting correlation shown in Fig. 6.10 was:

$$j_h = 1{\cdot}017\ Re^{-0{\cdot}37}$$

The average deviation of the experimental values of j_h from the above expression was 5·9%.

j_d Factor.

The values of j_d for the Series 2 pellets are shown in Tables 6.33 and 6.34. The factors given for the 2 in bed were calculated from the coefficients corrected for bed depth effect.

FIG 6.10

EFFECT OF REYNOLDS NO ON HEAT TRANSFER FACTOR FOR SERIES 2 PELLETS.

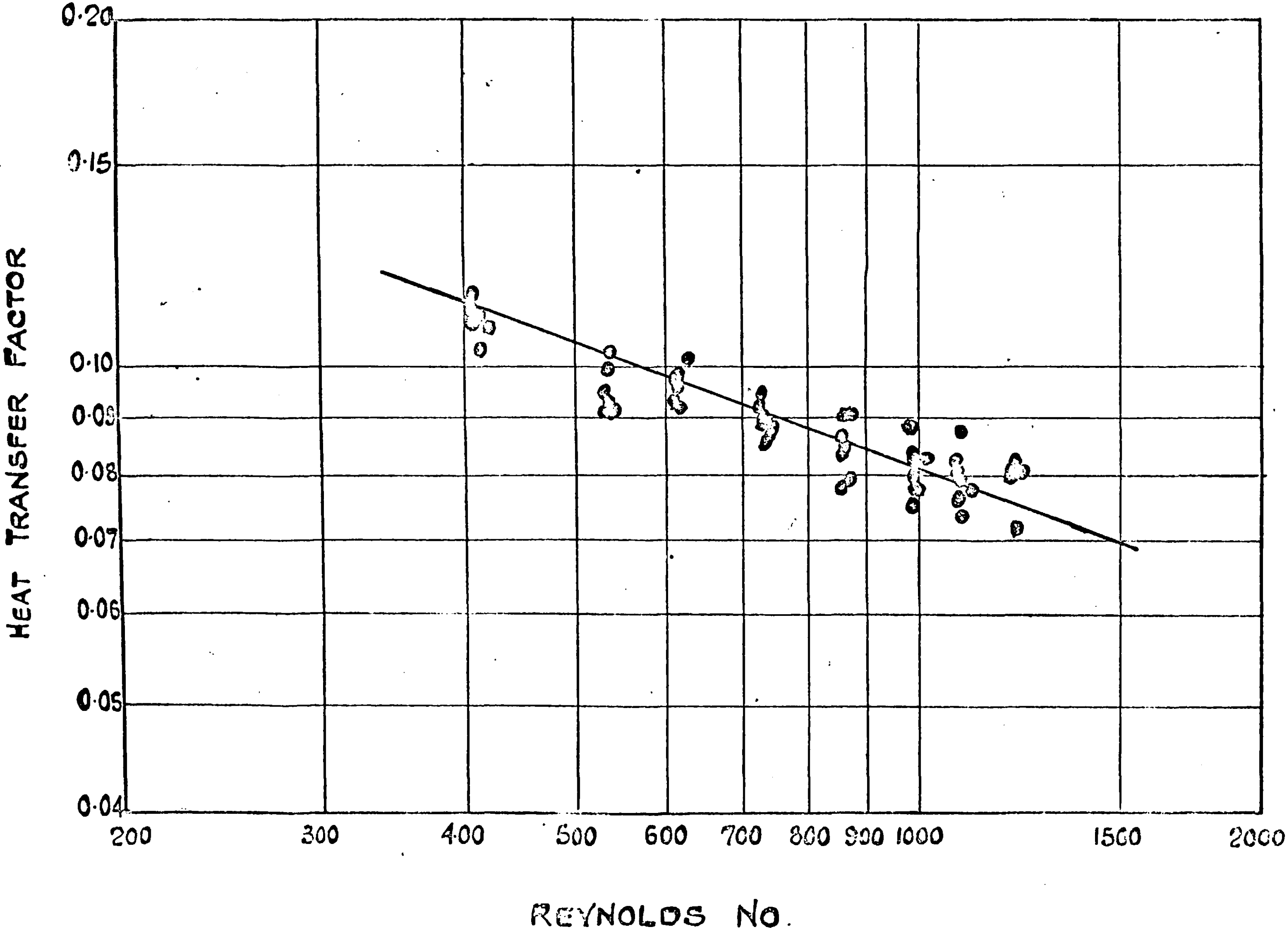

Table 6.33

Values of j_d for 1 in Bed of Series 2 Pellets.

G	t				
	35	42·5	50	50	60
300	0·0948	0·0852	0·0979	0·0950	0·1057
390	0·0731	0·0726	0·0847	0·0754	0·0742
450	0·0623	0·0717	0·0796	0·0743	0·0775
535	0·0694	0·0713	0·0705	0·0729	0·0773
630	0·0709	0·0628	0·0728	0·0685	0·0699
720	0·0708	0·0619	0·0678	0·0676	0·0705
785	0·0632	0·0586	0·0635	0·0715	0·0672
875	0·0660	0·0580	0·0668	0·0667	

Table 6.34

Values of j_d for 2 in Bed of Series 2 Pellets.

G	t	
	50	60
300	0·0971	0·1015
390	0·0807	0·0758
450	0·0782	0·0758
535	0·0716	0·0750
630	0·0676	0·0628
720	0·0630	0·0587
785	0·0636	0·0611
875	0·0648	

The j_d factors conformed to the same pattern as the j_h factors.

The value of the ratio j_h/j_d calculated from each set of drying conditions ranged from 1·17 to 1·28 the average value being 1·25.

The values of j_d were correlated with Re to give the following general mass transfer relationship for the Series 2 pellets:

$$j_d = 0{\cdot}783\ Re^{-0{\cdot}36}$$

The experimental values of j_d deviated by an average of 5·6% from the above correlation which is shown in Fig. 6.11.

FIG 6.11

EFFECT OF REYNOLDS No ON MASS TRANSFER FACTOR FOR SERIES 2 PELLETS.

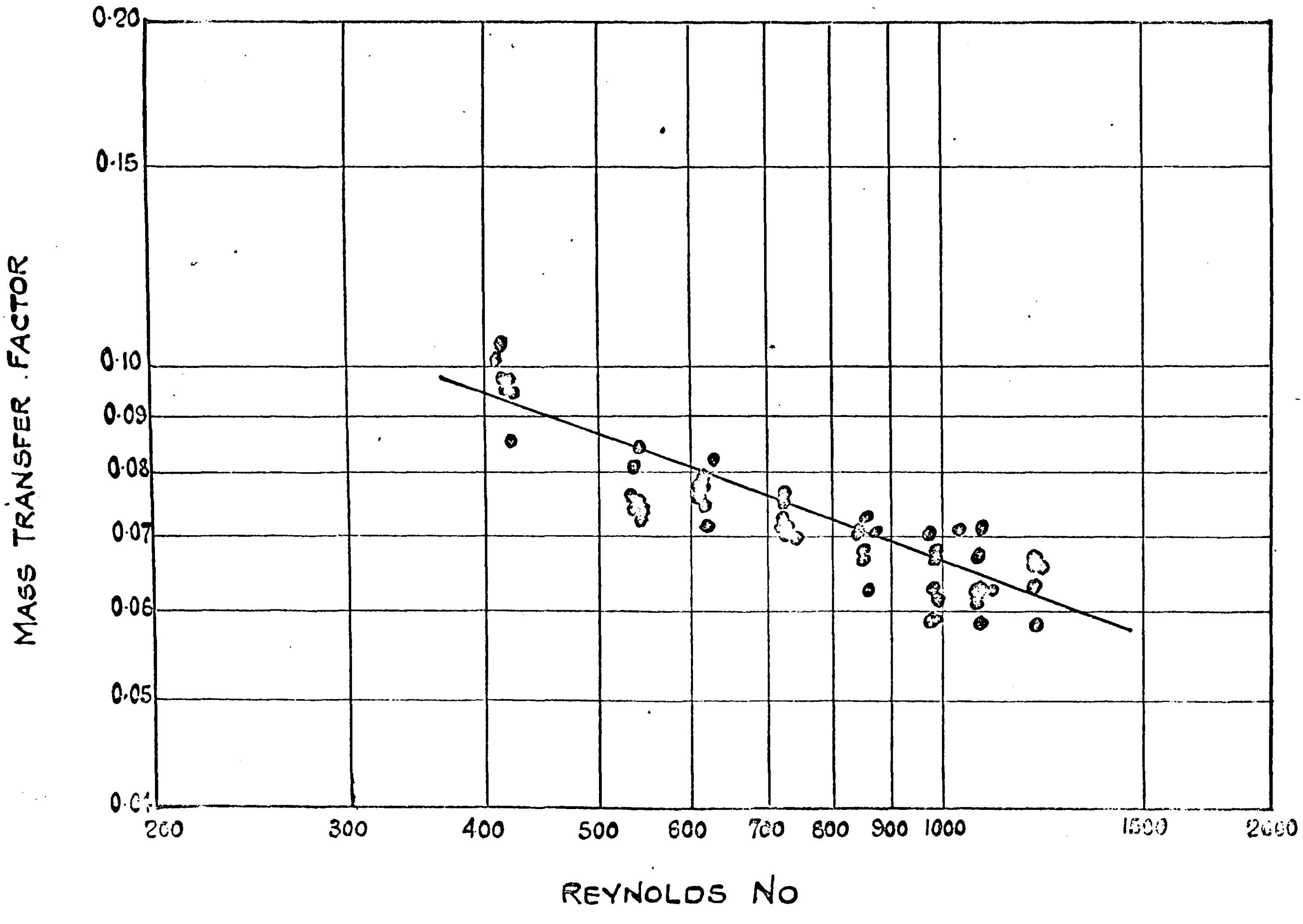

6.3 Series 3 Pellets.

The dimensions and physical properties of the pellets are given in Table 3.1 on page 34. Drying tests were carried out in the 12 in square basket using the following levels of W_B and t :

Table 6.35

Values of W_B and t for Series 3 Pellets.

W_B	t
3·78 (1 in layer)	35 42·5 50 60
5·80 (1·5 in layer)	50 60
7·86 (2 in layer)	60

The values of G used at each level of W_B and t are listed in Section 6.1. In the tests with the 1.5 in bed, the minimum level of t was restricted to 50°C as the air leaving the bed was approaching saturation at lower levels of t. For a similar reason, the value of t used in the tests with the 2 in bed was 60°C.

6.5.1 Constant Drying Rates.

The values of N_c', which were calculated from the experimental data as described in Section 5.4, are given for the 1 in bed of pellets in Table 6.36. Table 6.37 shows the rates obtained with the 1·5 in and 2 in beds.

Table 6.36

Values of N_c' for 1 in Bed of Series 3 Pellets.

G	t			
	35	42·5	50	60
300	0·542	0·561	0·772	0·868
390	0·619	0·735	0·881	1·093
450	0·733	0·839	1·011	1·209
535	0·841	1·008	1·156	1·500
630	0·934	1·135	1·378	1·667
720	1·098	1·262	1·569	1·832
785	1·146	1·304	1·728	1·986
875	1·294	1·489	1·810	2·155

Table 6.37

Values of N'_c for 1·5 in and 2 in Beds of Series 3 Pellets.

G	t		
	50	60	
	1·5 in bed	1·5 in bed	2 in bed
300	0·466	0·566	0·475
350	0·572	0·701	0·578
450	0·662	0·798	0·681
535	0·750	1·003	0·842
630	0·900	1·128	0·929
720	1·050	1·210	1·028
785	1·152	1·421	1·198
875	1·257	1·538	1·300

The results indicate that the values of N'_c followed the same pattern as those of the previous types of pellets.

Variation of N'_c with G.

The relationship between N'_c and G was represented by the same equation (6.1) as was used for the results of the Series 1 and 2 pellets.

The constants a_1 and b_1 of the equation were calculated as described in Section 6.1.2, and are given in Table 6.38.

Table 6.38

Values of a_1 and b_1 for Series 3 Pellets.

Z	t	a_1	b_1
1	35	0·00467	0·83
	42·5	0·00371	0·88
	50	0·00561	0·85
	60	0·00680	0·85
			av. 0·85
1·5	50	0·00201	0·95
	60	0·00256	0·94
2	60	0·00205	0·95

The constant b_1 was independent of t but increased from an average value of 0·85 at the 1 in bed of 0·95 at the 2 in bed. The variation of N_c' with G is expressed graphically in Fig. 6.12.

6.3.2 Heat and Mass Transfer Coefficients.

The coefficients h_g and k_g were computed for each of the drying tests using the procedure described in Appendix II.

h_g Coefficient.

The values of h_g, given in Table 6.39 for the 1 in bed tests and in Table 6.40 for the 1·5 in and 2 in bed tests, show that whereas the coefficients were independent of the inlet air temperature, they increased with the air rate but

FIG 6.12

EFFECT OF AIR RATE ON CONSTANT DRYING RATE FOR SERIES 3 PELLETS.

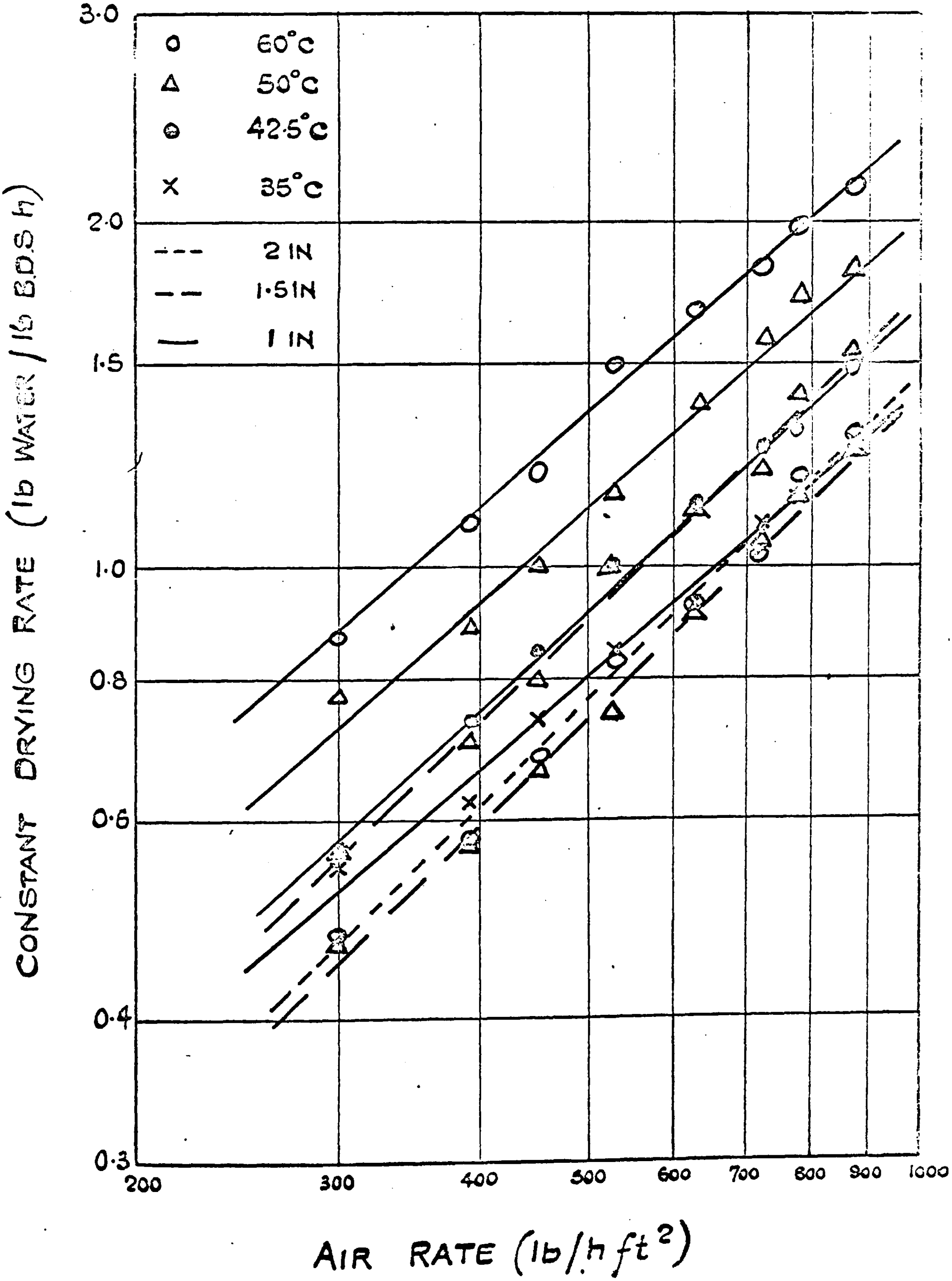

decreased as the bed depth increased. Similar trends were followed by the heat transfer coefficients derived from the tests carried out with the Series 1 and Series 2 pellets.

Table 6.39

Values of h_g for 1 in Bed of Series 3 Pellets.

G	t			
	35	42 5	50	60
300	10·8	9·75	11·3	11·4
390	12·4	12·1	12·7	12·9
450	13·6	14·8	14·8	13·2
535	15·8	16·1	15·2	16·1
630	18·3	18·0	19·0	18·7
720	19·7	18·7	20·6	19·1
785	21·1	19·4	22·8	19·7
875	21·8	21·5	23·1	19·9

Table 6.40

Values of h_g for 1·5 in and 2 in Beds of Series 3 Pellets.

G	t		
	50	60	
	1·5 in bed	1·5 in bed	2 in bed
300	7·20	6·95	5·60
390	8·15	8·40	6·52
450	9·23	9·75	7·43
535	11·3	12·2	8·45
630	13·1	12·8	9·82
720	14·0	13·6	11·6
785	15·1	15·1	12·1
875	17·2	17·5	12·8

Variation of h_g with G.

Because of their independence of t, the values of h_g at each level of G were grouped together and subjected with the values of G to regression analyses to give expressions of the form of equation (6.2). The values of the constants a_2 and b_2 in this equation obtained at each bed depth are given in Table 6.41.

Table 6.41

Values of a_2 and b_2 for Series 3 Pellets.

Z	a_2	b_2
1	0·223	0·68
1·5	0·069	0·81
2	0·062	0·82

Variation of h_g with Z.

The decrease in the value of h_g as the bed depth increased was also experienced by the coefficients evaluated from the experimental data obtained in the tests with the Series 1 and Series 2 pellets. However, when the thermal driving forces, used in the derivation of the coefficients for the tests carried out in the 1·5 in and 2 in beds of pellets, were corrected as described in Section 6.1.2, on page 45, it was found that the new coefficients were very similar to those obtained in the 1 in bed. The values of the modified coefficients, h'_g, are given in Table 6.42.

The modified coefficients were correlated with the air rate to give the following expression;

For the 1.5 in bed, $h'_g = 0·389\ G^{0·60}$

and for the 2 in bed, $h'_g = 0·280\ G^{0·65}$

Table 6.42

Values of h'_g for the 1·5 in and 2 in Beds of Series 3 Pellets.

G	t		
	50	60	
	1·5 in bed	1·5 in bed	2 in bed
300	11·6	11·5	11·0
390	14·8	13·9	13·6
450	15·5	14·9	15·9
535	17·0	16·8	16·2
630	18·8	18·9	18·8
720	20·3	21·0	19·9
785	20·3	21·2	21·3
875	22·9	21·5	22·5

Although the values of h'_g obtained in the 1·5 in and 2 in bed tests were similar to the values of h_g from the 1 in bed tests, the apparent independence of the coefficients on the bed depth was checked by determining whether the exponents of G, i.e. the values of b_2, obtained in the correlations of the coefficients at each bed depth varied significantly and by comparing the mean value of h_g at each bed depth. The differences between the exponents were tested by carrying out an Analysis of Variance as described in Appendix VIII. The results of the analysis, given in Table 6.43, indicated that there was no significant difference among the exponents.

Table 6.43

Analysis of Variance for Testing Differences in Values of b_2 for Series 3 Pellets.

Source of Variance	Degrees of freedom	Sum of squares	Mean sum of squares
Combined Regression	1	0·538828	0·538828
Difference of Regression	2	0·001898	0·000949
Combined Residual	50	0·018466	0·000369
Total within groups	53	0·559292	
F ratio = 2·6			
Value of F for significance at 5% level of probability = 3·2			

The mean values of the coefficients for each bed depth were very similar, being 16·3 Chu/h ft^2 °C for the 1 in bed, 17·2 Chu/h ft^2 °C for the 1·5 in bed and 17·0 Chu/h ft^2 °C for the 2 in bed. Hence the coefficients were independent of the depth of the pellet bed and were, consequently, grouped together and correlated with the air rate to give the following relationship, which is shown in Fig. 6.15:

$$h'_g = 0{\cdot}270\ G^{0{\cdot}65}$$

k_g Coefficient.

The values of k_g are given in Table 6.44 for the drying tests conducted in the 1 in bed while the coefficients obtained in the 1·5 in and 2 in bed tests are listed in Table 6.45.

FIG 6.13

EFFECT OF AIR RATE ON HEAT TRANSFER COEFFICIENT FOR SERIES 3 PELLETS.

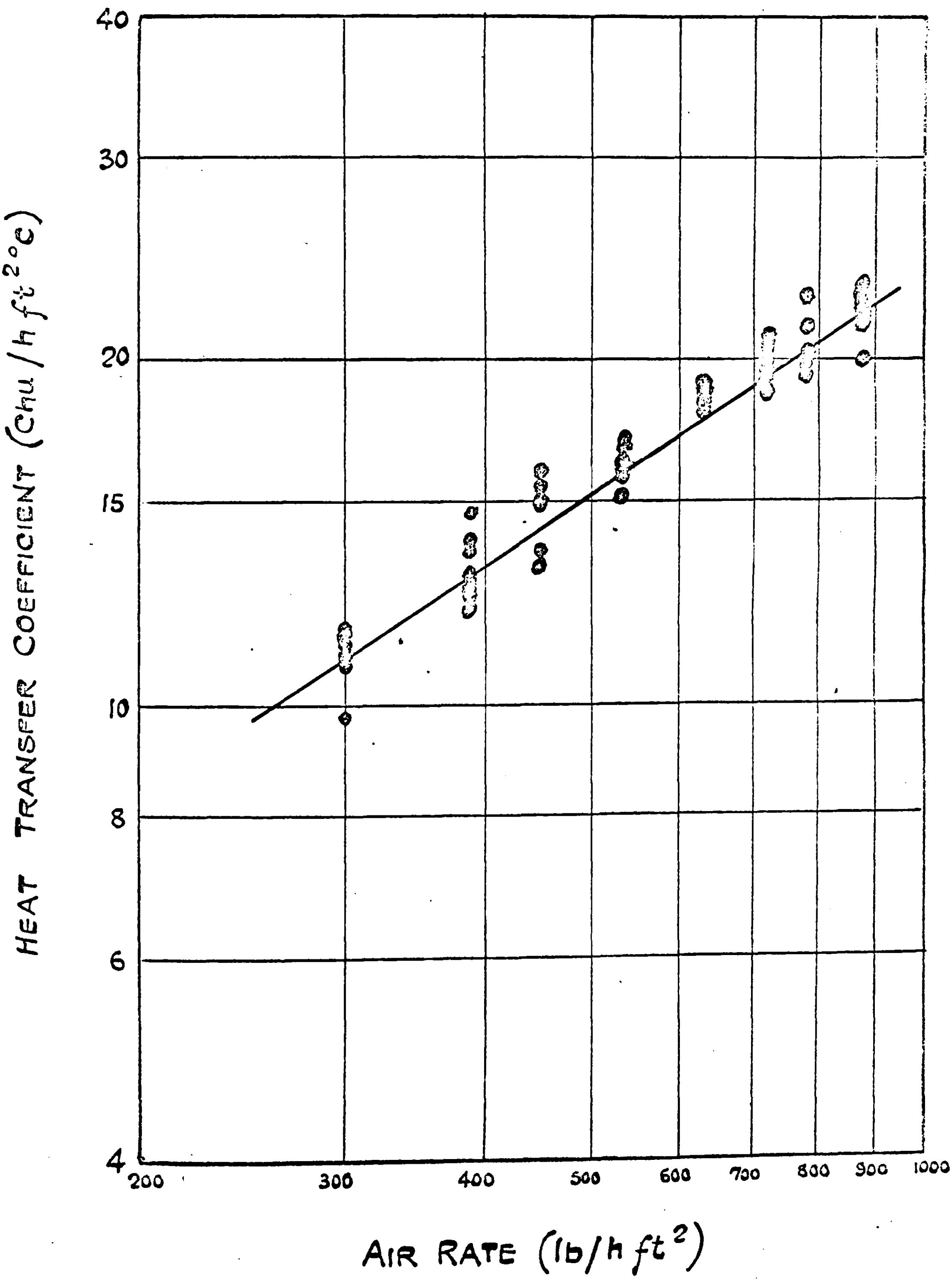

Table 6.44

Values of k_g for 1 in Bed of Series 3 Pellets.

G	t			
	35	42·5	50	60
300	41·5	37·5	43·9	42·2
390	48·2	47·2	49·1	49·2
450	52·8	56·0	56·7	50·1
535	60·5	62·3	58·5	61·6
630	70·5	69·9	72·6	71·5
720	75·4	72·0	79·7	74·0
785	81·3	72·6	88·7	76·5
875	83·7	82·9	89·8	76·7

Table 6.45

Values of k_g for 1·5 in and 2 in Beds of Series 3 Pellets.

G	t		
	50	60	
	1·5 in bed	1·5 in bed	2 in bed
300	29·0	26·6	21·8
390	31·5	32·4	25·4
450	35·1	38·2	28·7
535	44·2	46·7	32·4
630	51·0	49·4	38·5
720	53·8	52·6	44·6
785	57·9	58·7	47·6
875	66·9	67·5	49·7

The direct relationship, between the heat and mass transfer coefficients obtained with the Series 1 and Series 2 pellets, existed also between the coefficients derived from the tests with the Series 3 pellets so that the values of k_g behaved similarly to those of h_g. In these tests, the average value of the ratio h_g/k_g was 0·260.

Variation of k_g with G.

The variation of the mass transfer coefficients with the air rate was studied by grouping together the coefficients at each bed depth and correlating the grouped data with the values of G in the form of equation (6.3). The values of the constants a_3 and b_3 for each bed depth are given in Table 6.46.

Table 6.46

Values of a_3 and b_3 for Series 3 Pellets.

Z	a_3	b_3
1	0·821	0·69
1·5	0·251	0·82
2	0·195	0·82

Variation of k_g with z.

The mass transfer coefficients in the deeper beds were corrected for the error in the driving force used in the derivation of the coefficients, by applying the same factor as that used in the modification of the corresponding heat transfer coefficients. Consequently at each set of conditions, the ratio of the modified coefficients, h'_g/k'_g was identical to that of the original coefficients. The values of k'_g for the 1·5 in and 2 in beds are given in Table 6.47.

Table 6.47

Values of k'_g for the 1·5 in and 2 in Beds of Series 3 Pellets.

G	t		
	50	60	
	1·5 in bed	1·5 in bed	2 in bed
300	44·9	44·0	38·9
390	56·9	53·8	53·0
450	58·7	58·6	61·4
535	66·0	64·6	61·9
630	73·1	72·2	73·9
720	77·7	80·9	77·0
785	77·6	82·7	83·1
875	87·7	82·9	87·5

The modified coefficients were correlated with the air rate to give the following relationships:

For the 1·5 in bed, $k'_g = 1{\cdot}50\ G^{0{\cdot}60}$

and for the 2 in bed, $k'_g = 0{\cdot}735\ G^{0{\cdot}71}$

As the values of h_g for the 1 in bed tests and of h'_g for the 1·5 in and 2 in bed tests were found to be independent of the bed depth, the corresponding values of k_g and k'_g were also assumed to be unaffected by the bed depth. Consequently, these mass transfer coefficients were grouped together and correlated with the air rate to give the expression:

$$k'_g = 0{\cdot}989\ G^{0{\cdot}66}$$

This is expressed graphically in Fig. 6.14.

6.3.3 Heat and Mass Transfer Factors.

The derivation of the values of j_h and j_d are described in Appendix II.

j_h Factor.

The heat transfer factors derived from the 1 in bed tests are given in Table 6.48 while Table 6.49 contains the factors calculated from the 1·5 in and 2 in bed tests.

FIG 6.14

EFFECT OF AIR RATE ON MASS TRANSFER COEFFICIENT FOR SERIES 3 PELLETS

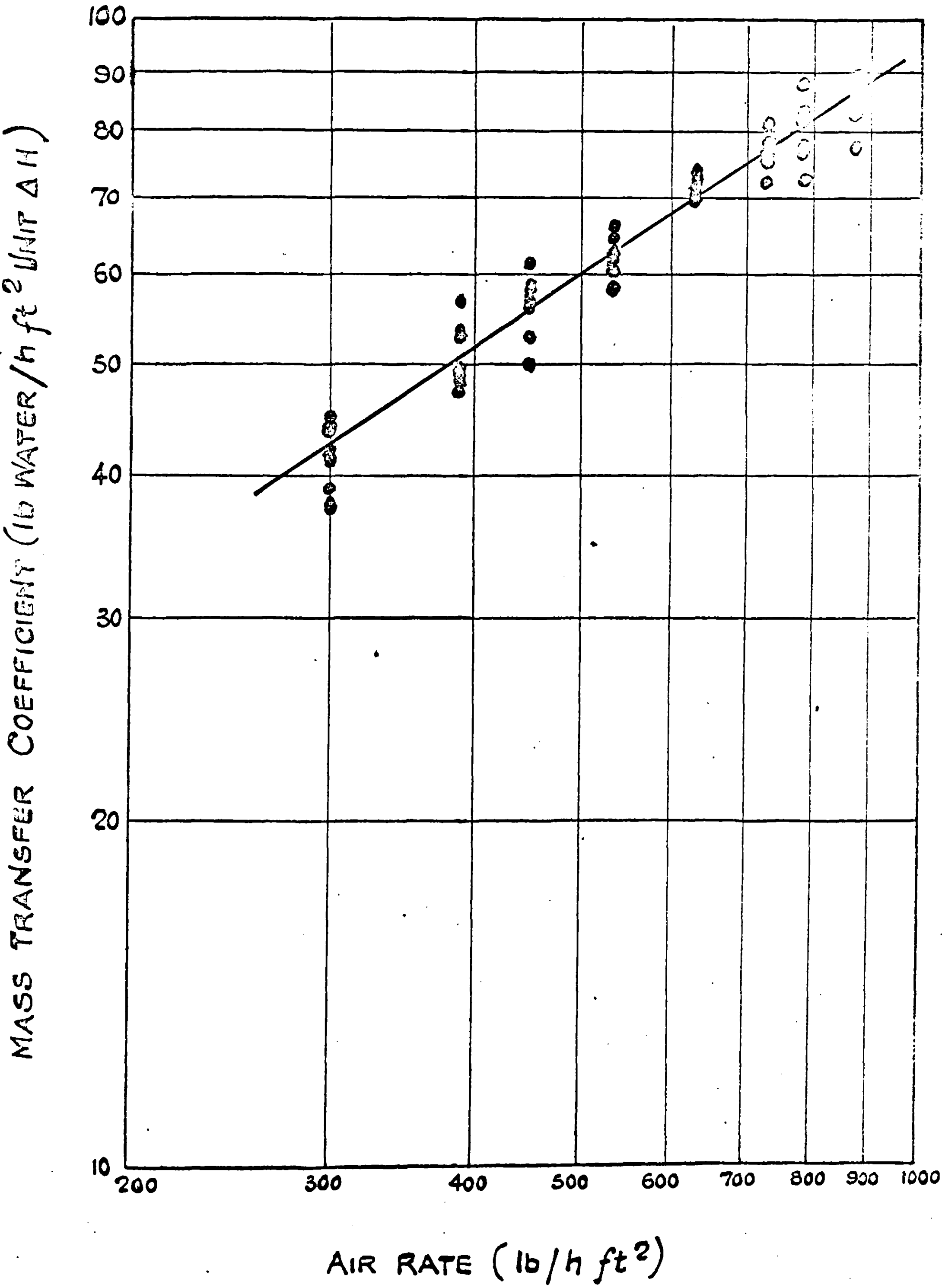

Table 6.48

Values of j_h for 1 in Bed of Series 3 Pellets.

G	t			
	35	42·5	50	60
300	0·1230	0·1106	0·1292	0·1298
390	0·1088	0·1064	0·1118	0·1134
450	0·1039	0·1132	0·1130	0·1008
535	0·1002	0·1020	0·0968	0·1021
630	0·0993	0·0975	0·1033	0·1016
720	0·0935	0·0887	0·0983	0·0907
785	0·0919	0·0844	0·0988	0·0854
875	0·0853	0·0838	0·0903	0·0771

Table 6.49

Values of j_h for 1·5 in and 2 in Beds of Series 3 Pellets.

G	t		
	50	60	
	1·5 in bed	1·5 in bed	2 in bed
300	0·1315	0·1310	0·1342
390	0·1293	0·1220	0·1193
450	0·1179	0·1159	0·1224
535	0·1082	0·1075	0·1031
630	0·1021	0·1017	0·1024
720	0·0965	0·0997	0·0949
785	0·0883	0·0923	0·0926
875	0·0895	0·0839	0·0822

The factors behaved similarly to the values h_g and h'_g which they were computed in that they were independent of the depth of the pellet bed and of the inlet air temperature. However, they differed from the heat transfer coefficients in that they decreased as the air rate increased whereas the coefficients increased with the air rate.

The general heat transfer relations for the Series 3 pellets was derived by correlating the values of j_h with the corresponding Reynolds numbers Re, as described in Section 6.1.3. The following general correlation which is shown in Fig. 6.15 was obtained:

$$j_h = 0.932 \, Re^{-0.36}$$

The average deviation of the experimental values of j_h from this correlation was 4.0%.

j_d Factor.

The values of j_d computed from the 1 in bed tests are shown in Table 6.50 while Table 6.51 contains the values of j_d derived from the 1.5 in and 2 in bed tests.

FIG 6.15

EFFECT OF REYNOLDS NO ON HEAT TRANSFER FACTOR FOR SERIES 3 PELLETS.

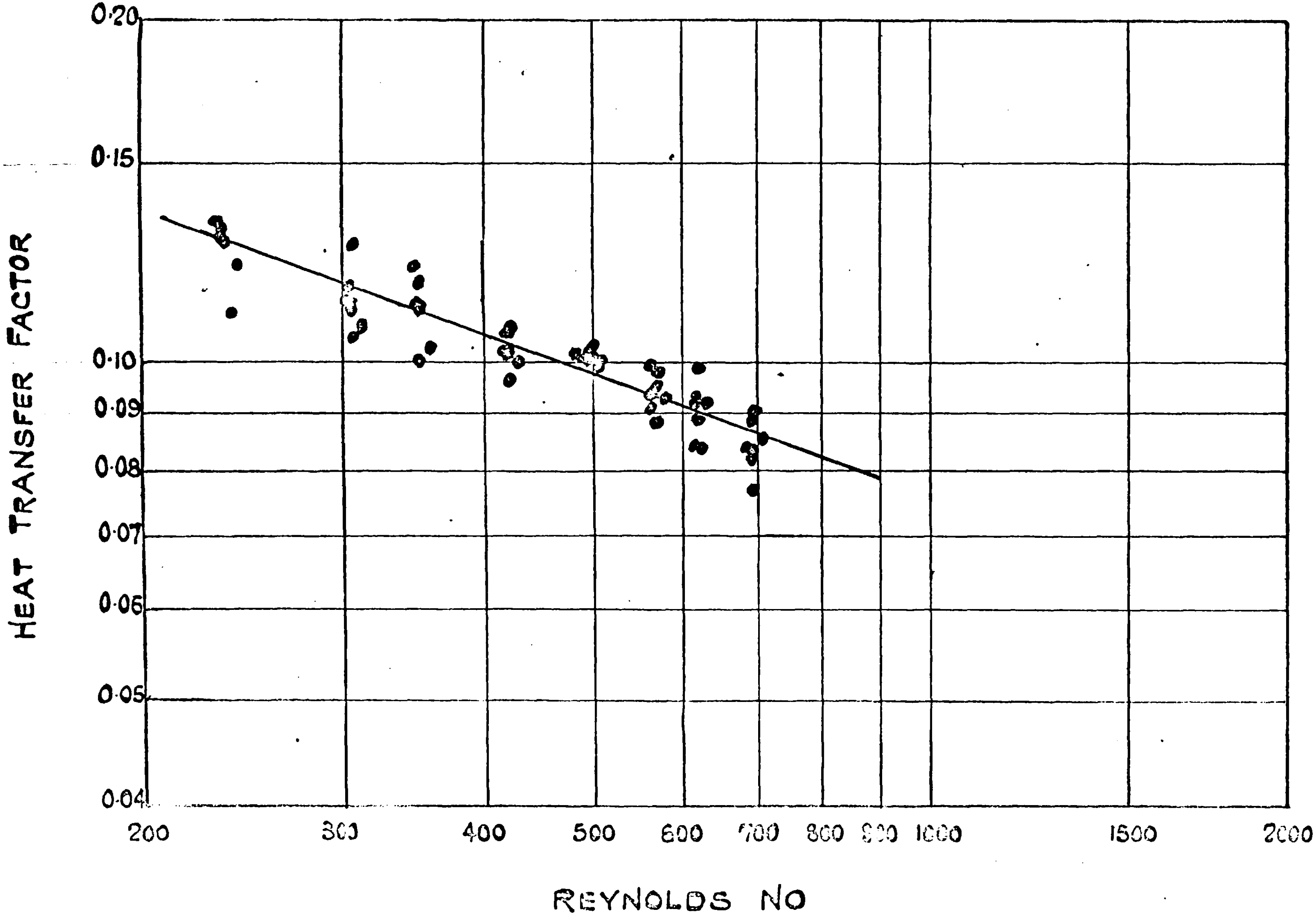

Table 6.50

Values of j_d for 1 in Beds of Series 3 Pellets.

G	t			
	25	42·5	50	60
300	0·0988	0·0892	0·1050	0·1030
390	0·0883	0·0865	0·0902	0·0900
450	0·0842	0·0891	0·0904	0·0800
535	0·0806	0·0829	0·0781	0·0823
630	0·0790	0·0793	0·0826	0·0813
720	0·0749	0·0715	0·0793	0·0737
785	0·0737	0·0659	0·0806	0·0694
875	0·0683	0·0676	0·0734	0·0627

Table 6.51

Values of j_d for 1·5 in and 2 in Beds of Series 3 Pellets.

G	t		
	50	60	
	1·5 in bed	1·5 in bed	2 in bed
300	0·1069	0·1048	0·1091
390	0·1043	0·0984	0·0970
450	0·0936	0·0934	0·0987
535	0·0880	0·0860	0·0825
630	0·0830	0·0820	0·0839
720	0·0772	0·0804	0·0765
785	0·0706	0·0750	0·0753
875	0·0716	0·0677	0·0688

The mass transfer factors showed the same characteristics as the heat transfer factors; namely, they were independent of the bed depth and air inlet temperature but decreased as the air rate increased.

The value of the ratio j_h/j_d, derived from each set of test conditions ranged from 1·22 to 1·28, the average value being 1·24.

The general mass transfer relationship for the Series 3 pellets was obtained by correlating the values of j_d with Re. The resulting correlation, which is shown in Fig. 6.16 may be expressed mathematically as:

$$j_d = 0{\cdot}742\ Re^{-0{\cdot}36}$$

The average deviation of the factors from the relationship was 4·2%.

FIG 6.16

EFFECT OF REYNOLDS NO ON MASS TRANSFER FACTOR FOR SERIES 3 PELLETS.

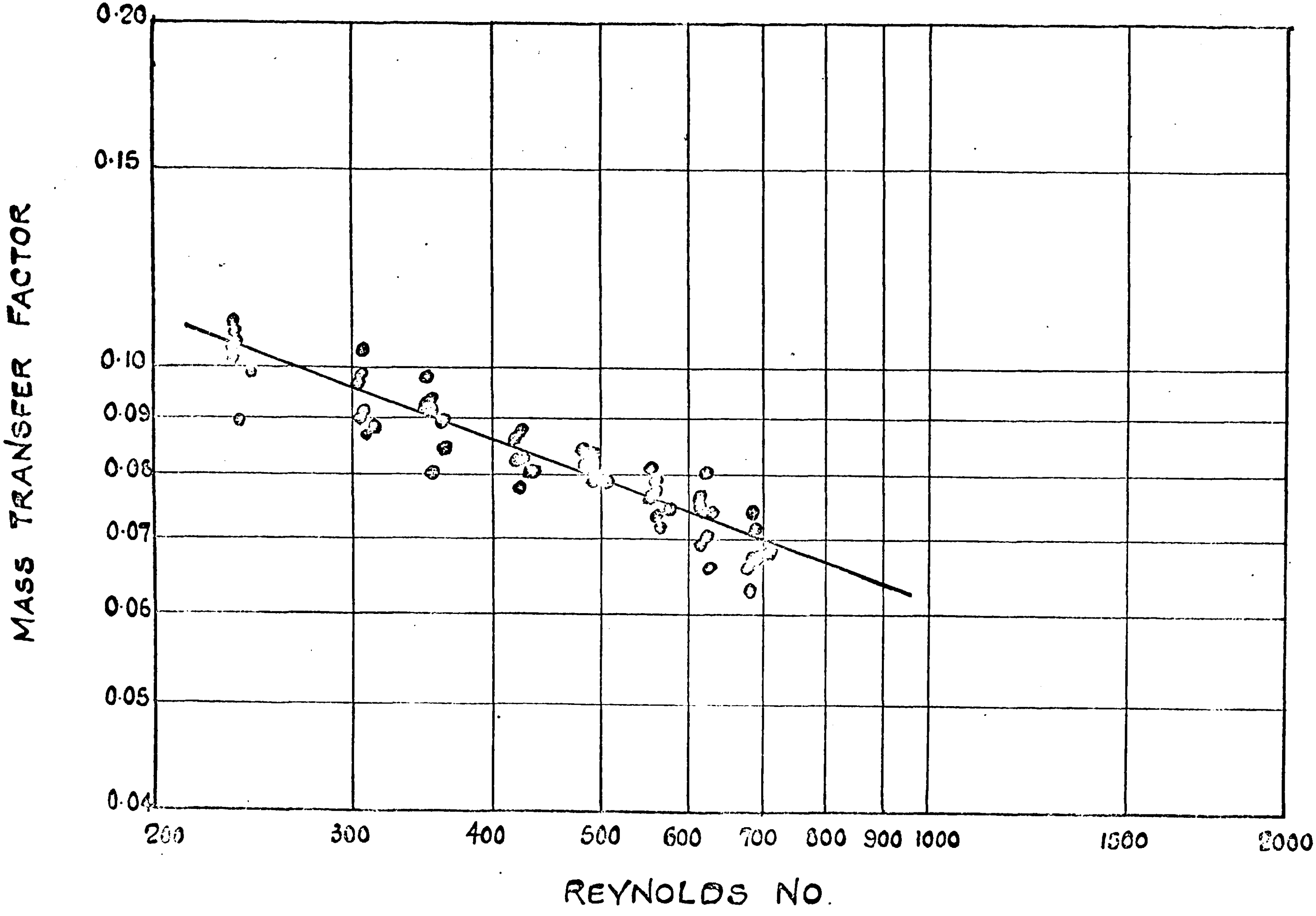

6.4 Series 4 Pellets.

The pellets, whose dimensions and physical properties are given in Table 5.1 on page 34, were the same diameter as the Series 1 pellets but were 0·210 in thick, compared with a thickness of 0·161 in for the Series 1 pellets.

In the tests which were carried out in the 12 in square basket, the values of w_B and t were as follows:

Table 6.52

Values of w_B and t for Series 4 Pellets.

w_B	t
2·5 (1 in layer)	35
	42·5
	50

The values of G used at each level of t are given in Section 6.1.

6.4.1 Constant Drying Rates.

The values of N'_c obtained in the 24 tests are given in Table 6.53. The derivation of these quantities is described in Section 5.4.

Table 6.53

Values of N_c' for 1 in Bed of Series 4 Pellets.

G	t		
	35	42·5	50
300	0·64	0·85	0·94
390	0·80	1·02	1·18
450	0·88	1·20	1·45
535	1·05	1·36	1·53
630	1·23	1·58	1·69
720	1·38	1·68	1·99
785	1·53	1·83	2·14
875	1·61	2·00	1·23

The length of the constant drying period in the tests covered a range similar to those of the other three series of pellets.

Variation of N_c' with G.

The effect of G on N_c' which is shown in Fig. 6.17 was expressed in the form of equation 6.1 as described in section 6.1. Values of a_1 and b_1 are given in Table 6.54 and show that the exponent b_1 was independent of the level af t.

FIG 6.17

EFFECT OF AIR RATE ON CONSTANT DRYING RATE FOR SERIES 4 PELLETS

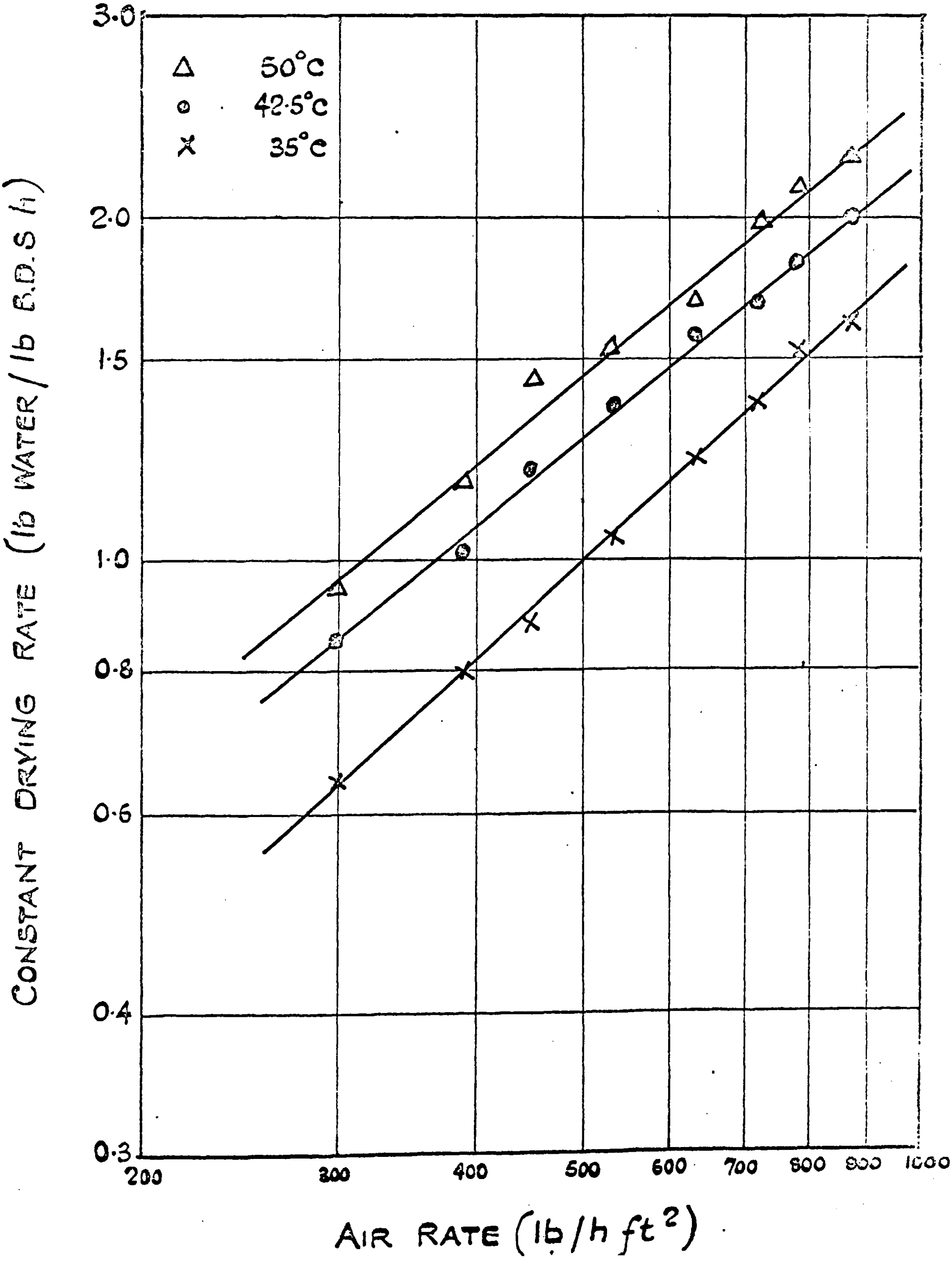

Table 6.54

Values of a_1 and b_1 for Series 4 Pellets.

	t		
	35	42·5	50
a_1	0·00392	0·00895	0·00981
b_1	0·89	0·80	0·81

6.4.2 Heat and Mass Transfer Coefficients.

The values of h_g and k_g, calculated as described in Appendix II are given in Tables 6.55 and 6.56. The coefficients showed the same characteristics as those obtained with the other Series of pellets:

(1) h_g and k_g were directly related, the average value of h_g/k_g for each set of operating conditions being 0·260

(2) h_g and k_g increased with G.

(3) h_g and k_g were independent of t; (the lower values obtained in the tests with an inlet air temperature of 50°C, were caused by an increase of approximately 15% in the humidity of the inlet air in these tests).

Table 6.55

Values of h_g for 1 in Bed of Series 4 Pellets.

G	t		
	35	42.5	50
300	12.3	11.9	10.0
390	13.2	12.2	11.6
450	14.3	14.9	13.1
535	15.9	15.8	13.2
630	19.1	18.2	15.5
720	19.2	18.8	18.2
785	20.4	20.3	18.9
875	21.5	21.9	19.1

Table 6.56

Values of k_g for 1 in Bed of Series 4 Pellets.

G	t		
	35	42.5	50
300	48.2	45.6	38.4
390	51.2	46.9	44.7
450	54.6	57.6	50.2
535	61.0	60.8	50.9
630	73.0	70.1	59.0
720	73.8	68.7	69.7
785	79.0	74.9	72.9
875	82.8	84.3	72.9

Effect of G on h_g and k_g.

The relationship between h_g and G was investigated further by grouping all the h_g values together and subjecting them to a regression analysis to give the expression:

$$h_g = 0{\cdot}384\ G^{0{\cdot}60}$$

The corresponding expression relating to k_g to G was:

$$k_g = 1{\cdot}47\ G^{0{\cdot}59}$$

These expressions are shown in Fig. 6.18 and 6.19.

6.4.3 Heat and Mass Transfer Factors.

The values of j_h and j_d, shown in Tables 6.57 and 6.58 were calculated as described in Appendix II. The average value of the ratio j_h/j_d was 1·24.

Table 6.57

Values of j_h for 1 in Bed of Series 4 Pellets.

G	t		
	35	42·5	50
300	0·1395	0·1357	0·1137
390	0·1157	0·1065	0·1016
450	0·1089	0·1140	0·0993
535	0·1007	0·1000	0·0837
630	0·1035	0·0977	0·0841
720	0·0913	0·0892	0·0865
785	0·0884	0·0883	0·0819
875	0·0840	0·0853	0·0746

FIG 18

EFFECT OF AIR RATE ON HEAT TRANSFER COEFFICIENT
FOR SERIES 4 PELLETS.

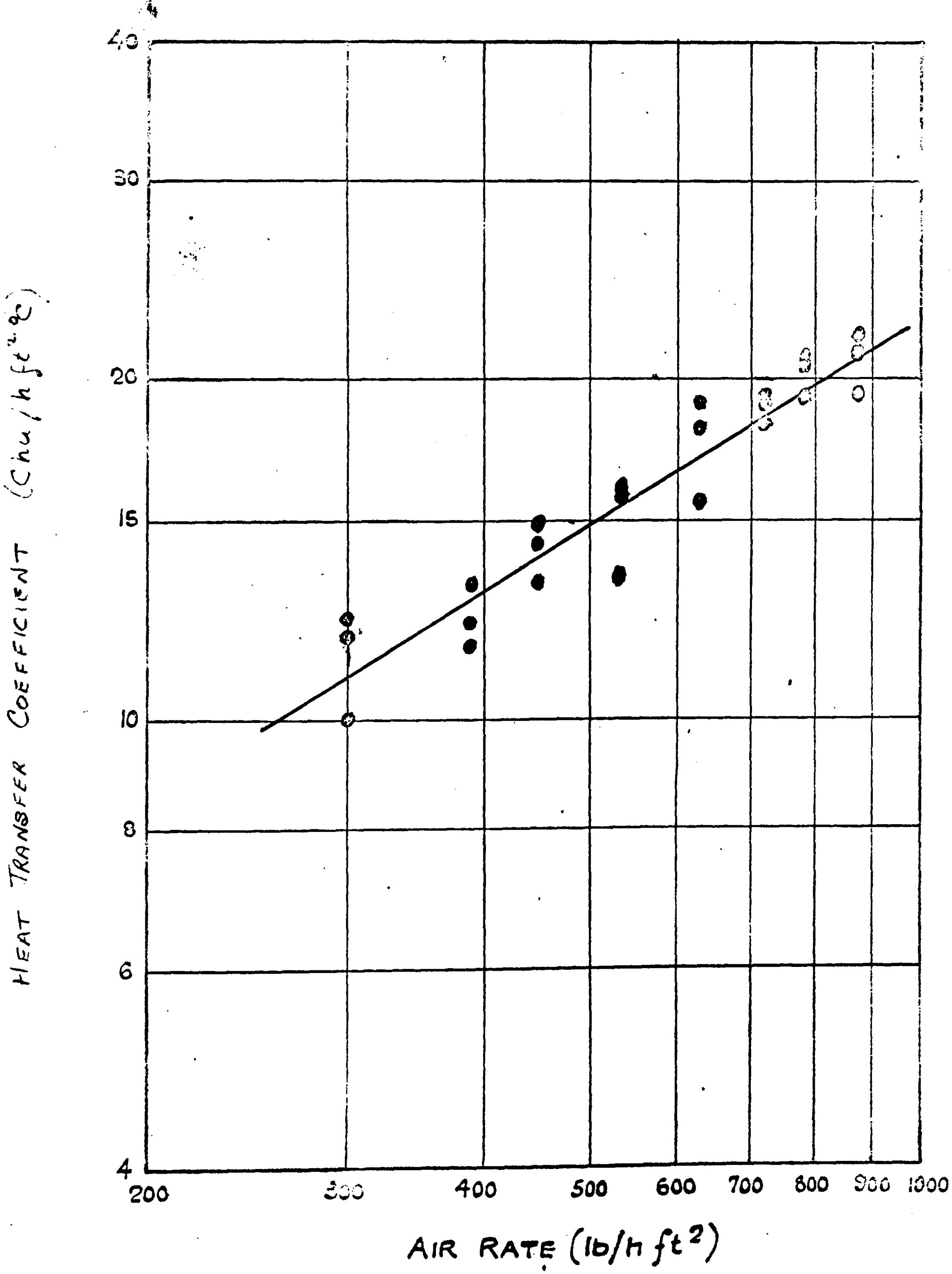

FIG 19

EFFECT OF AIR RATE ON MASS TRANSFER COEFFICIENT
FOR SERIES 4 PELLETS.

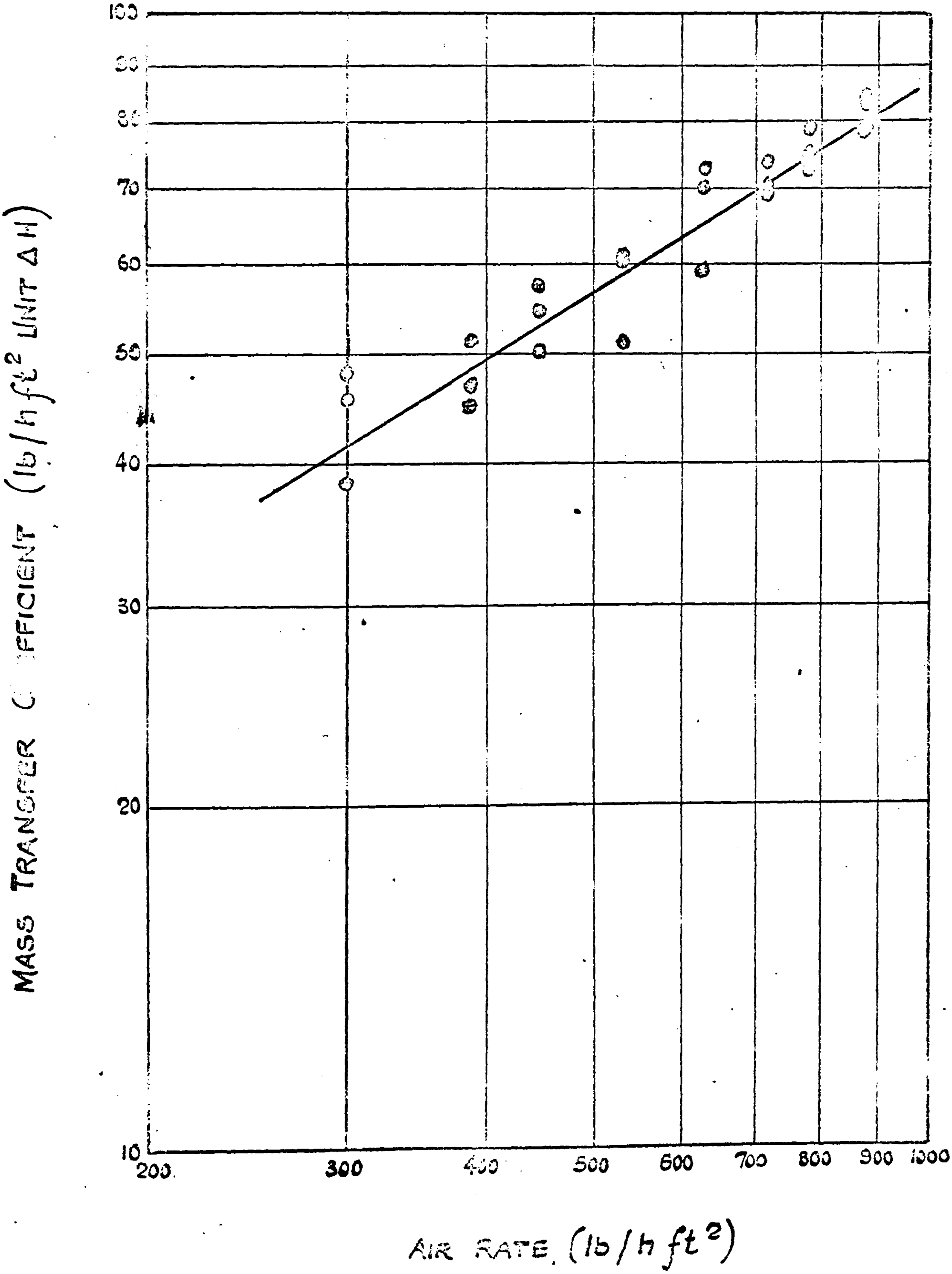

Table 6.58

Values of j_d for 1 in Bed of Series 4 Pellets.

G	t		
	35	42·5	50
300	0·1148	0·1086	0·0915
390	0·0936	0·0858	0·0819
450	0·0870	0·0917	0·0801
535	0·0812	0·0810	0·0679
630	0·0829	0·0796	0·0674
720	0·0733	0·0687	0·0693
785	0·0717	0·0686	0·0662
875	0·0676	0·0688	0·0596

The transfer factors behaved in a similar fashion to those obtained with the other types of pellets in that they were independent of the air inlet temperature but decreased as the air rate increased.

The general heat and mass transfer relationships for this type of pellet were determined as described in Section 6.1.3. The relationships, which are shown in Fig. 6.20 and 6.21 may be expressed as:

$$j_h = 1.242\ Re^{-0.39}$$

and $$j_d = 1.114\ Re^{-0.41}$$

The experimental values of j_h and j_d deviated on average from the respective correlations by 6·0% and 7·0%.

FIG 6. 20

EFFECT OF REYNOLDS NO ON HEAT TRANSFER FACTOR FOR SERIES 4 PELLETS.

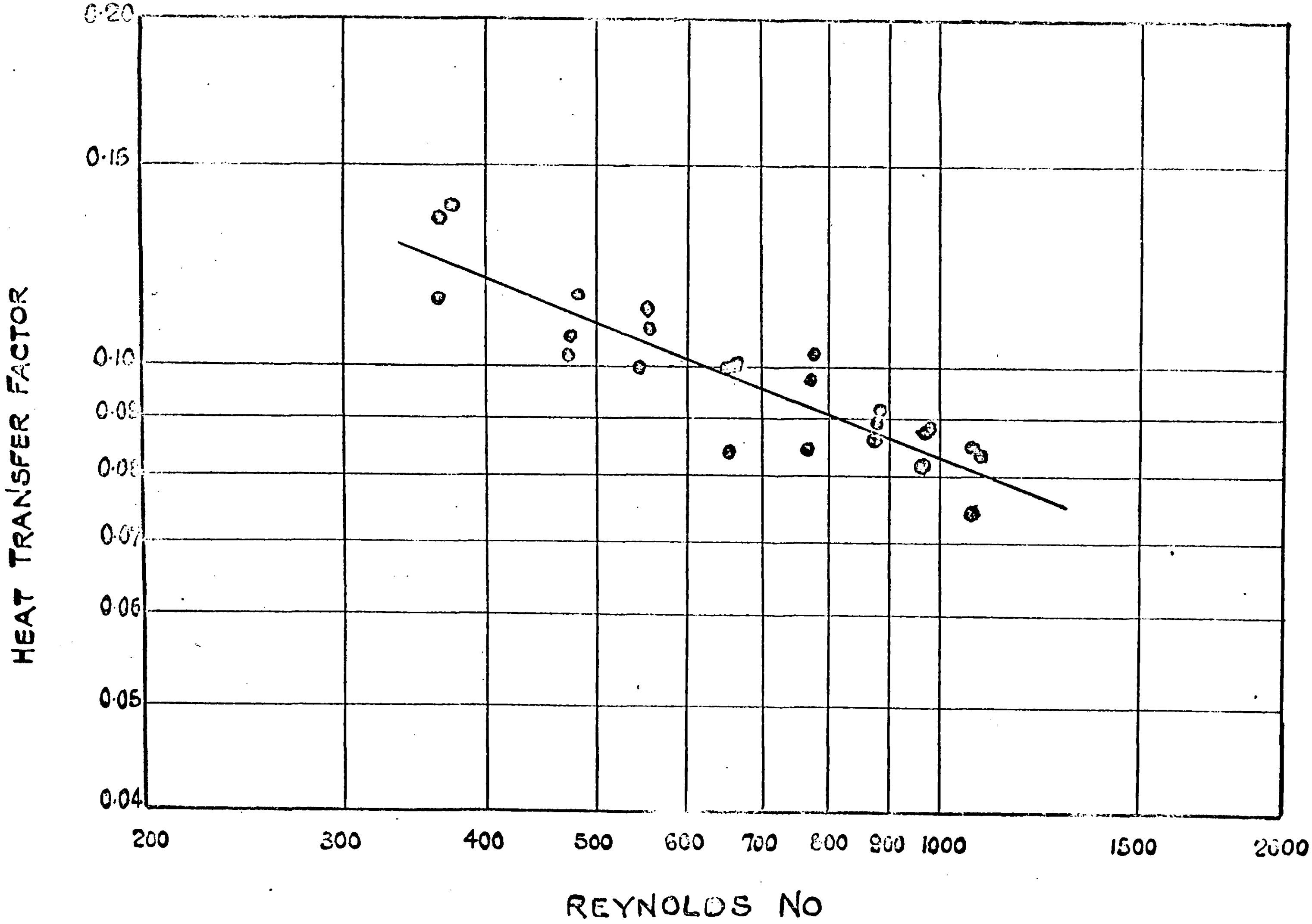

FIG 6.21

EFFECT OF REYNOLDS NO ON MASS TRANSFER FACTOR FOR SERIES 4 PELLETS.

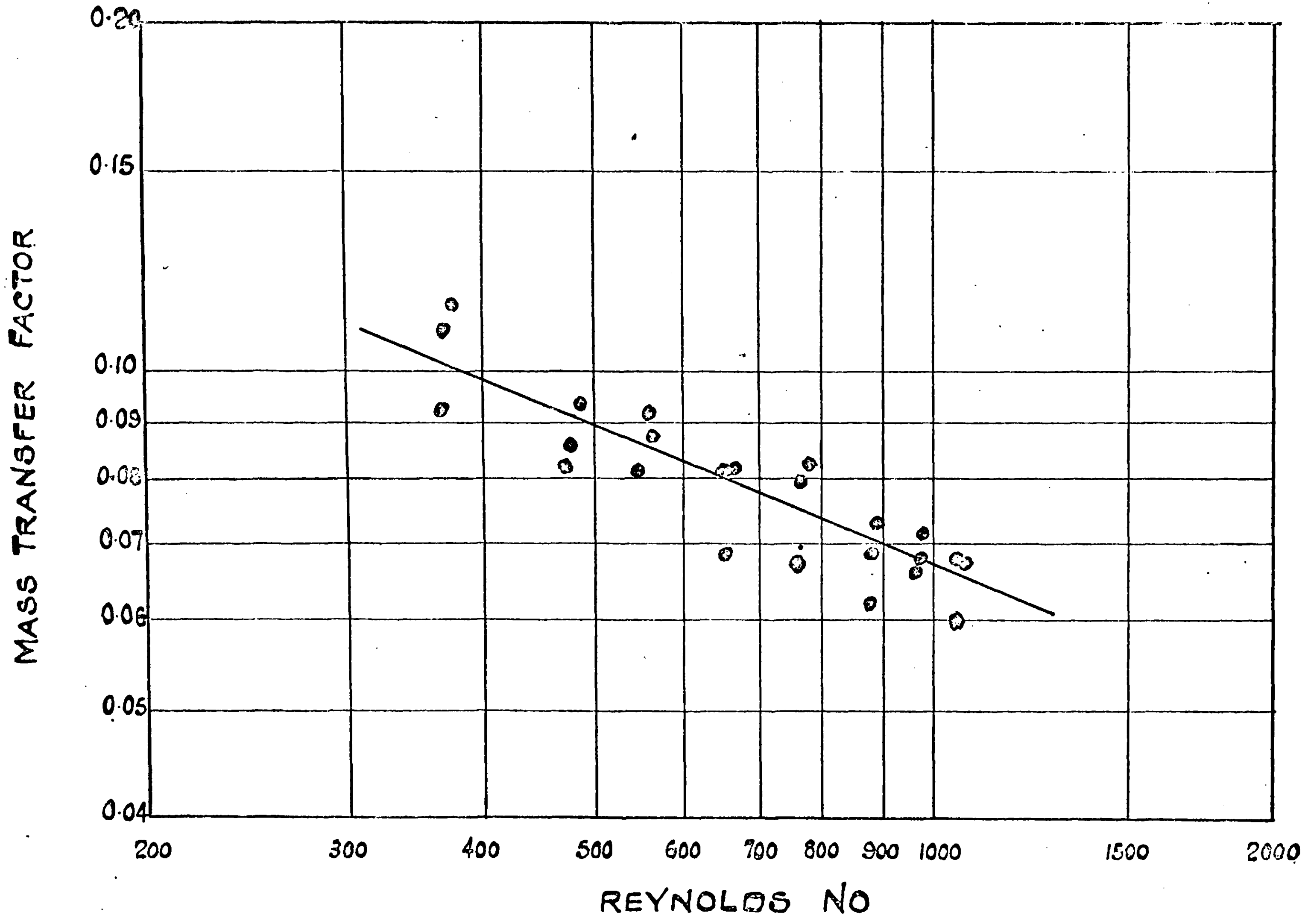

6.5 Comparison of Transfer Relationships.

The heat transfer relationships derived from the tests carried out with the four pellet sizes were:

Series 1	j_h	=	$0{\cdot}729\ Re^{-0{\cdot}32}$
Series 2	j_h	=	$1{\cdot}017\ Re^{-0{\cdot}37}$
Series 3	j_h	=	$0{\cdot}932\ Re^{-0{\cdot}36}$
Series 4	j_h	=	$1{\cdot}242\ Re^{-0{\cdot}39}$

Comparing the values of the exponent of the Reynolds numbers, it is apparent that, although the exponents range from -0·39 to -0·32, the values in the correlations for the smallest particles, (Series 3) and the largest particles (Series 2) are very similar, being -0·36 and -0·37 respectively and that the exponents for the intermediate pellet sizes, i.e. Series 1 and Series 4 pellets, lie on either side of these values. Hence it may be assumed that the exponent of the Reynolds number is independent of the size of particle.

Therefore, a simple comparison may be made by averaging the four exponents and using the mean exponent to recalculate each constant preceding the Reynolds number. The four correlations then become:

Series 1	j_h	=	$0{\cdot}896\ Re^{-0{\cdot}35}$
Series 2	j_h	=	$0{\cdot}940\ Re^{-0{\cdot}35}$
Series 3	j_h	=	$0{\cdot}862\ Re^{-0{\cdot}35}$
Series 4	j_h	=	$0{\cdot}982\ Re^{-0{\cdot}35}$

It can now be seen that the new correlation for the

Series 1 pellets is 4% greater than that for the Series 3 pellets but 5% less than the correlation for the Series 2 pellets. As these values are within the standard deviation of 6·2% of the original correlation for the Series 1 pellets, it is considered that the differences between the correlation for the Series 1 pellets and the correlations for the Series 2 and Series 3 pellets are due to experimental error.

Similarly, the difference between the correlations for the Series 2 and Series 4 pellets is within the standard deviation of either of the original correlations and consequently this difference may also be accounted for by the experimental variance.

Hence, it may be assumed that there are no significant differences between the four heat transfer relationships which may be combined to give the following general correlations with a standard deviation of 5·9%:

$$j_h = 0{\cdot}900\ Re^{-0{\cdot}35}$$

As the heat and mass transfer factors are directly related to each other, a similar procedure was followed in comparing the four mass transfer relationships which were combined to give the following correlation:

$$j_d = 0{\cdot}678\ Re^{-0{\cdot}34}$$

The standard deviation of the above expression was 6·1%. The overall correlations are shown in Fig. 6.22 and 6.23.

FIG 6.22

OVERALL HEAT TRANSFER CORRELATION

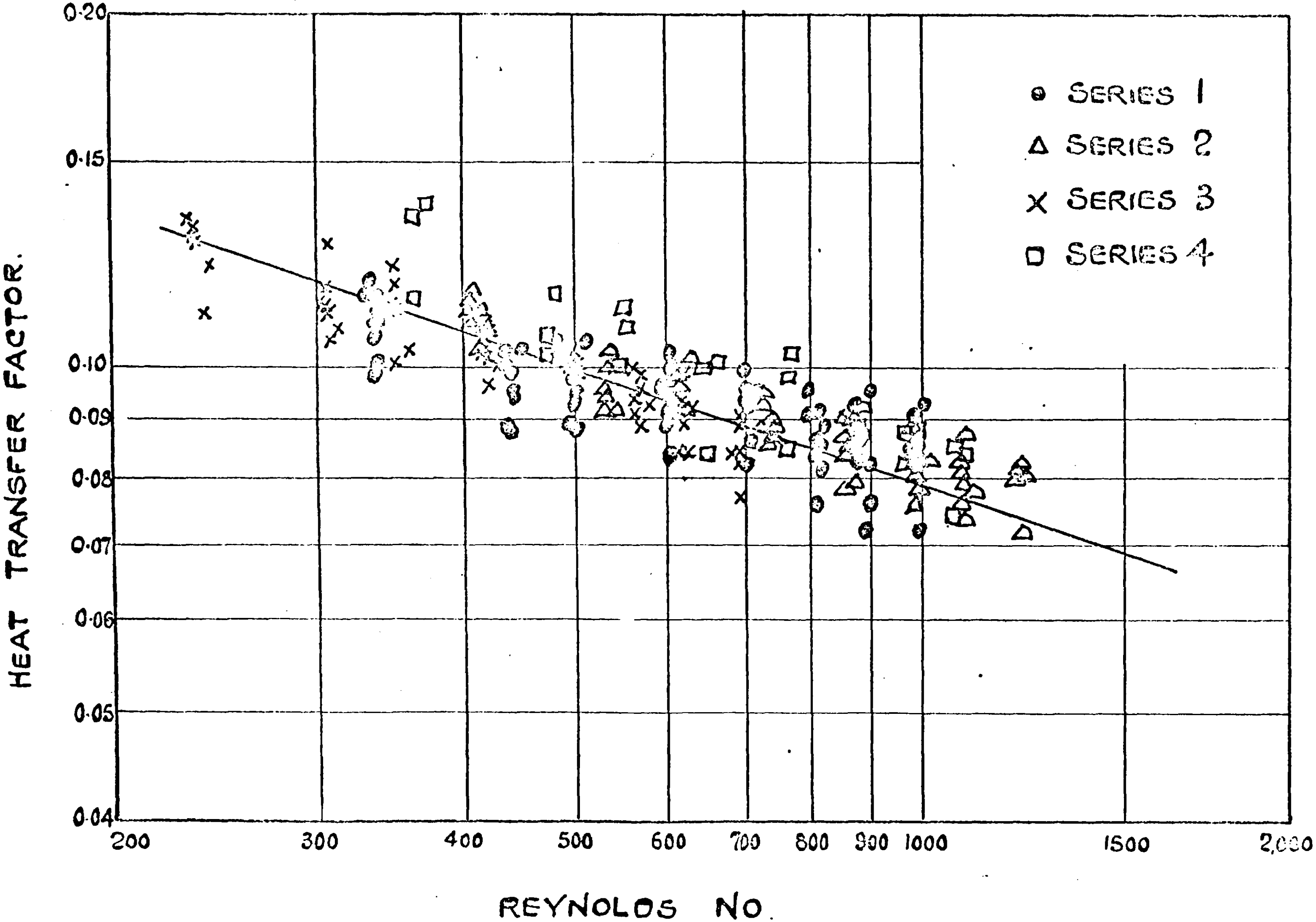

FIG 6.23

OVERALL MASS TRANSFER CORRELATION

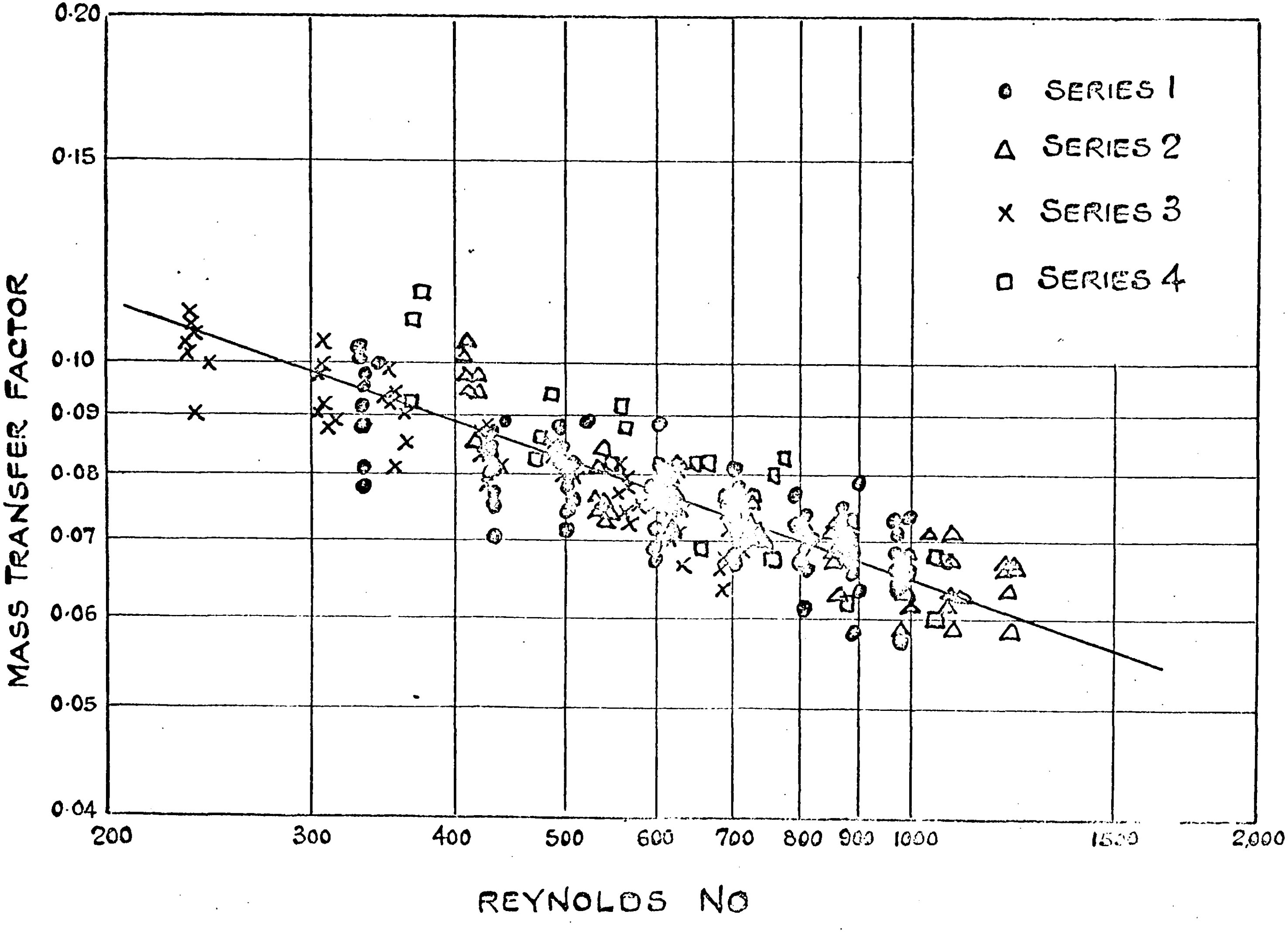

6.6 Discussion.

6.61 Constant Drying Rate.

Although it is generally accepted that drying rates are increased by reducing the particle size of the material, the constant drying rates did not conform to this pattern when they were put on a comparable basis for each pellet size by expressing them in the units lb water/h ft^2 of pellet surface (N''_c). This seems to suggest that there were other uncontrolled factors in the system which influenced the drying rates more than the particle size but it is apparent from the mean values of N''_c given in Table 6.59 for the 1 in beds of pellets that the slowest rates were obtained with the series 2 pellets which were the largest particles. In every other respect, however, the rates conformed with established drying theory.

Table 6.59

Mean Values of N''_c for 1 in Beds of Pellets.

Series	Pellet Diameter (in)	t		
		35	42·5	50
1	0·406	0·213	0·275	0·329
2	0·500	0·201	0;252	0·326
3	0·312	0·227	0·263	0·330
4	0·406	0·243	0·310	0·354

Drying tests conducted with beds of pellets of differing cross-sectional area showed that the drying rates were not affected by the ratio of bed area to pellet size.

It is seen from Tables 6.4, 6.22, 6.38 and 6.54 that the exponent of G in the correlations of N_c' with G was independent of the particle size but increased as the bed depth increased. This interaction between the air rate and bed depth has led to values from 0·49 to 0·89 being reported for the exponent in the literature and it is possible that a value of unity may be obtained when the air becomes saturated within the bed so that the drying rate is independent of the bed depth and depends solely upon the conditions of the air entering the bed. Therefore it is evident that experimental drying tests covering a wide range of bed loadings and air conditions should be performed before drying rates can be predicted accurately.

6.6.2 Heat and Mass Transfer Coefficients.

A comparison of the transfer coefficients evaluated from the experimental data indicated that they were independent of the inlet air temperature, increased with the air rate but decreased as the depth of the pellet bed increased. This reduction was caused by the actual driving force differing from the logarithmic driving force used in the derivation of the coefficients and disappeared when the coefficients obtained in the deeper beds were modified by applying a correction factor which consisted of the ratio of the area under the logarithmic mean curve to the area under the curve drawn through the measured outlet temperatures at the intermediate bed depths. Hence it was evident that more transfer was occurring than that corresponding to the conditions represented by the logarithmic mean driving force.

In most of the heat and mass transfer studies reported in the literature, the transfer coefficients were independent of bed depth even although they were evaluated using the logarithmic mean driving force. However, the air conditions covered in those studies were not far removed from ambient conditions so that the transfer rates were slow and the profile of the experimental driving force would be relatively flat and approximate to the logarithmic mean curve.

However, in the present study, high transfer rates were obtained so that the ratio of inlet to outlet driving forces was often as great as 10:1 and the difference between the logarithmic driving force and the actual mean driving force was as much as 40%. These observations are in agreement with the results of Bradshaw and Myers[33] who recommended that the logarithmic mean driving force may be used satisfactorily for evaluating transfer coefficients provided that the ratio of inlet to outlet driving forces is less than 6.

Comparing the values of the heat transfer coefficients derived for each pellet system, it was found that the coefficients decreased as the particle size increased, the average values ranging from 14·8 Chu/h ft^2 ^oC for the largest pellets i.e. series 2 to 17·0 Chu/h ft^2 ^oC for series 3 which were the smallest pellets.

The values of the ratio of the coefficients, h_g/k_g, for each drying test was found to be constant; the average value of 0·260 of the ratio h_g/k_g corresponded to the value of the constant in the equation relating the humidity of the air to the wet bulb depression of the air.

The exponent of G in the correlations of the unmodified coefficients with G was found to increase with the bed depth, the values ranging from 0·60 to 0·75 for the 1 in bed tests and from 0·73 to 0·85 for the 2 in bed tests. This interaction between the air rate and bed depth disappeared when the coefficients were corrected for the error in the driving force.

6.6.3 Heat and Mass Transfer Factors.

The values of the factors conformed to the pattern set by transfer coefficients from which they were evaluated in that they were independent of the air inlet temperature and depth of the pellet bed but decreased as the pellet size increased. However, by virtue of their definition, the factors decreased as the air rate increased whereas the coefficients increased with the air rate.

The value of the ratio j_h/j_d was approximately constant for all the drying tests, the average value being 1·24. This value is considerably greater than values of 1·06 to 1·12 reported in the literature. Ideally, for a direct analogy between heat and mass transfer the ratio should have a value of unity, but some of the conditions, which must be satisfied for attainment of the direct analogy, are so limiting that they are almost impracticable. To give an example, it is essential for an exact analogy that the mass transport and therefore the driving force be as small as practically possible because, at high transfer rates, the velocity profile in the gas film across which transfer is taking place becomes distorted and therefore the mass transfer coefficient is dependent on the rate of mass transfer.

In the present study the relatively high value of j_h/j_d is thought to be caused principally bu the use of the constant 0·260 in the air humidity wet bulb depression relationship as the values of this constant determines the ratio of the transfer coefficients from which j_h and j_d are derived. If a constant of 0·24 had been used in the humidity equation as is sometimes recommended, the ratio of h_g/k_g would also have become 0·24 and the ratio of j_h/j_d would have dropped to a value of 1·12 which was obtained by Bradshaw and Myers, their value of h_g/k_g being 0·243.

A small heat loss by radiation from the sides of the drying chamber may also have contributed slightly to the high values of j_h/j_d found in the present work.

6.6.4 Shape Factor.

The j_d factors obtained in the tests were used to determine the shape or area availability factor f which was introduced originally by Gupta and Thodos[35] to correlate in general relationships, heat and mass transfer data from diverse packed bed systems. These relationships were:

$$\frac{\varepsilon j_d}{f} = \frac{0.300}{\left[\frac{\sqrt{A_p}G}{\mu}\right]^{0.35} - 1.90} \qquad \ldots\ldots(4.31)$$

and

$$\frac{\varepsilon j_h}{f} = \frac{0.322}{\left[\frac{\sqrt{A_p}G}{\mu}\right]^{0.35} - 1.90} \qquad \ldots\ldots(4.32)$$

The shape factor, which is defined as the ratio of particle surface available to transfer to the surface area of a sphere having the same volume as the particle, was evaluated by substituting the appropriate values in equation (4.31) which may be rearranged as:

$$f = 3.33\, j_d \varepsilon \left\{ \left[\frac{\sqrt{A_p}G}{\mu}\right]^{0.35} - 1.90 \right\} \qquad \ldots\ldots(4.33)$$

The average values of f, calculated for each series of pellets, are shown in Table 6.60, together with experimental and theoretical values of f which were given by Gupta and Thodos for various particle shapes. A plot of $\frac{\varepsilon j_d}{f}$ against $\left[\frac{\sqrt{A_p}G}{\mu}\right]$ for the present experimental study is shown in Fig. 6.24 with the relationship of Gupta and Thodos.

FIG 6.24

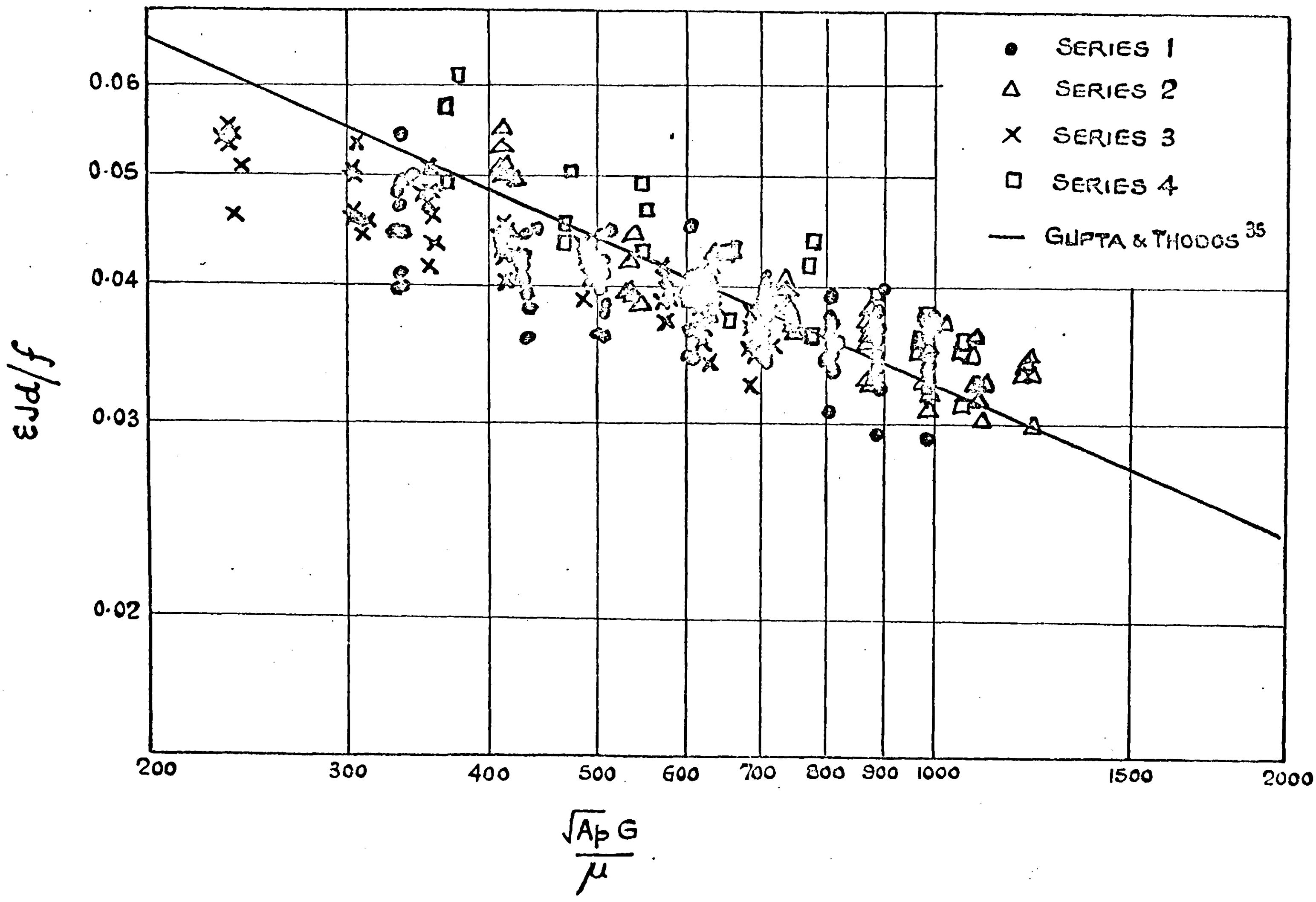

SERIES 1
SERIES 2
SERIES 3
SERIES 4
GUPTA & THODOS 35
0.06
0.05
0.04
0.03
0.02
$f/\rho\varepsilon^3$
200
300
400
500
600
700
800
900
1000
1500
2000
$\frac{\sqrt{A_p}\,G}{\mu}$

Table 6.60

Values of f.

Particle Shape		f exp.	f theor.
Tabloid	Series 1	0·862	
	Series 2	0·916	
	Series 3	0·807	
	Series 4	0·957	
	Average	0·872	
Spheres		1·000	1·000
Regular cylinders		0·865	0·952
Cubes		0·825	0·820
Partition rings		1·24	1·24
Raschig rings		1·34	1·22
Berl saddles		1·36	1·48

The theoretical values of f given in Table 6.60 were determined by taking the arithmetic mean area of the cases when the entire particle surface is available to transfer and when all probable areas are not available to transfer. By virtue of its definition, the value of f for spherical particles is unity.

The calculation of the theoretical f value for the tabloid pellets requires a knowledge of minimum pellet surface area which may be available to transfer. Although this area is extremely difficult to compute as the surfaces of pellets are curved, it is highly probable that the area will occur when the pellets are packed one upon the other with their major diameters in a horizontal or vertical plane.

Although it is perhaps more realistic to compare the experimental f value for the pellets with its theoretical value, it is nevertheless of interest to determine the relation between the average value of f exp. for tabloid pellets and the other f values given in Table 6.60. This relation may be evaluated by comparing the shape of the pellet with other particle shapes whose f values have been determined previously.

As the ends of a tabloid pellet have a radius of curvature almost three times that of the pellet itself, they may be considered to be relatively flat compared with the cylindrical body of the pellet and hence the shape of the pellet may be likened to that of an irregular cylinder.

Although an experimental f value for irregular cylinders has not been reported in the literature, it may be estimated from the experimental f value for regular cylinders by comparing the theoretical f values for regular and irregular cylinders. From this estimate, the theoretical shape factor for tabloids may be assessed.

In order to compare the experimental shape factor of the tabloids with the factors for other particles, the maximum values of f , corresponding to a fluidised bed system, were calculated for the tabloid pellets, regular cylinders and irregular cylinders which had the same diameter and volume as the tabloids. The values of f max. are given in Table 6.61 together with theoretical f values for both types of cylinders.

<u>Table 6.61</u>

Particle Shape		ƒ max.	ƒ theor.
Tabloid	Series 1	1·22	
	Series 2	1·23	
	Series 3	1·20	
	Series 4	1·15	
	Average	1·20	
Cylinder	Having same vol. & diam as S1	1·38	0·942
	" " " " " " S2	1·38	0·943
	" " " " " " S3	1·36	0·938
	" " " " " " S4	1·26	0·920
	Average	1·35	0·936
Cylinder Regular		1·15	0·952

From Table 6.61, it can be seen that the sphericity of the tabloid particles lies between those of the regular and irregular cylinders. It is also apparent that the value of ƒ theor. for the irregular cylinders is less than that for the regular cylinders and hence it is reasonable to assume that ƒ exp. for irregular cylinders will be less than the corresponding ƒ value of 0·865 for regular cylinders. Assuming also that the difference (ƒ theor. - ƒ exp.) is the same for both types of cylinders, the value of ƒ exp. for irregular cylinders becomes 0·849.

Considering now the tabloid pellets, the minimum surface area which is accessible to transfer in a bed of tabloid pellets will be slightly greater than the corresponding area in a bed of cylinders as less surface will be covered when the particles are packed upon each other. Consequently, the experimental f value for tabloids should be slightly greater than the estimated f value of 0·849 for irregular cylinders. The f value of 0·872 obtained in the present tests thus conformswith the pattern set by the other shape factors.

In their development of the shape factor, Gupta and Thodos evaluated f values for various types of particle on the basis that $f = 1{\cdot}00$ for spheres; this assumes that the entire surface area of a sphere is available to heat and mass transfer for both packed and fluidized beds. However, it is inevitable, that at points of contact between spheres, some surface area will be covered or be in a stagnant region in which the fluid medium will be saturated and no mass transferred.

Although the proportion of inaccessible surface at the points of contact will be very small or perhaps even negligible for beds of spheres, it might become significant in beds of other particle shapes such as cylinders where there may be lines of contact between particles instead of points. This may account for the difference which Gupta and Thodos found between the experimental and theoretical values of f for packed beds of cylinders.

Consequently, a knowledge of this inaccessible area would enable the area corresponding to minimum transfer conditions to be determined precisely. The corresponding theoretical shape factors would then be more accurate and the prediction of heat and mass transfer rates from the general transfer relationships more reliable.

7. Conclusions

In the drying tests carried out with four sizes of tabloid pellets, the constant drying rates which were obtained over a comprehensive range of operating conditions, conformed with the established theory of through-circulation drying.

The interaction, between the effects of the air rate and bed depth on the drying rates and heat and mass transfer coefficients, resulted from the air becoming almost saturated on leaving the deeper beds and it is probable that the exponent of G in the correlation of N_c' with G would have a value of unity if the air leaving the bed was saturated. Hence, as the exponent of G depends on the depth of the bed, it is expedient for experimental drying tests to be performed over a wide range of loading and air conditions before drying rates can be estimated accurately.

The use of the logarithmic mean driving force in the computation of heat and mass transfer coefficients is satisfactory provided that the ratio of inlet to outlet driving forces is small. If this ratio is as high as 10, as was experienced in the deeper beds, the actual driving force, derived using the outlet conditions in the intermediate bed depth, is approximately 30-40% less than the logarithmic driving force and the coefficients derived from the actual driving force are independent of the depth of the pellet bed. In such conditions, the heat and mass transfer coefficients and factors for deep beds may be computed accurately if conditions at the intermediate bed depth are known.

The general heat and mass transfer relationships derived from the drying tests showed reasonable agreement with correlations reported in the literature.

For the tabloid pellets, the average value of 0·872 for the area availability or shape factor f , introduced by Gupta and Thodos, was found to lie between the factors for spherical and regular cylindrical particles. A comparison of the shape of the tabloid pellets and regular and irregular cylindrical particles indicated that the experimental value for the tabloid pellets conformed with the pattern set by the theoretical and experimental f values for the cylindrical particles.

The values of f , given by Gupta and Thodos for various particles shapes, were derived on the basis that f equals unity for spherical particles. This assumes that the entire surface of a sphere is available to heat and mass transfer in both packed and fluidised beds. Although this is not strictly true as some surface at points of contacts between spheres will be rendered ineffective, the proportion of inactive surface may perhaps be negligible for the case of spherical particles but might become significant in beds of other particle shapes such as cylinders where there are lines of contact between particles instead of points. This may account for the differences which have been found to exist between the theoretical and experimental shape factors for various particles shapes.

Hence, it is considered that further work, investigating the proportion of particles surface area which takes part in the transfer operation, would be most useful and, in fact, is essential for coefficients and factors in this type of heat and mass transfer to be predicted accurately.

PART III

THE ROTARY DRYER

8. Introduction

The rotary dryer has been developed from the rotary furnace or kiln, which consists of an inclined tube, where rotation moves its contents slowly along its lenght. Drying is accomplished by passing hot air or furnace gases over the material in the tube. A general discussion of rotary kilns has been published by Dickie[54] and Perry[55].

The rotary dryer differs from the kiln in having internal baffles or flights to agitate the material passing through the dryer. Many types of baffles have been designed to increase the contact between the hot gases and material,[56,57,58] but simple radial flights are frequently used.

The majority of the earlier dryers were constructed for the treatment of sand or lignite, but other applications included the drying of sugar beet[59] seaweed[60] and inorganic salts, pharmaceuticals, cork and rubber[61]. Because the rotary dryer is essentially a continuous system, it is now commonplace in industry, and present-day knowledge has been advanced by its use in the fertiliser industry[62].

Modifications of the rotary dryer, including the rotary louvre type and steam tube dryers, have been developed. The design and operation of the rotary louvre dryer, which is basically a through-circulation unit, has been described by

Lapple et al.[63]. A description of the steam tube dryer, which is a rotary dryer with steam tubes replacing the flights and ambient air passing through the dryer, is given by Perry.

8.1 Material Transport.

Early workers, investigating the conveying properties of rotary kilns and dryers, gave primary consideration to the retention time of the material in the tube. An alternative criterion has been introduced by Friedman and Marshall[64], who proposed that the volumetric percentage hold-up of the dryer is the constant to be fixed for design purposes. This is defined as the ratio of the volume occupied by the material in the dryer to the total internal volume of the dryer.

The hold-up and retention time are related by the expression:

$$\theta'_R = \frac{L_R \; X'}{100F'} \qquad \text{.....(8.1)}$$

where θ'_R = retention time (h)

L_R = length of dryer (ft)

X' = percentage hold-up

F' = feed rate ($ft^3/h\ ft^2$ of dryer cross section)

This theoretical retention time is the average time of passage, and the actual time spent by individual material particles deviates about this value. This deviation is important where heat sensitive material is being dried, and several workers [71, 73, 74, 65, 66, 67], have studied this aspect of material transport.

The first data on retention times were obtained from tests on rotary kilns carried out by Sullivan et al.[68], who derived the following equation from their results:

$$\theta'_R = \frac{0{\cdot}00517\, L_R \gamma^{\frac{1}{2}}}{S_d\; D_R\; R} \qquad \ldots\ldots(8.2)$$

where γ = dynamic angle of repose of material (degrees)

S_d = slope of kiln (ft/ft)

D_R = diameter of kiln (ft)

R = rate of rotation of kiln (rev/min)

L_R = length of kiln (ft)

Ginstling et al.[69] independently derived the following expression for predicting the time of passage through a rotary dryer:

$$\theta'_R = \frac{0{\cdot}00783\, L_R}{S_d\; D_R\; R} \qquad \ldots\ldots(8.3)$$

Equation (8.3) gives an estimate retention time 2·4 times greater than the value given by equation (8.2) if a representative value of 40° is assumed for the angle of repose. A similar relationship was given by Saeman[70] from a mathematical analysis of the likely paths of material through a kiln. These formulae, however, give misleading results for low kiln slopes and cannot be applied to high loadings in horizontal cylinders.

An important effect in considering material transport in a rotary dryer, is that of the air stream through which the material cascades. According as the air flow is co-current or counter-current, the material will be assisted or retarded in its passage. Consequently, Smith[71] suggested the constant 0·00783 in equation (8.3) should be replaced by a constant k which varied from 0·0042 to 0·017 for counter-current dryers and from 0·017 to 0·0058 for co-current dryers.

From a series of tests where optimum loading conditions were used, i.e. where all the material was carried along by the action of the flights, Prutton et al.[94] postulated the relationship:

$$\theta'_R = \frac{k\ L_R}{S_d\ D_R\ R} + m'V \qquad .....(8.4)$$

where V = air velocity (ft/min)

m' = a constant, positive for counter-current air flow and negative for co-current air flow.

Friedman and Marshall[64] suggested that to maintain a constant hold-up, the feed rate must be varied directly with the rate of rotation of the dryer raised to some power less than one. From experimental data, they obtained the relationship:

$$X_s = \frac{0{\cdot}294\ F_s}{S_d\ R^{0\cdot 9}\ D_R} \qquad .....(8.5)$$

For air flow conditions, the same workers presented the expression:

$$X = X_s + m''G \qquad .....(8.6)$$

where X = hold-up in dryer with air flow

X_s = " " " " without air flow

G = mass air flow (lb/h ft^2)

m'' = constant, depending on material being positive for counter-current flow and negative " co " " .

It is important to realise how loading of a dryer affects its performance. Low loadings may produce uneven distribution of the cascading material and consequent short-circuting of the air stream, whereas high loadings will produce a bed of material moving along the bottom of the dryer by kiln action.

Allowing for this loading effect in their theoretical considerations, Saeman <u>et</u> <u>al</u>.[65] presented this formula for hold-up in rotary dryers and coolers:

$$X = \frac{F\,L_R}{K(X)\;D_R\;N\;(S_d - m'''V)} \qquad \ldots.(8.7)$$

where $K(X)$ = a constant varying from 2 to π depending on the dryer loading

m''' = a constant.

This relationship was subsequently corroborated by Porter and Masson [73] for rotary coolers ranging from 6 to 9 ft in diameter. It gives a simplified representation of the dominant variables which influence material transport and should be used as a first approximation only. For a more accurate estimate of the rate of material transport, a step by step derivation of the continuous transport distribution is recommended by Saeman[62].

The above equations should be applied only to materials which exhibit no appreciable change in handling characteristics throughout the length of the dryer since Friedman and Marshall[64] and Spraul[61] reported anomalies with materials, whose flow properties altered in their passage through the dryer.

8.2 Heat and Mass Transfer.

This aspect of rotary drying has received intensive examination by several workers[65,73,74,75], employing varying and complicated approaches in an effort to find a consistent and valid basis for design and scale-up.

One of the main problems confronting workers in this field is the accurate measurement of temperature inside the dryer. Although a satisfactory method of determining material temperatures has been developed by Friedman and Marshall[64], no similar reliable technique has been applied to the measurement of the air temperature gradient along the dryer. Attempts have been made using a high velocity filtered thermocouple but the results obtained were erratic and non-reproducible. The introduction of a probe into the dryer may be partially responsible for these inconsistencies since it alters the steady conditions in the dryer.

An average air temperature at a point inside the dryer can be estimated from a knowledge of material moisture contents and temperatures and inlet air conditions using a psychrometric chart. Previous studies have been based on the assumption that the air temperature is constant along any single particle trajectory, but Saeman and Mitchell[65] reported an appreciable difference between the air temperatures at the top and bottom of the cascading curtains of material.

The rotary dryer can be considered as a multi-pass heat exchanger and Miller et al.[74] utilised this approach in deriving the following equation:

$$q = 0{\cdot}187 \quad (N_f - 1)\ L_R D_R G^{0{\cdot}46}\ \Delta Tm \qquad \ldots.(8.0)$$

q = heat transfer rate (Btu/h)

N_f = no. of flights

ΔT_m = logarithmic mean temperature difference (^oF)

The logarithmic mean temperature difference, however, cannot be applied since the derivation of the log mean overall thermal driving force is dependent upon:

(1) The heat capacities of both fluid and material remaining constant

(2) The heat transfer coefficient being constant

(3) The heat transfer rate being proportional to the temperature difference.

In a rotary dryer, these conditions are not fulfilled and this method of computing heat transfer rates is not strictly applicable.

Friedman and Marshall[75] extended work on the correlation of rotary dryer performance and showed that dryer hold-up exerted a dominant effect on heat transfer. They also found that the heat transfer coefficient in a rotary dryer was inversely proportional to the diameter and suggested the relationship:

$$U_a = \frac{10\ G^{0.16}}{D_R} \qquad \ldots.(8.9)$$

where U_a = Overall volumetric heat transfer coefficient (Btu/h ft^3 of dryer volume)

The form of this expression was later confirmed by Saeman and Mitchell[65] for the constant geometry and peripheral shell speed.

The effect of hold-up on heat transfer was also substantiated by Saeman and Mitchell[65], who suggested that the cascade rate i.e. the actual rate of discharge of material from the flights, was a factor in the heat transfer rate. From experimental data, they deduced the equation:

$$q = C(0.6 + 2.5e^{-4.8}\ Z_f)\ \ L_R\ \Delta Tm \qquad \ldots.(8.10)$$

where C = Cascade rate (ft^3/ft^2 min or lb/min)

= X_f AN_f R

= 2x R(assuming contents cascade twice per revolution)

X_f = Flight loading (ft^3/ft^2 or lb/ft)

Z_f = radial flight depth (ft)

ΔT_m = mean temperature difference (^oF)

A general correlation expressing gas velocity effects on heat transfer in direct heat rotary dryers was proposed by McCormick[76], and experimental data from previous workers in this field [65,74,75] were used to verify the relationship.

The change in condition of the air passing through the dryer may be represented by a curve on a psychometric chart. Kawabute[77] applied a method developed by Inaxumi[78] for the prediction of air conditions during humidification to the rotary dryer and derived a formula for the slope of the temperature-humidity curve on the psychometric chart. Its application is limited, however, since the treatment assumes that the decrease in drying rate during the falling rate period is caused by the gradual decrease in the wetter surface area and not by diffusional kinetics.

A design method, based on measureable quantities rather than on empirical constants measured on other equipment, has been described by Porter[79]. He considered the transient heat transfer which occurs within the solid particles. Considerations of residence time and flight design were also involved in the design for heat transfer.

Sharples, Glikin and Warne[48] constructed a mathematical model for either co-current or counter-current dryers from equations describing the material transport and heat and mass transfer in a dryer. The model, which was programmed for stepwise integration by a digital computer, was applied to an industrial dryer by determining heat transfer and drying rate coefficients which made the inlet and outlet conditions of the model equivalent to the corresponding conditions on the production unit.

9. EXPERIMENTAL METHODS

9.1 Classical Method of Experimentation.

The derivation of the empirical relationships discussed previously appears to have followed a planned experimental programme, which Brownlie[80] calls the "classical method of experimentation". By this method, the individual effect of each factor on the system is found by varying each in turn, the remaining factors being held constant.

This method assumes that the effect of each factor is independent of the values of the other factors. When this assumption does not hold the factors are said to interact; e.g. the effect of changing factor A from value A_1 to value A_2, when factor B is held at B_1, may be different from the effect of the same alteration when B is held at B_2.

Another discrepancy in the classical method is that the effect of each factor is determined while the rest are kept constant at arbitrarily fixed values. If any of the factors interact, the estimated effect of each depends on the constant values chosen for the others. An estimate of the combined effect of all the factors will therefore be accurate only if the interaction is small or if the proposed design values of the various factors are close to the constant experimental values. If these conditions are not satisfied, gross inaccuracies may be obtained.

The classical method cannot detect interactions between factors and consequently provides a modified picture of the system. A complete investigation of the system requires the effect of a factor to be evaluated over a range of values of the other factors in the system. This procedure is followed in the factorial method of experimentation.

9.2 Factorial Method of Experimentation.

In the factorial method of experimentation, which was developed by Fisher[81] and Yates[82] to analyse the results of agricultural experiments, the effect of each factor is determined over a range of values of the other factors.

The factorial approach is used in the preliminary study of a complex process to ascertain the dominant variables and the range over which further intensive examination of the variables should take place. It is usually sufficient in a preliminary investigation to test two values (levels) of each factor; therefore in a factorial experiment to determine the effects of three factors A, B and C on a process, eight tests, covering all combinations of factor levels would be required. Denoting the lower and higher levels by subscripts 1 and 2, the tests would be:

$A_1 B_1 C_1$ $A_1 B_2 C_1$ $A_1 B_1 C_2$ $A_1 B_2 C_2$

$A_2 B_1 C_1$ $A_2 B_2 C_1$ $A_2 B_1 C_2$ $A_2 B_2 C_2$

The factorial method ensures a complete and comprehensive study of a system and increased experimental sensitivity and efficiency.

9.3 Comparison of the Classical and Factorial Methods of Experimentation.

The factorial method has four distinct advantages over the classical method of experimentation.

(1) The factorial design shows greater economy than the classical approach in permitting more precise estimation of the effects of factors for a given effort, since the results of each test is used many times in determining the effect of each factor.

(2) Since the factorial method requires tests to be made over a range of values of each factor, interactions between factors can be detected; in the classical approach, the possibility of factors interacting is not considered.

(3) The conclusions, obtained from a factorial method, are valid over a much wider range of operating conditions than those drawn from the classical method.

(4) The symmetrical form of the complete factorial design provides an estimate of the experimental error without the need for duplicate tests; the aim, in the classical approach, is to minimise random errors and, consequently, duplicate tests are required before the error can be estimated.

These differences may be illustrated by applying both methods to a hypothetical experiment to investigate the effect on a process yield of y changing three process variables, A, B, and C from their normal values A_1 B_1 C_1 to some new values A_2 B_2 C_2.

?.?.1 Classical Method.

A test is made with the factors at their normal levels A_1 B_1 C_1 to find the yield $(A_1\ B_1\ C_1)_y$, obtained under normal conditions. To estimate the effect of changing factor A from A_1 to A_2, a second test is made with the values A_2 , B_1 , C_1 to give the yield $(A_2\ B_1\ C_1)y$. The estimate effect of factor A is the difference between these fields. Thus:

$$\text{Effect of A} = (A_2\ B_1\ C_1)y - (A_1\ B_1\ C_1)y$$

Similarly, the effects of B and C are found by comparing the standard test with tests A_1 B_2 C_1 and A_1 B_1 C_2 respectively.

$$\text{Effect of B} = (A_1\ B_2\ C_1)y - (A_1\ B_1\ C_1)y$$

$$\text{Effect of C} = (A_1\ B_1\ C_2)y - (A_1\ B_1\ C_1)y$$

From these tests, however, no assessment of random errors is possible and in order to ascertain whether any of these effects are real or due to experimental error, it is necessary to repeat each experiment at the very least, so that eight tests must be made. Moreover, the effect of change in means is only estimated on the basis of two results and these will not be precise.

Such an experiment gives no information about interactions between variables and it is necessary to make additional tests to determine whether moving B from B_1 to B_2 affects the change brought about by altering A from A_1

to A_2 and so on.

[illegible].[illegible].2 Factorial method.

In the factorial design, the eight tests shown on page 122 are made. This experimental scheme can be represented by the co-ordinates of the corners of a cube, whose axes are A, B and C.

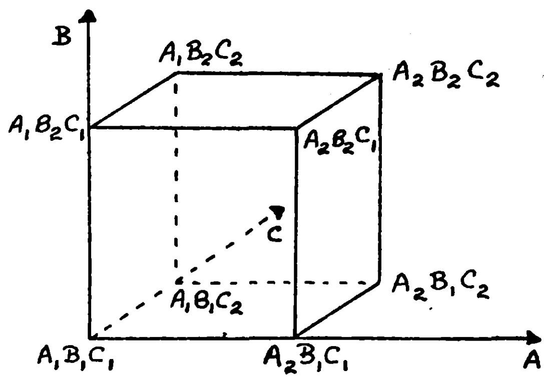

In this case, the estimate effect of the changing A from A_1 to A_2 is the difference between the average yield of the tests in the A_1 plane (i.e. the average of $(A_1\ B_1\ C_1)$ y, $(A_1\ B_2\ C_1)$y and $(A_1\ B_2\ C_2)$y) and the average yield of the tests in the A_2 plane (i.e. the average of $(A_2\ B_1\ C_1)$y, $(A_2\ B_2\ C_1)$y and $(A_2\ B_1\ C_2)$y and $(A_2\ B_2\ C_2)$y). This estimate effect of A is independent of the values of B and C used since, to a first approximation, the changes produced by B and C varying over each plane cancel out.

The main effects of B and C are obtained from averaging over their corresponding planes in a similar manner.

This hypothetical experiment illustrates the immediate advantage of the factorial design in that the main effects are obtained as the difference between sets of four yields instead of two yields as in the classical design of comparable size. This gives a more precise estimate of the effect of each factor and underlines the superiority of the factorial experiment which lies in the fact that the result of each test is used many times, while only the standard test is used more than once in the classical experiment.

In addition to estimating the main effects of A, B and C, the factorial method permits a direct estimation of interactions between factors. To estimate the interaction between the A and B factors, the four yields in the C_1 plane are averaged with the corresponding four yields in the C_2 plane.

e.g. $$\frac{(A_1\ B_1\ C_1)y + (A_1\ B_1\ C_2)y}{2} = (A_1\ B_1)\bar{C}\ y$$

$\bar{C}$ indicating that the yields are averaged over C. The four averages thus obtained are:

$(A_1\ B_1)\bar{C}\ y$ $\quad$ $(A_2\ B_1)\bar{C}y$

$(A_1\ B_2)\bar{C}\ y$ $\quad$ $(A_2\ B_2)\bar{C}\ y$

The difference between the top row averages gives the effect of changing A from A_1 to A_2 at $B = B_1$, and the difference between the bottom row averages gives the effect of changing A from A_1 to A_2 with B at B_2. Since each of the four averages was the mean of two tests, the experimental error can be used to determine whether the effect of A at B_1 is significantly different from the effect of A at B_2. (The test of significance used is described under the Analysis of Variance). If the two effects differ significantly, A and B are said to interact.

9.4 Analysis of Variance.

In an industrial process, large random errors may be introduced by the operating conditions, which do not permit a strict control of process variables. This creates a problem for a process engineer in interpreting the results of an industrial experiment consisting, for economic reasons, of a limited number of tests, since considerable sums of money may depend on the conclusions drawn from the experiment.

There are, however, statistical tests of significance which, by analysing the experimental data, can distinguish between real effects and interactions and those due to experimental error, and also indicate the probability of an incorrect conclusion.

The series of tests, which comprises the factorial experiment, is so designed that the effects and interactions estimated from the test results can be effeciently analysed by the test of significance known as the "Analysis of Variance".

The theory of the analysis of variance is given in several statistical text books, [83,84,85,86] but the principles of the analysis may be outlined in the following manner.

The test results, obtained from the factorial experiment, produce a range of values of the dependent variable, each value corresponding to a different combination of independent variables. The scatter of these values may be measured by a statistical quantity known as the "variance". In addition to the total variance obtained, smaller variances can be attributed to the effects of various factors and to interactions between them. Variance, however, is an additive quantity and the total variance consists of the sum of the component variances plus a residual variance attributed, theoretically, to a complex interaction, which, for physical reasons, does not exist of itself. This residual variance, therefore, may be used as an estimate of the experimental error. An estimate of the error may be obtained directly by duplicating each test in the factorial experiment.

The method used to determine whether the effect of a factor can be considered significant is to postulate that the effect does not exist and then to ascertain the probability of the observed difference between the variance attributed to this effect and the experimental error variance occuring by chance. The significance of interactions between factors is tested in a similar manner.

The differences between the two variances is calculated by the ratio:

$$\frac{\text{Variance due to effect or interaction}}{\text{Variance due to experimental error}} = F$$

and, from tables of F[87], the probability of an equally large value of F occurring by chance (i.e. when there is no significant effect or interaction) is found. In industrial experimentation, this probability must be less than an arbitrary level of 5% before an effect or interaction is considered significant. There are however, other probability or significance levels, e.g. 10%, 0·1%, which may be used depending on the degree of certainty required by the conclusions drawn from an experiment.

9.5 The Scope of the Present Investigation.

A two-level factorial experiment is applied to the drying of barley in a pilot rotary dryer and is used to examine the effects of the rate and temperature of the air, the rate of rotation of the dryer and the feed rate of the barley on the material transport and drying mechanisms in the dryer.

10. EXPERIMENTAL APPARATUS AND PROCEDURE.

10.1 Description of the Experimental Rotary Dryer.

The rotary dryer used in this investigation is shown in Fig. 10.1. The drying tube, made of "Pyrex" heat resisting glass, had an internal diameter of 5 in and was 40 in long. 8 angled aluminium flights fitted to the inside of the tube were held by brass rings at either end of the tube.

The drying tube was rotated by a pinion, which engaged peripheral teeth on the ring at the feed end of the dryer. The pinion was driven through a gearbox and three step pulley by a D.C. motor, which enabled a wide range of dryer speeds to be obtained.

The wet material was fed into the dryer by a conveyor belt system. Difficulties, encountered in the design of a system to give a constant feed rate, were overcome by fitting a drum with a wire mesh periphery into the feed storage hopper situated above the conveyor belt. This drum was driven by a pulley from the driving shaft of the conveyor belt, the whole assembly being driven through a variable "Zeromax" gearbox by a constant speed A.C. motor. The belt, made of rubber, dropped the wet material about 2 in inside the dryer and any material, which, by reason of material gradient or air flow, started to travel in the reverse direction, was lifted by the flights and dropped on to the conveyor belt.

The dried product was collected in a large glass bottle, which was attached by a canvas sleeve to an aluminium shute

FIG 10.1

ROTARY DRYER

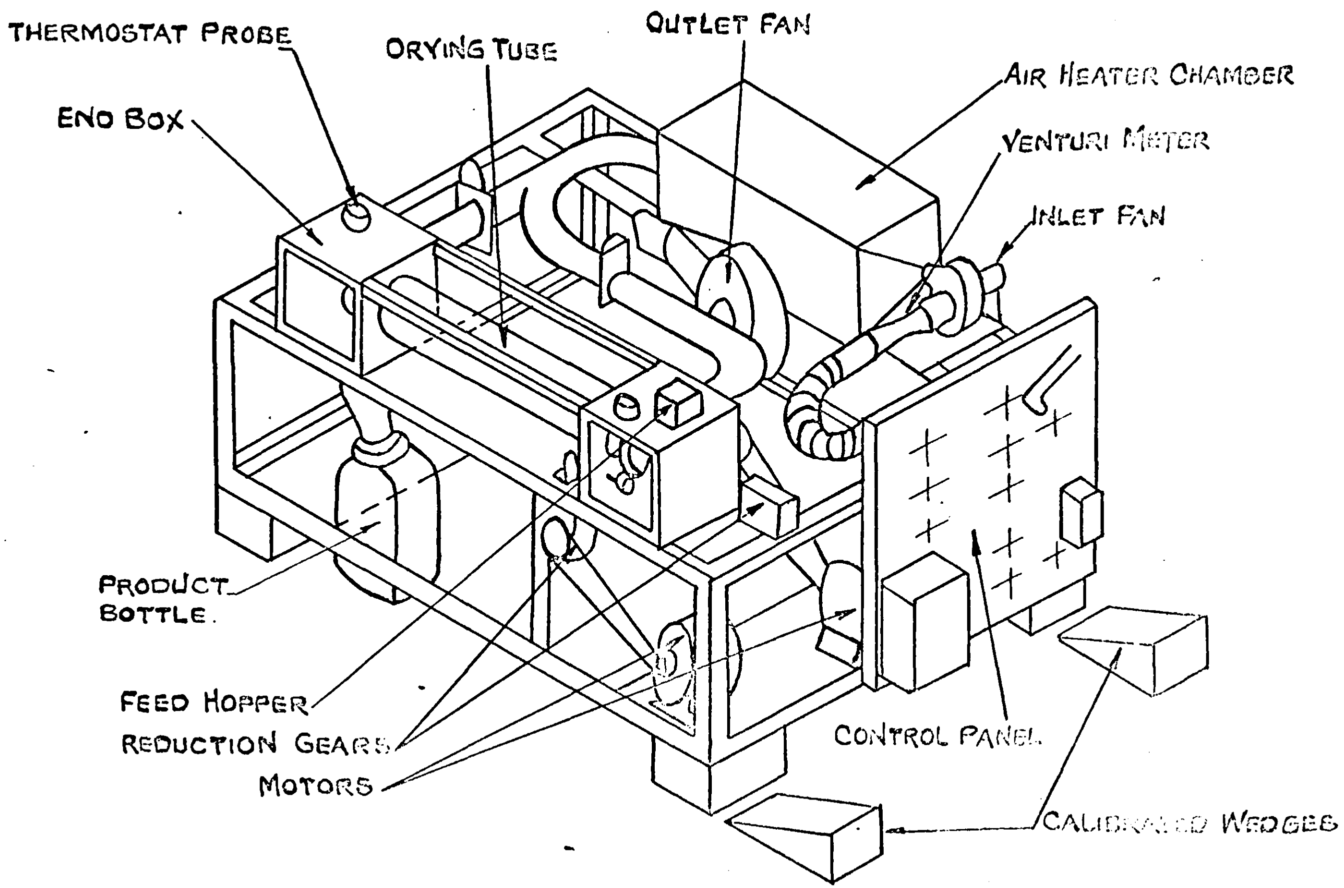

under the discharge end of the drying tube.

The feed and discharge mechanisms were enclosed in chambers made of "Sindanyo" wood fitted with glass fronts.

The air flow, which was supplied by two variable speed D.C. fans, was metered by a venturi tube situated in the inlet ducting and passed through a heating chamber to the drying tube. Lagged copper ducting, which conveyed the heated air to the tube, was constructed to give either co-current or counter-current air flows. In the present study, only counter-current flow was used. Variation and control of the air flow was accomplished by adjusting the speed of the forced draught fan through a potentiometer mounted on the control panel.

The pressure tappings from the venturi meter were connected to an inclined manometer which was also situated on the panel. As air leaks may occur in the end boxes,joints etc. , the venturi meter was calibrated against a vane anemometer placed in the drying tube.

The heating chamber contained 2 electrical elements of 2 kw, 2 of 1 kw and 1 of 0·5 kw, one of the 1 kw units being controlled by a "Sunvic" thermostat positioned in the inlet air stream. The thermostat controlled in the inlet air temperature to $\pm$ 0·25°C.

In order to minimise heat losses, which tend to be important in a small unit of this type, a glass jacket was fitted round the drying tube, which was also lagged with asbestos rope. A separate supply of hot air was passed into the jacket and a uniform temperature was provided by a high speed propeller fan.

The whole unit was mounted on a frame of slotted angle iron, re-inforced in places with a sheet material. This facilitated the alteration of the slope of the drying tube by jacking up one end of the frame and inserting calibrated wooden wedges.

10.2 EXPERIMENTAL WORK.

10.2.1 Measurement of Feed Rate.

The feed rate was measured by collecting product samples over selected time intervals. The samples were dried and weighed and the feed rate calculated. This method gave results with a variation of less than 2% and avoided any possibility of entrainment in the air flow at the feed end having any effect on the value of the feed rate.

10.2.2 Measurement of Material Velocities and Moisture Content.

To deduce the actual drying curve, material velocities at several points along the drying tube must be known. A uniform material velocity under constant feed conditions implies a uniform loading of material along the dryer. This may not occur if the decrease in moisture content as the material passes along the dryer alters its surface properties and bulk density. In the case of vegetable materials, the handling characteristics are very dependent on moisture content and alteration in moisture content produces marked variation in material velocities along the dryer.

Velocity at any point is inversely proportional to the loading at that point and is given by the equation:

$$V_s = \frac{F'}{X_L} \qquad \text{....(10.1)}$$

where V_s = velocity (in/min)

F' = feed rate (lb B.D.S./min)

X_L = loading (lb B.D.S./in)

The loading inside the dryer was measured by inserting a trough fitted with removable transverse sections, 1 in between parallel faces. The dryer was rotated until its contents were transferred to the trough and the moisture content and, hence, the weight of bone dry solid, of the sample collected by each section was determined by drying the sample in a vacuum oven. The accuracy of this method, which assumes that each section collects material in proportion to its length, was checked by Smith[88]. (1954

10.1.3 Experimental Procedure.

The inlet fan, jacket fan and heaters were switched on and their controls adjusted to give the required operating conditions. The drying tube was allowed to rotate slowly to avoid local overheating until the whole unit had attained working conditions.

When these conditions had been reached, the tube was set to the desired speed, the feed hopper filled with wet material and the conveyor system energised. The system was adjusted to give the required feed rate and the dryer was operated steadily until a constant discharge was obtained. The test was continued for twice the estimated retention time before any measurements were taken.

At the end of the run, the heaters and fans were switched off and the trough containing removable sampling sections was immediately inserted to collect the contents of the dryer. The contents of each section were transferred to the air-tight aluminium weighing dishes. Samples of feed and dried material were also taken and the moisture content of all the samples determined by drying them in a vacuum oven.

The hold-up of the dryer was measured by drying and weighing the entire contents of the dryer.

10.3 Material.

Barley grain appeared to be suitable for study in the rotary dryer due to its uniform particle size and free-flowing properties. It is used widely in the brewing and distilling industry for the preparation of beer, whisky and malt products.

Dehydration of barley for use in brewing is important where even germination is desirable and a low moisture content necessary for safe storage of the grain is required.

A typical chemical analysis of barley is given as:

water 15%, cellulose 6%, starch and other carbohydrates 60%, lipids 2%, other non-nitrogenous material 4%, protein 10% and ash 3%.

10.4 Selection of Variables to be Studied.

In the complex rotary drying system, there are eleven prominent and independent variables which may be divided into two classes:

(1) System Variables.

These consist of the character and temperature of the material, and the diameter, length, slope, flight capacity and number of flights of the dryer.

(2) Operating Variables.

These are the feed rate of material, air flow rate and temperature, and the rotational speed of the dryer.

The first class of variables are usually fixed for a particular dryer system while the second class of variables may fluctuate during the drying operation. Consequently, the experimental error in a particular test is due entirely to these fluctuations and not to any variation in the system variables. It seems more logical, therefore, to study the effect of the factors whose operational variations account for the random error. Hence, the variables selected for study were:

the feed rate of wet material F

the air flow rate G

rotational speed of the dryer R

inlet temperature of airflow T

The effect of each variable was studied at two levels:

F_1 = 5·0 lb B.D.S./h F_2 = 5·75 lb B.D.S./h

G_1 = 600 lb/h ft^2 G_2 = 800 lb/h ft^2

R_1 = 8 rev/min R_2 = 13 rev/min

T_1 = 100°C T_2 = 110°C

With a dryer slope of 1·7%, these levels gave satisfactory differences in the value of the product moisture content and avoided excessively long or excessively short retention times.

11. RESULTS OF THE ROTARY DRYING OF BARLEY.

11.1 Introduction.

In the study of the performance of a rotary dryer, two approaches may be followed:

(a) Theoretical Approach.

This approach is concerned with the investigation of the conditions existing inside the dryer. These conditions may refer to heat and mass transfer between the solids and gas or to the transport of the solids along the dryer.

(b) Practical Approach.

This approach relates the operating conditions of the dryer to a characteristic property of the dryer, which is of practical importance. The final moisture content of the solids in such a property, since it is usually specified in a dryer design.

In this project, both approaches were considered; the theoretical approach consisted of the study of the solids hold-up and retention time in the dryer whereas the practical approach dealt with the moisture content profile of the solids along the dryer.

These approaches may be combined to define the optimum conditions of the dryer, i.e. the conditions which produce a maximum drying rate. In addition, they may be incorporated into the design of a dryer, the retention time affecting the constraints which limit the choice of dryer dimensions and operating conditions and the moisture content profile determining the required dryer length for a specified product moisture content. The retention time should be considered with the air flow rate and temperature so that the maximum solids temperature is not exceeded.

11.2 Experimental Test Programme.

The effects of the four variables F, G, R and T on the performance of the rotary dryer were studied at the two levels of each factor given on pages 135 and 136. The programme of tests was designed according to the factorial method of experimentation, which required tests to be performed at all combinations of factor levels. In order to give an estimate of the experimental error, duplicate tests were carried out and consequently a total of 32 tests were made.

To minimise the change of bias in the test results, the tests were performed in a random order.

The results of a typical drying test are given in Appendix IX.

11.3 MATERIAL TRANSPORT RESULTS.

11.3.1 Hold-up of Material in Dryer.

The experimental values of the solids hold-up in the dryer, obtained from the 32 tests, as described in Section 10.2.3, are shown in Table 11.1, together with the corresponding theoretical values calculated from equation (8.7), using a value of 0·002 for the air drift coefficient, m'''.

Table 11.1

Comparison of Experimental and Theoretical Values of Hold-up of Barley in a Rotary Dryer.

Test Conditions	Experimental Value (lb B.D.S.)	Theoretical Value (lb B.D.S.)
F_1 G_1 R_1 T_1	1·428 1·300	1·472 1·573
F_1 G_1 R_1 T_2	1·353 1·595	1·430 1·712
F_1 G_1 R_2 T_1	0·717 0·766	1·129 1·043
F_1 G_1 R_2 T_2	0·803 1·030	1·091 1·232
F_1 G_2 R_1 T_1	1·540 1·531	1·595 1·570
F_1 G_2 R_1 T_2	1·577 1·740	1·478 1·742
F_1 G_2 R_2 T_1	1·030 0·829	1·069 1·144
F_1 G_2 R_2 T_2	1·098 1·126	1·203 1·241
F_2 G_1 R_1 T_1	2·233 2·277	2·222 2·200
F_2 G_1 R_1 T_2	2·275 2·222	2·255 2·182
F_2 G_1 R_2 T_1	1·685 1·896	1·753 1·693
F_2 G_1 R_2 T_2	1·681 1·558	1·907 1·797
F_2 G_2 R_1 T_1	2·383 2·270	2·530 2·336
F_2 G_2 R_1 T_2	2·499 2·512	2·565 2·750
F_2 G_2 R_2 T_1	2·259 2·264	2·409 2·365
F_2 G_2 R_2 T_2	2·044 2·116	2·059 2·211

The theoretical and experimental hold-up values were subjected to a regression analysis to determine the significance of equation (8.7) for the prediction of hold-up values. The method of conducting a regression analysis is outlined in Appendix VII. The results of the analysis, given in Table 11.2, indicate that the correlation coefficient is highly significant and, consequently, the experimental hold-up values exhibit a linear relationship with the theoretical values calculated from equation (8.7).

Table 11.2

Regression Analysis of Experimental and Theoretical Hold-up Values.

Source of Variance	Degrees of Freedom	Sum of Squares
Due to Regression	1	9·266604
About Regression	30	0·433481
Total	31	0·700085
Correlation Coefficient r = 0·985		
From Tables[87], value of r significant at 1% level of probability = 0·554		

11.3.2 Material Retention Times.

The experimental values of the retention time, θ_m, of the material in the dryer are given in Table 11.3 which also contains the retention time, θ_{em}, estimated from the material velocities in the dryer. The derivations of θ_m and θ_{em} are described in Appendix IX.

Table 11.3

Values of θ_m and θ_{em} for the Rotary Drying of Barley.

Test Conditions	θ_m min	θ_{em} min	Test Conditions	θ_m min	θ_{em} min
F_1 G_1 R_1 T_1	26·0 29·5	26·5 29·4	F_2 G_1 R_1 T_1	24·8 25·5	25·3 25·6
F_1 G_1 R_1 T_2	30·5 30·0	30·4 29·9	F_2 G_1 R_1 T_2	24·8 25·1	25·2 25·2
F_1 G_1 R_2 T_1	12·3 14·2	12·7 14·9	F_2 G_1 R_2 T_2	18·6 20·0	18·3 19·6
F_1 G_1 R_2 T_2	14·2 16·1	15·0 16,0	F_2 G_1 R_2 T_2	17·1 16·8	17·3 17·3
F_1 G_2 R_1 T_1	35·0 35·6	34·6 35·2	F_2 G_2 R_1 T_1	26·0 26·9	27·5 25·2
F_1 G_2 R_1 T_2	38·7 36·2	37·5 34·0	F_2 G_2 R_1 T_2	26·7 25·2	26·0 25·2
F_1 G_2 R_2 T_1	20·9 15·7	22·0 16·3	F_2 G_2 R_2 T_1	20·3 20·7	19·4 20·2
F_1 G_2 R_2 T_2	19·9 21·6	20·6 21·0	F_2 G_2 R_2 F_2	21·3 20·7	21·6 20·2

The effects of the factors F,G,R and T on θ_m were determined by subjecting the values of θ_m from the 32 tests to an Analysis of Variance as described in Appendix VI.

The analysis was carried out on the values of $\log_{10} \theta_m$ instead of θ_m since, by taking logarithms, the relationship, derived from the results of the analysis, might be simplified.

e.g. if $\theta_m = f(FGR) + f(FGT)$,

by taking logarithms, the expression might reduce to

$$\log_{10} \theta_m = f(FG) + f(FR) + f(GT)$$

Since duplicate tests were performed in the factorial experiment, the form of the analysis enabled a direct estimate of the experimental error made, which was compared with the effects of the various factors and interactions in order to measure their significance. In the results of the analysis, shown in Table 11.4, effects and interactions, significant at the 5% level of significance, are identified by an asterisk.

Table 11.4

Analysis of Variance on Values of $\log_{10} \theta_m$ for the Rotary Drying of Barley.

Source of Variance	Degrees of Freedom	Crude Sum of Squares	Mean Sum of Squares
F	1	0·002080	0·002080
G	1	0·049928	0·049928
R	1	0·339900	0·339900
T	1	0·002080	0·002080
FG	1	0·012482	0·012482 *
FR	1	0·058654	0·058684 *
FT	1	0·007022	0·007022 *
GR	1	0·002888	0·002888
GT	1	0·000265	0·000265
RT	1	0·000046	0·000046
FGR	1	0·000008	0·000008
FGT	1	0·000760	0·000760
FRT	1	0·000778	0·000778
GRT	1	0·000924	0·000924
FGRT	1	0·000421	0·000421
Residual	16	0·014687	0·000919
Total	31	0·492923	

The Analysis of Variance indicated that the FG, FR and FT interactions were significant. The retention time θ_m of the material in the dryer may therefore be derived from an expression of the form:

$$\log_{10}\theta_m = f(FG) + f(FR) + f(FT)$$

In order to simplify this expression and give a better understanding of the mechanism of material transport through the dryer, further analyses were carried out on the values of $\log_{10} \theta_m$ obtained at each level of the feed rate F.

These analysis produced the following relationships:

$$\text{at } F_1, \quad \log_{10} \theta_m = f(G) + f(R) + f(T)$$

$$\text{at } F_2, \quad \log_{10} \theta_m = f(G) + f(R)$$

11.4 Material Moisture Contents.

In studying the rotary dryer, there are several measurable quantities which characterise its drying performance. Since the rotary dryer is a continuous system any time-based characteristic, such as the rate of water evaporation in the dryer, is of secondary importance to the moisture content of the material in the dryer.

The change in material moisture content along the dryer, produced by various test conditions, may be represented either by the difference in material moisture content between two positions in the dryer or by the profile of the material moisture content along the dryer.

Since a moisture content difference is calculated from two moisture contents determined experimentally it is more susceptible to experimental error than the moisture content profile, which is computed from a number of similar moisture contents. Consequently, the moisture content profile was selected as a measure of the rotary dryer's efficiency providing that it could be evaluated in terms of a simple factor.

On constructing a profile, by drawing a curve through the moisture contents determined from samples extracted from the dryer, it was found that the profile was approximately linear. Assuming a linear profile, the values of the material moisture contents were subjected to a regression analysis, which was found to be highly significant. The value of the regression coefficient, b_r, therefore represented the moisture content profile of the material in the dryer.

The method of conducting the regression analysis is described in Appendix VII.

It is advantageous to consider the effect of the moisture content of the feed to the dryer on its drying performance, since the feed moisture content might vary from one set of test conditions to another. There were two possible factors producing this variation:

(1) The soaking conditions of the barley

(2) The conditions experienced by the barley prior to entering the dryer.

The effect of the first factor was minimised by using the same soaking conditions for each test. The second factor, however, could not be controlled directly, since the conditions existing in the feed chamber, through which the feed was conveyed, were dependent on the operating conditions inside the dryer. These conditions varied with the different combinations of test factors but were constant during a test when equilibrium conditions had been attained inside the dryer. Consequently, during the actual test period, the moisture content of the feed remained constant. This factor necessitated the determination of feed moisture contents by extrapolation from the moisture content profile and not from a direct moisture content determination of the barley in the feed hopper.

In order to investigate the effect of the feed moisture content on the moisture content profile of the barley in the dryer, three tests were performed under the same operating conditions but with varying feed moisture contents. The results of these tests given in Table 11.5, and shown in Fig. 11.1, indicate that the moisture content profile is dependent on the feed moisture content.

Table 11.5

Effect of Feed Moisture Content on the Value of b_r for the Rotary Drying of Barley.

Feed Moisture Content lb water/lb B.D.S.	$b_r \times 10^3$ lb water/lb B.D.S. in
0·510	8·83
0·685	9·55
0·880	11·70

In order to minimise the error caused by feed moisture content variation, the feed moisture contents in the tests of the factorial experiment were in the range 0·68 to 0·75

FIG 11.1

ROTARY DRYING OF BARLEY

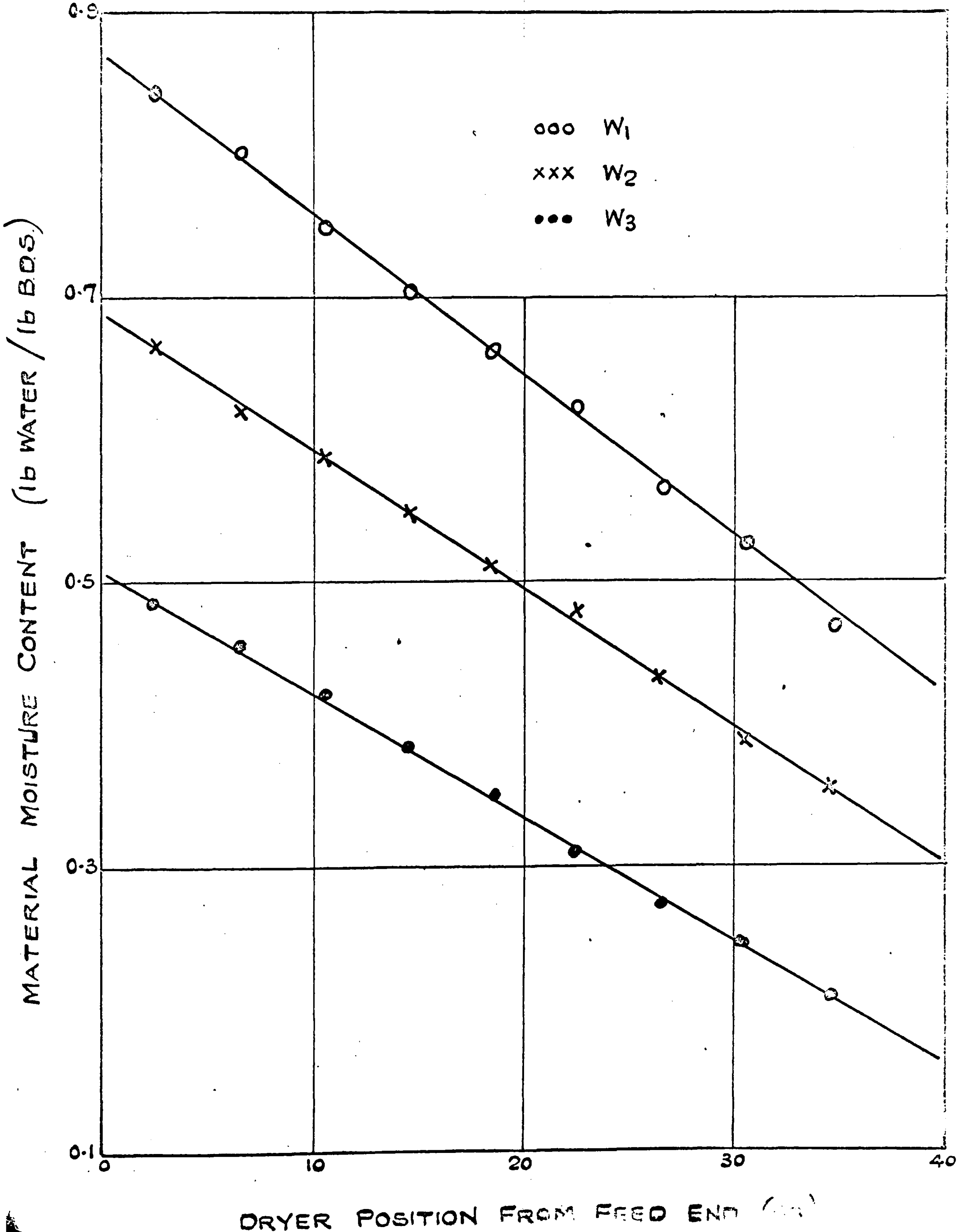

lb water/lb B.D.S.

The moisture content profiles obtained for each set of test conditions are shown in Figs. 11.2, 11.3, 11.4, and 11.5, and the values of the regression coefficients, b_r, computed for all the factorial tests are given in Table 11.6.

Table 11.6

Values of b_r for the Rotary Drying of Barley.

Test Conditions	$b_r \times 10^3$ lb water/ lb B.D.S.in	Test Conditions	$b_r \times 10^3$ lb water/ lb B.D.S.in
$F_1\ G_1\ R_1\ T_1$	8·75 8·63	$F_2\ G_1\ R_1\ T_1$	6·01 6·35
$F_1\ G_1\ R_1\ T_2$	9·59 11·15	$F_2\ G_1\ R_1\ T_2$	7·13 6·71
$F_1\ G_1\ R_2\ T_1$	7·09 7·67	$F_2\ G_1\ R_2\ T_1$	6·02 6·30
$F_1\ G_1\ R_2\ T_2$	9·64 9·69	$F_2\ G_1\ R_2\ T_2$	6·31 7·03
$F_1\ G_2\ R_1\ T_1$	10·70 10·60	$F_2\ G_2\ R_1\ T_1$	7·05 7·03
$F_1\ G_2\ R_1\ T_2$	12·65 11·94	$F_2\ G_2\ R_1\ T_2$	7·20 6·98
$F_1\ G_2\ R_2\ T_1$	9·37 8·58	$F_2\ G_2\ R_2\ T_1$	6·22 6·38
$F_1\ G_2\ R_2\ T_2$	9·27 10·06	$F_2\ G_2\ R_2\ T_2$	7·03 7·14

FIG 11.2

ROTARY DRYING OF BARLEY

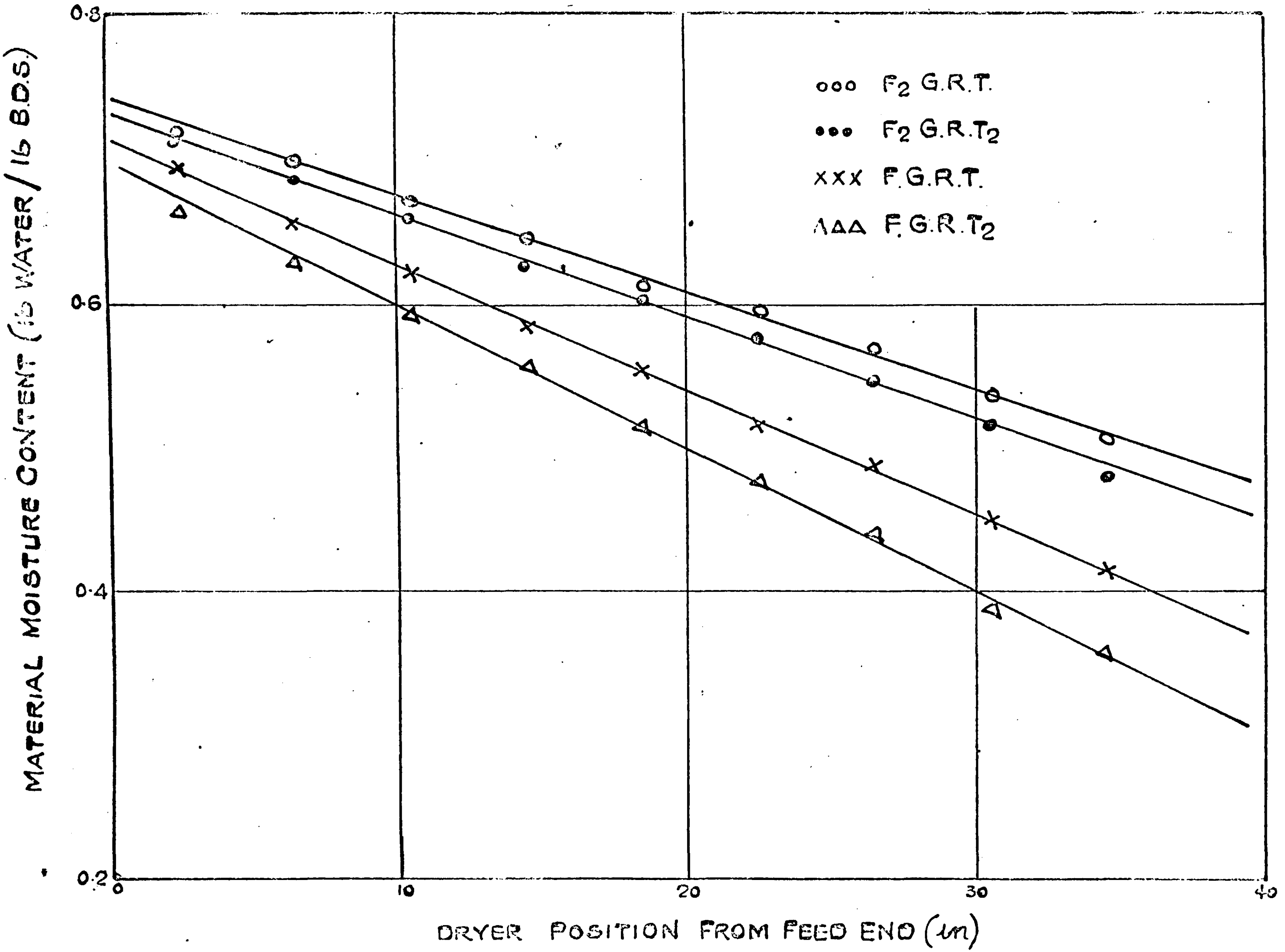

FIG 11.3
ROTARY DRYING OF BARLEY

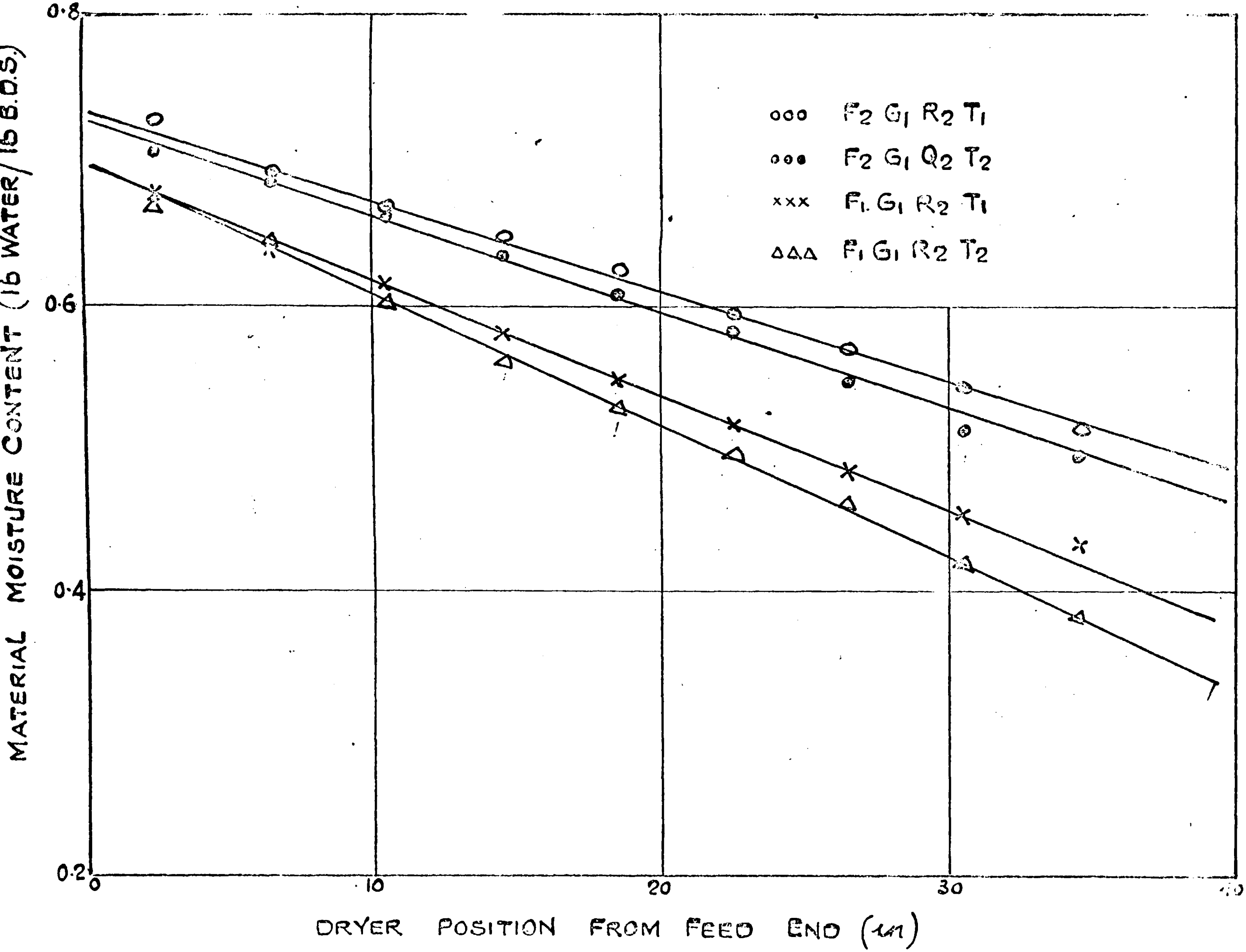

FIG 11.4

ROTARY DRYING OF BARLEY

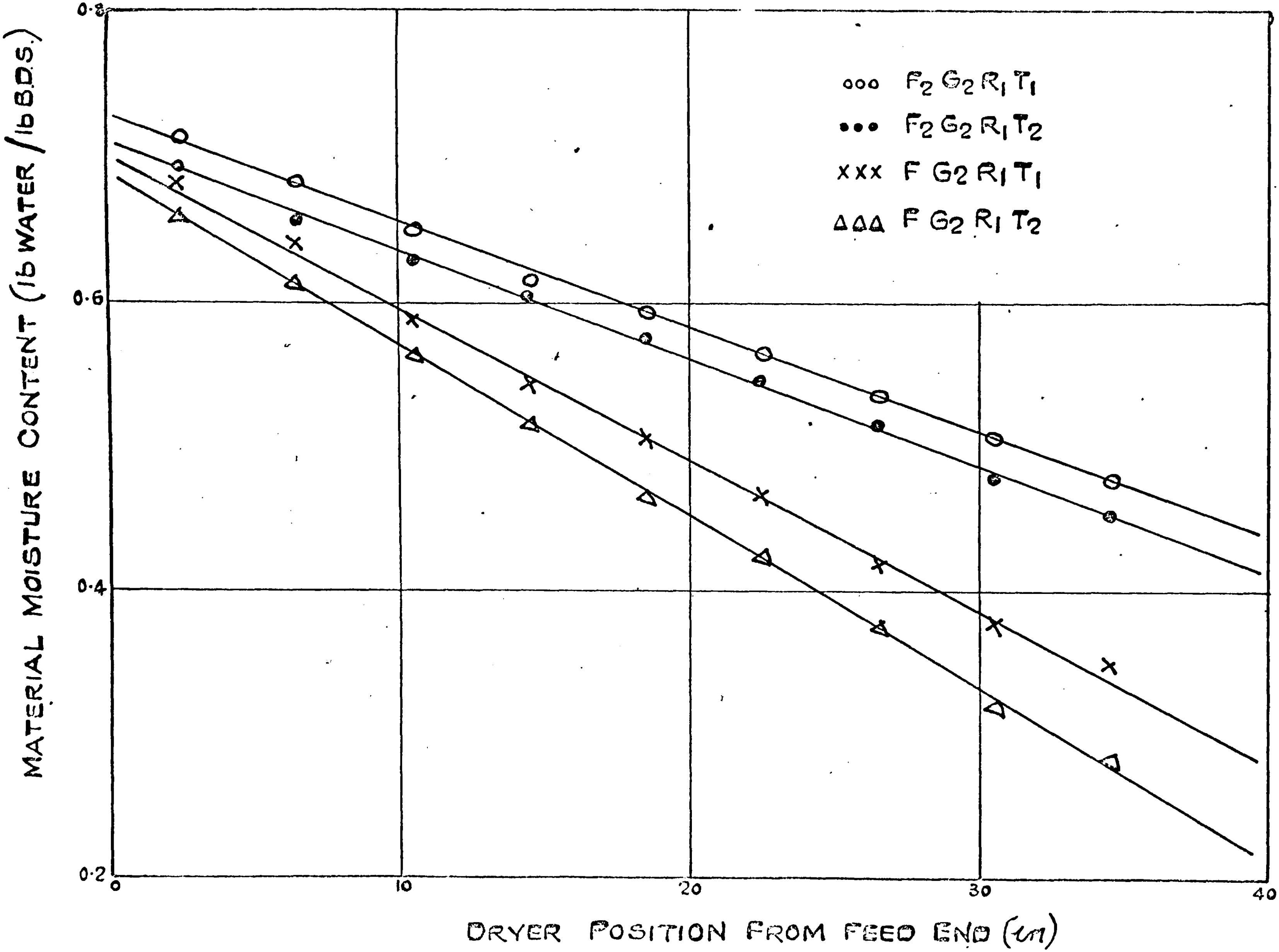

FIG 11.5

ROTARY DRYING OF BARLEY

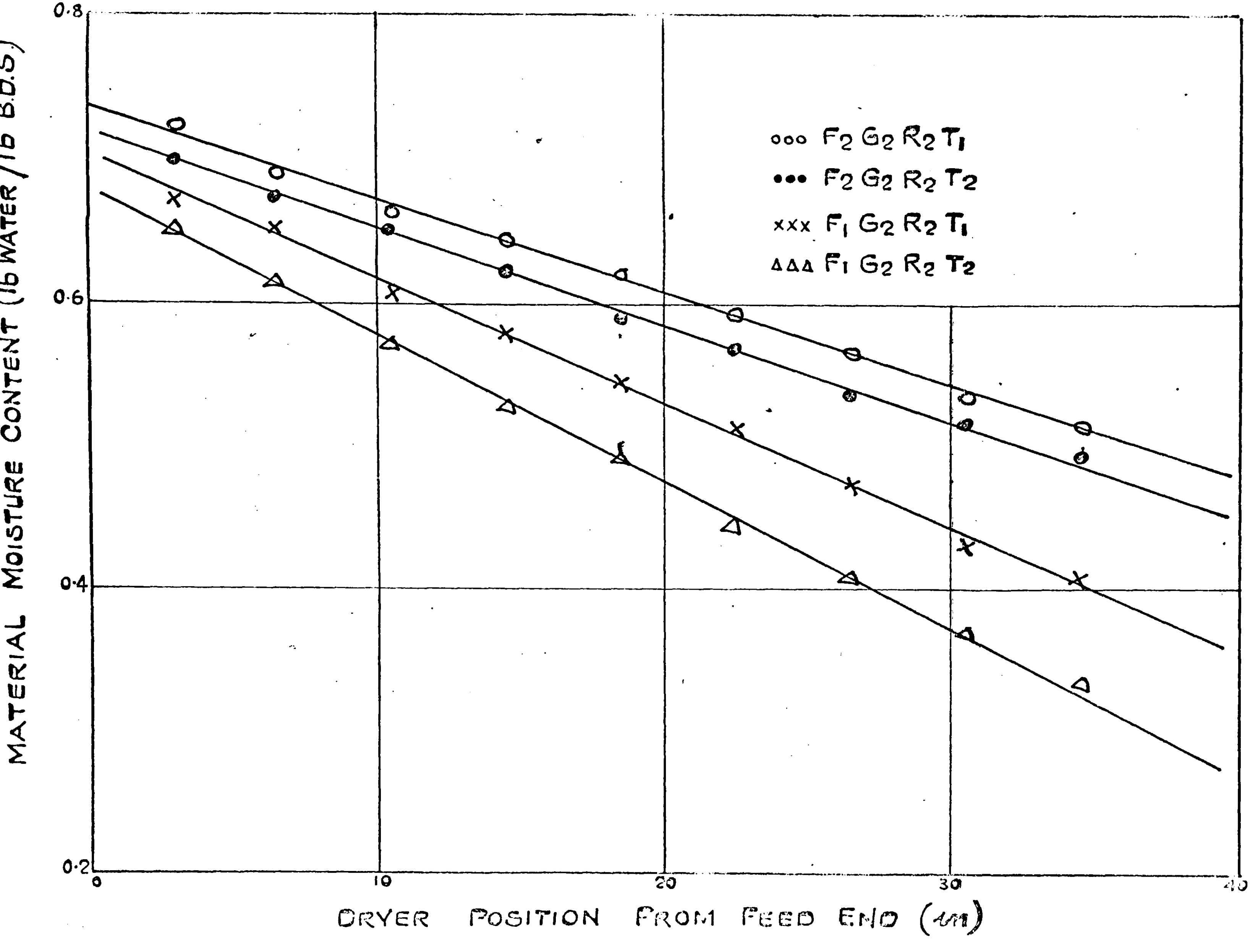

Values of log 1000b_r were subjected to an Analysis of Variance, the results of which are given in Table 11.7.

Table 11.7

Analysis of Variance on Values of $\log_{10}$ 1000b_r for the Rotary Drying of Barley.

Source of Variance	Degrees of Freedom	Crude Sum of Squares	Mean Sum of Squares
F	1	0·201390	0·201390
G	1	0·015488	0·015488
R	1	0·014999	0·014999
T	1	0·022535	0·022535
FG	1	0·002581	0·002581
FR	1	0·005708	0·005708
FT	1	0·002824	0·002824
GR	1	0·001501	0·001501
GT	1	0·002035	0·002035
RT	1	0·000253	0·000253
FGR	1	0·000290	0·000290
FGT	1	0·000604	0·000604
FRT	1	0·000056	0·000056
GRT	1	0·000011	0·000011
FGRT	1	0·002272	0·002272 *
Residual	16	0·006528	0·000408
Total	31	0·279075	

Effects and interactions, significant at the 5% probability level, are identified by an asterisk.

The Analysis of Variance indicated that the effect of the variables on the moisture content profile may be represented by the following expression:

$$\log_{10} 1000b_r = f(FGRT)$$

As in the results of the retention time of the material in the dryer, additional analyses were carried out on the values of $\log_{10} 1000b_r$ obtained at each level of the feed rate F. These analyses gave the following expressions:

$$\text{at } F_1, \quad \log_{10} 1000b_r = f(G) + f(R) + f(T)$$

$$\text{at } F_2, \quad \log_{10} 1000b_r = f(G) + f(T)$$

12. DISCUSSION

12.1 Introduction.

In the study of a system, the method of experimentation is an important factor to be considered. Most published work on rotary dryers has been based on the classical method of experimentation in which the effect of a factor on a system is determined by varying the factor while the other factors in the system are held constant at arbitrarily fixed values. This method is only strictly valid for simple systems in which the factors do not interact i.e. the effect of a factor is independent of the values of the other factors. This condition depends on the complexity of the system and a comprehensive study of a complex system is only attained when the effect of a factor is determined over a range of values of the other factors.

The rotary dryer is typical of a system in which the effects of several of the controlling factors are dependent upon the values of the factors. The effective study of a complex system may be achieved by using the factorial method of experimentation, which investigates the effect of a factor while the remaining factors vary over a range of values. In addition to its economic efficiency over the classical method, the factorial method enables a statistical analysis to be carried out on the test results. This analysis identifies real effects from those which are caused by random error.

This series of tests was concerned with the performance of a given dryer under various operating conditions and not with the dryer dimensions. The interest centred not in the material being dried but in the characteristics of the dryer. The statistical form of the tests resulted in the derivation of several expressions which contained functions of little physical significance. These functions, however, may be interpreted to give an insight into the complexities of the system enabling a limited amount of co-ordination of possible mechanisms to be achieved.

12.2 Material hold-up.

The regression analysis, which was carried out on the experimental hold-up values and the theoretical hold-up values calculated from equation (8.7) and is given in Table 11.2, indicated that this equation, proposed by Saeman and Mitchell, represents the transport of material through a rotary dryer.

This relationship contains an air velocity drift coefficient, m''', whose value depends on the dryer system. In these tests, the most satisfactory value of m''', which suited this system, was 0·002. This was less than the values used by Saeman and Mitchell for their dryer system. This difference in the values of m''', however, may be attributed partly to the difference in the dryer diameters in two systems.

If there is no kiln action in the dryer, i.e. all the material is lifted by the flights, the movement of a particle through the dryer consists of alternate periods of falling and drying (of duration θ_d) and of resting on a flight (of duration θ_p). In the dryer used in these tests, the distance through which a particle falls from a flight is less than the corresponding distance fallen in the dryer of larger diameter used by Saeman and Mitchell. Consequently, the ratio θ_d/θ_p, for the same dryer rotational speed, is less in a dryer of diameter of 5 in than in a dryer of diameter of 1 ft or more, and the drag effect of the air, which is directly proprotional to this ratio, will be less in the smaller dryer.

This confirms the work of Saeman and Mitchell, who suggested that the air velocity drift coefficient should be expressed as a function of the cascading period of the particle.

A comparison of the experimental and theoretical hold-up values, given in Table 11.1, revealed that the theoretical values were approximately 20% higher than the corresponding test values at low hold-up values. This discrepancy may be accounted for by the action of the barley as it strikes the dryer floor. At low hold-up values, the forward movement of the barley is accelerated by a bouncing effect as it strikes the glass floor of the dryer, whereas a cushioning effect, produced by a bed of barley on the dryer floor, is present at high hold-up values.

It was found that, on average, the theoretical hold-up values were higher than the test values by approximately 5%.

12.3 Material Retention Times.

Although the solids hold-up and retention times are related by equation:

$$\theta_m = \frac{A}{F} \qquad .....(12.1)$$

a comprehensive study of the retention time of the material is advantageous over a similar study of its hold-up, since θ_m is independent of small variations in F ; values of A, however, are directly proportional to small fluctuations in F. A consideration of retention times is important in the design of a counter-current dryer so that the maximum allowable solids temperature is not exceeded.

The statistical analysis of the test results shown in Table 11.4, indicated that, over the range of values studied, all the four factors, i.e. feed rate of material, inlet temperature and flow rate of the air stream and the rotational speed of the dryer, affected the retention time of the material and the interactions FG, FR and FT were significant at the 5% probability level. The overall effects of F and T, however, were insignificant at this level of significance.

The significance of the FT interaction, which means that the effect of the air inlet temperature is dependent on the level of the feed rate was confirmed by the additional analysis carried out on the results of the tests at F_1 and F_2. These analyses described in Section 11.3.2, revealed that the effect of T was significant at F_1 but insignificant at F_2. It is probable that, at the lower feed rate, an increase in air temperature reduces the moisture content and density of the barley particles thereby increasing the drag effect of the air and also the material retention time. This was verified by comparing the retention times given in Table 11.3 for each level of air temperature.

It was also eveident from the values of θ_m that the effect of G was reduced when the feed rate was increased; for instance, in the tests carried out at the level R_1T_1, the average increases in θ_m produced by increasing G were 7·5 min at F_1 and 1·3 min at F_2. This change in the effect of G is represented by the significance of the FG interaction in the analysis of variance.

The retention time is influenced by the type of particle movement which takes place at the foot of the cascading curtains of material. This movement depends on the conditions existing on the floor of the dryer. At the lower feed rate, the bed of material on the dryer floor is very thin and does not completely cover the dryer floor so that, when the falling material strikes the glass floor, it undergoes a bouncing movement which occurs in the direction of the dryer slope. At the higher feed rate, however, the dryer contains a thick bed of relatively soft material compared with glass and the bouncing motion of the cascaded material is reduced by the dampening effect of the bed of material on the dryer floor thereby increasing the retention time of the material in the dryer. The effect of this bouncing action will be greater at the faster rotational speed of the dryer when the particles on falling through the hot air strike the dryer bottom more frequently than at the slower dryer speed.

On examining further the values of θ_m in Table 11.3, it was found that the retention times at the higher dryer speed, conformed with the above picture in that the material retention time increased with the feed rate. At the lower dryer speed, however, the retention time decreased when the feed rate was increased. It is apparent, therefore, that the air and temperature effects described previously are the controlling effects at the lower dryer speed while the particles bouncing effect is controlling at the faster dryer speed.

Although the theoretical picture, presented above, is only representative of the conditions studied in this system, it infers that the type of particle movement occurring at the foot of the cascading curtains should be considered in the estimation of retention times at low hold-up values, the movement being dependent of the shape of the particle.

The insignificance of the overall effects of F and T conforms with the mechanism of material transport proposed by Saeman and Mitchell in their derivation of equation (6.7).

12.4 Moisture Content of Material.

The result of the analysis of variance, carried out on the logarithmic values of the moisture content profile coefficient b_r and given in Table 11.7, revealed that the coefficient was dependent on the feed rate of material, the dryer speed and the temperature and flow rate of the air. However, the significance of the interaction FGRT in the analysis indicated the complexity of the drying action taking place inside the dryer, the effect of each factor being dependent on the level of the other factors. Moreover the interaction prevented the elucidation of the drying mechanisms in a rotary dryer and the development of a simple, but comprehensive model to describe these mechanisms.

However, a little information may be gleaned from the analyses which were conducted on the values of $\log_{10} 1000b_r$ in the tests at each level of F. The results of these analyses given on page 149, indicated significant effects for the factors G, R and T at the level F_1, but at the F_2 level, only the factors G and T were significant.

The insignificance of the factor R at the F_2 level, which infers that the dryer speed does not affect the coefficients at the high feed conditions, may have been caused by the fact that, under high feed conditions, drying occurs slowly so that an increase in the speed of the dryer, which reduces the time during which the material is exposed to the drying conditions, doesnot significantly reduce the drying of the materia.

The linear variation of the moisture content of the barley as it progressed along the dryer simplified the method of presenting the results and enabled the efficiency of the dryer to be evaluated in terms of a single factor.

13. CONCLUSIONS.

The application of the factorial method of experimentation to the drying of barley in a rotary dryer has shown that the effects of the dominant factors in the system, i.e. the air flow, air temperature, dryer speed, and feed rate of the barley, cannot be determined independently of each other but are combined in interacting groups of factors.

The linear profile of the moisture content of the material in the dryer simplified the method of presenting the results, but the effect of each factor on the profile coefficient was found to be dependent on the values of the other three factors, the interaction FGNT being significant in the analysis of variance at the 5% level of probability. Unfortunately, this interaction prevented a lucid interpretation of the tests results, and the extension of the factorial experiment to a third level, which is necessary for the prediction of moisture content profiles, was not considered to be merited.

The hold-up and retention time of the material in the dryer conformed to the model proposed by Saeman and Mitchell for the transport of material through a rotary dryer, although at low hold-up values the rate at which material progressed through the dryer was increased by a bouncing motion which the material experienced as it struck the floor of the dryer. Under these conditions, the experimental hold-up values were

20% less than the corresponding values predicted from the expression of Saeman and Mitchell.

<u>Suggestions for Future Work.</u>

The experimental results upon which the foregoing conclusions were based may have depended considerably on the small scale of the dryer used in the tests as the ratio of the periods during which the material is being dried or resting on a dryer flight is considerably less in the pilot dryer than in commercial dryers of 10 ft. or more in diameter.

One method of overcoming this scale-up problem is either to increase the rotational speed of the smaller dryer or to decrease the speed of the large dryer. Although in these circumstances the times during which the material in the two dryers is exposed to the hot air stream would be comparable, it would create other conditions which are not comparable and furthermore, which are not consistent with industrial practice. It is quite probable, therefore that for satisfactory reproducibility of results and compatibility with industrial dryers, the diameters of pilot scale dryers should be greater than a minimum limiting value.

In any future work, it is suggested that the diameter of any small scale dryer be at least 2 ft. in diameter although this would require using feed rates twenty times as great as that used in the present work and almost puts such a dryer in the semi-production class. The length of the dryer should be sufficient to give a satisfactory difference in inlet and exit conditions.

It is difficult to forecast whether the application of the factorial method of application to the operation of a larger diameter dryer would lead to the derivation of simpler expressions as previous studies reported in the literature have shown that the mechanism by which drying takes place in a rotary dryer is rather complex and difficult to predict accurately. However, it may well be that the effect of feed rate alone would be less pronounced but at the same time it could possibly emphasise the importance of treating dryer hold-up as a separate factor in rotary dryer design.

In order to determine the dominant factors in a rotary dryer system and as a result predict the performance of a rotary dryer, the following method of experimentation is suggested:-

(1) a preliminary two-level factorial experiment treating the eleven dryer design factors given on page 135 in groups of four

(2) a factorial three-level experiment to elucidate any interactions produced in the preliminary tests.

It is possible that to carry out these experiments, factors which are generally accepted as being independent of each other may have to be grouped together to form secondary factors.

However, until such an experimental programme is successfully carried out it is evident that the most reliable results for dryer design are obtained from full scale industrial dryers.

14. REFERENCES.

1. Treybal, R.E. "Mass Transfer Operations", 1955. (New York: McGraw-Hill.)

2. Norman, W.S. "Absorption, Distillation and Cooling Towers", 1961. (London: Longmans.)

3. Sherwood, T.K., and Pigford, R.L. "Absorption and Extraction", 2nd Edn., 1952. (New York: McGraw-Hill.)

4. Whitman, W.G. Chem. and metall. Engng, 1923, 29, 147.

5. Gilliland, E.R., and Sherwood, T.K. Ind. Engng Chem., 1934, 26, 516.

6. Morris, G.A., and Jackson, J. "Absorption Towers", 1953. (London: Butterworth.)

7. McCarter, R.J., and Stutsman, C.F. A.I.Ch.E.Jl, 1959, 5, 502.

8. Norman, W.S., and Sammak, F.Y.Y. Trans. Instn chem. Engrs, 1963, 41, 109.

9. Calderbank, P.H., and Moo-Young, M.B. "International Symposium on Distillation", 1960. (London: The Institution of Chemical Engineers.)

10. Higbie, R. Trans. Am. Instn chem. Engrs, 1935, 31, 365.

11. Danckwerts, P.V. Ind. Engng Chem., 1951, 43, 1460.

12. Kishinevskii, M.Kl. Journal of Applied Chemistry,

U.S.S.R., 1954, 27, 4, 382.

13. Kishinevskii, M.Kh., and Macholova, I. ibid., 1958, 31, 1013.

14. Danckwerts, P.V. A.I.Ch.E.Jl, 1955, 1, 456.

15. Hanratty, T.J. ibid., 1956, 2, 359.

16. Toor, H.L., and Marchello, J.M. ibid., 1958, 4, 1, 97.

17. Carberry, J.J. ibid., 1960, 6, 460.

18. Colburn, A.P. Trans. Am. Instn chem. Engrs, 1933, 29, 174.

19. Chilton, T.H., and Colburn, A.P. Ind. Engng Chem., 1934, 26, 1183.

20. Gamson, B.W., Hougen, O.A., and Thodos, G. Trans. Am. Instn chem. Engrs, 1943, 39, 1.

21. Heergees, F.H., and Ringens, W.P. Chem. Engng Sci., 1956, 5, 226.

22. De Acetis, J., and Thodos, G. Ind. Engng Chem., 1960, 52, 12, 1003.

23. Gupta, S., and Thodos, G. A.I.Ch.E.Jl, 1963, 9, 6, 751.

24. McCune, L.K., and Whilhelm, R.H. Ind. Engng Chem., 1949, 41, 1124.

25. Taecker, R.C., and Hougen, O.A. Chem. Engng Prog., 1949, 45, 188.

26. Gaffney, B.J., and Drew, T.B. Ind. Engng Chem., 1950, 42, 1120.

27. Dryden, C.E., Strang., D.A., and Withrow, A.E. Chem. Engng Prog., 1953, 49, 191.

28. Satterfield, C.N., and Resnick, W. ibid., 1954, 50, 504.

29. Resnick, W., and White, R.R. ibid., 1949, 45, 377.

30. Hurt, D.M. Ind. Engng Chem., 1943, 35, 522.

31. Bar-Ilan, M., and Resnick, W. Ind. Engng Chem., 1957, 49, 2, 313.

32. Bradshaw, R.D., and Bennett, C.D. A.I.Ch.E.Jl., 1961, 7, 1, 48.

33. Bradshaw, R.D., and Myers, J.E. ibid., 1963, 9, 5, 590.

34. Wilson, E.J., and Geankoplis, C.J. Ind. Engng Chem. Fundamentals, 1966, 5, 1, 9.

35. Gupta, S., and Thodos, G. Chem. Engng Prog. 1962, 58, 7, 58.

36. Chu, J.C., Kalil, J., and Wetteroth, W.A. ibid., 1953, 49, 141.

37. Ergun, S. ibid., 1952, 48, 5, 227.

38. McConnachie, J., and Thodos, G. A.I.Ch.E.Jl, 1963, 9, 1, 60.

39. Wilke, C.R., and Hougen, O.A. Trans. Am. Instn chem. Engrs, 1945, 41, 445.

40. Shulman, H.L., and De Gouff, J.I. Ind. Engng Chem., 1952, 44, 1915.

41. Shulman, H.L., Ulrick, C.F., and Wells, N. A.I.Ch.E.Jl, 1955, 1, 247.

42. Shulman, J.L., Ulrick, C.F., and Proulx, A.A., and Zimmerman, J.O. ibid., 1955, 1, 2, 253.

43. Shulman, H.L., Ulrick, C.F., Wells, N., and Proulx, A.Z. ibid., 1955, 1, 259.

44. Shulman, H.L., and Margolis, J.E. ibid., 1957, 3, 2, 157.

45. Gupta, S., and Thodos, G. ibid., 1962, 8, 5, 608.

46. Hobson, M., and Thodos, G. Trans. Am. Instn chem. Engrs, 1949, 45, 135.

47. Evans, G.C., and Gerald, C.F. Chem. Engng Prog., 1953, 49, 135.

48. Sharples, K., Glikin, P.G., and Warne, R. Trans. Instn chem. Engrs, 1964, 42, T275.

49. Glaser, M.B., and Thodos, G. A.I.Ch.E.Jl, 1958, 4, 1, 63.

50. Baumeister, E.B., and Bennett, E.O. ibid., 1958, 4, 1, 69.

51. Evonchiles, S., and Thodos, G. ibid., 1961, 7, 1, 78.

52. Yen, Y., and Thodos, G. ibid., 1962, 8, 1, 34.

53. Garner, F.H., and Suckling, R.D. ibid., 1958, 4, 1, 114.

54. Dickie, W.S. Chem. and metall. Engng, 1939, 46, 526.

55. Perry, J.H. "Chemical Engineering Handbook", 4th Edn.,

1963, (New York: McGraw-Hill).

56. B.P. 160, 358.

57. U.S.P. 2,378,186.

58. B.P. 605,221.

59. Ware, L.A. "Beet Sugar Manufacture", 1905. (London: Chapman and Hall).

60. Clark, D.E., Pratt, L.D., Coleman, S.A., and Green, H.C. U.S.P. 2,350,209.

61. Spraul, J.R. Ind. Engng Chem., 1955, 47, 368.

62. Saeman, W.C. Chem. Engng Prog., 1962, 58, 49, 56.

63. Lapple, W.C., Clark, W.E., and Dybdal, E.C. Chem. Engng, 1955, 62, 11, 177,

64. Friedman, S.J., and Marshall, W.R. Chem. Engng Prog., 1949, 45, 8, 482.

65. Saeman, W.C., and Mitchell, T.R. ibid., 1954, 50, 467.

66. Miskell, F., and Marshall, W.R. ibid., 1949, 45, 9, 573.

67. Smith, B.A. Private Communication.

68. Sullivan, J.D., Maier, G.C., and Ralston, O.C. U.S. Bureau of Mines, Technical Paper No. 384, 1927.

69. Ginstling, A.M., Silberman, D.M., and Gvozdev, N.V. Khim. Mashino Stroenie, 1939, 8.

70. Saeman, W.C. Chem. Engng Prog., 1951, 47, 509.

71. Smith, B.A. Ind. Engng Chem., 1938, 30, 993.

72. Poutton, C.G., Miller, C.O., and Schuette, W.H. Trans. Am. Instn chem. Engrs, 1942, 38, 123.

73. Porter, S.J., and Masson, W.G. Proceedings, No. 61, The Fertiliser Society, 1960.

74. Miller, C.O., Smith, B.A., and Schuette, W.H. Trans. Am. Instn chem. Engrs, 1942, 38, 841.

75. Friedman, S.J., and Marshall, W.R. Chem. Engng Prog., 1949, 45, 573.

76. McCormick, P.Y. ibid., 1962, 58, 6, 57.

77. Kawabuti, H. Chem Engng (Japan), 1956, 20, 223.

78. Inasumi, H. ibid., 1953, 17, 58.

79. Porter, S.J. Trans. Instn chem. Engrs, 1963, 41, 273.

80. Brownlee, K.A. "Industrial Experimentation", 4th Edn., 1949. (H.M.S.O.: London).

81. Fisher, R.A. "The Design of Experiments", 4th Edn., 1947. (London: Oliver and Boyd).

82. Yates, F. "Design and Analysis of Factorial Experiments" 1937. (Harpenden: Imperial Burea of Soil Science).

83. Davies, O.L. "Statistical Methods in Research and Production", 1947. (London: Oliver and Boyd).

84. Davies, O.L. "The Design and Analysis of Industrial Experiments", 1954. (London: Oliver and Boyd).

85. Cox, D.R. "Planning of Experiments", 1958. (London: Chapman and Hall).

86. Bennett, C.A., and Franklin, N.L. "Statistical Analysis in Chemistry and in the Chemical Industry",

1954, (New York: Wiley and Sons).

87. Lindley, D.V., and Miller, J.C.P. "Cambridge Elementary Statistical Tables", 1958. (Cambridge: University Press).

88. Smith, J.C. Ph.D. Thesis, 1959. (Glasgow University).

89. Wadell, H. <u>Journal of Franklin Institute</u>, 1934, <u>217</u>, 459.

90. Leva, M. "Fluidisation", 1959. (New York: McGraw-Hill).

91. Leva, M., Weintraub, M., Grummer, M., Pollchik, M., and Storch, H.H. <u>U.S. Bur. Mines Bull</u>., 1951, 504.

92. Dallavalle, J.M. "Micromeritics", 2nd Edn., 1948. (London: Pitman and Sons.).

93. Heywood, H. <u>Proc. Instn mech. Engrs</u>, 1938, <u>140</u>, 25

94. Heywood, H. "Symposium on Particle Size Analysis", 1947. (London: The Institution of Chemical Engineers

95. Heywood, H. "Symposium on Interaction Between Fluids and Particles", 1962. (London: The Institution of Chemical Engineers.).

96. Green, H. <u>Journal of Franklin Institute</u>, 1927, <u>192</u>, 637.

97. Martin, G. <u>Trans. Brit. Ceram. Soc</u>., 1923, <u>23</u>, 61.

98. Fair, G.M., and Hatch, L.P. <u>Jl. Am. Water Works Assoc</u>. 1933, <u>25</u>, 1551.

99. Blake, F.C. <u>Trans. Am. Instn chem. Engrs</u>, 1922, <u>14</u>, 415.

100. Schiller, L. Z. angur. Math. Mech., 1923, 3, 2.

101. Kozeny, J. S.B. Akad. Wiss. Wien, Abt. IIa, 1927, 136, 271.

102. Ergin, S., and Orning, A.A. Ind. Engng Chem., 1949, 41, 1179.

103. Carman, P.C. Trans. Instn. chem. Engrs, 1937, 15, 150.

104. Muskat, M., and Botset, H.G. Physics, 1931, 1, 27.

105. Coulson, J.M. Trans. Instn chem. Engrs, 1949, 27, 237.

106. Wyllie, M.R.J., and Gregory, A.R. Ind. Engng Chem., 1955, 47, 1379.

107. Evans, P.E., and Millman, R.S. "Perspectives in Powder Metallurgy", 1967. (New York: Plenum Press.

108. Orr, C. "Particulate Technology", 1966. (New York: Macmillan.).

109. Gray, W.A. "The Packing of Solid Particles", 1968. (London: Chapman and Hall.).

NOMENCLATURE

A	=	drying surface available (ft^2)
a_s	=	active surface area (ft^2)
a, a_1, a_2, a_3	=	empirical constants
A_p	=	surface area of particle (in^2 or ft^2)
a_p	=	specific surface area of packed bed (ft^2/ unit vol of bed)
$A(x)$	=	empirical constant
b, b_1, b_2, b_3	=	regression coefficients
b_R	=	regression coefficient (lb water/lb B.D.S. in)
C	=	material cascade rate (ft^3/ft^2 min or lb/ min)
C_p	=	specific heat capacity at constant pressure (Btu/lb ^oF or Chu/lb ^oC)
D_c	=	diameter of column (ft)
d_p or D_p	=	particle diameter (in or ft)
D_R	=	diameter of dryer (ft)
D_v	=	diffusivity (cm/s or ft/h)
F	=	feed rate (lb B.D.S./h)
F'	=	feed rate (lb B.D.S./min)
F'_v	=	feed rate (ft^3/ft^2 of dryer cross section)
f	=	shape factor
G	=	mass air velocity (lb/h ft^2 of dryer cross section)

G'	=	mass air velocity (lb/h)
h_g	=	heat transfer coefficient (Chu/h ft^2 ^oC)
h'_g	=	modified heat transfer coefficient (Chu/h ft^2 ^oC)
K_c	=	mass transfer coefficient (ft/h)
K_g	=	mass transfer coefficient (lb/h ft^2 unit humidity difference)
K'_g	=	modified mass transfer coefficient (lb/h ft^2 unit humidity difference)
K_p	=	mass transfer coefficient (lb mol/h ft^2 atm.)
K'	=	empirical constant
K''	=	empirical constant
L	=	liquid velocity (lb/h ft^2)
L_h	=	latent heat (Chu/lb)
L_R	=	length of rotary dryer (ft)
m', m'', m'''	=	air velocity coefficients
N	=	$dw/d\theta$ = drying rate (lb water/h)
N	=	mass transfer rate of diffusing component A (lb mol/h ft^2)
N'	=	$dw'/d\theta$ = drying rate (lb water/lb B.D.S. h)
N'_c	=	constant drying rate (lb water/lb B.D.S. h)
N_f	=	number of flights
p	=	partial pressure of component (atm.)

Q = heat transfer rate (Btu/h or Chu/h)

q = heat transfer rate (Chu/h ft^2)

N = rate of rotation of dryer (rev/min)

S_d = slope of dryer, (ft/ft)

t = temperature (^oC)

U = air velocity (superficial) (ft/sec)

U_v = overall volumetric heat transfer coefficient (Btu/h ft^3)

V = air velocity (ft/min)

V_s = velocity of material in rotary dryer (in/min)

w = weight of water (lb)

w_B = bed loading (lb B.D.S./ft^2 of dryer cross section)

w_c = critical moisture content (lb water/lb B.D.S.)

w_e = equilibrium moisture content (lb water/lb B.D.S.)

w_s = weight of bone dry solid (B.D.S.) (lb)

W' = $\frac{w}{w_s}$ = moisture content (lb water/lb B.D.S.)

X = dryer hold-up (lb B.D.S.)

X_a = dryer hold-up corrected for air flow (lb)

X_f = flight loading (ft^3/ft^2 or lb/ft)

X_L = hold-up in dryer (lb B.D.S./in)

X' = percentage hold-up

Z = height of bed (in)

ω_f	=	radial flight depth (ft)
ω_r	=	thickness of laminar film (ft)
μ	=	viscosity of fluid (lb/h ft)
λ	=	thermal conductivity (Chu/h ft ^oC)
γ	=	dynamic angle of repose of material (deg)
$(\Delta t)_m$	=	log mean temperature differential (^oF or ^oC)
θ	=	time (h)
θ_{em}	=	estimated retention time (min)
θ_m	=	retention time (min)
θ_R	=	retention time (h)
θ'	=	time (min)
φ	=	fraction of surface taking part in transfer process.

Subscripts

o	=	outlet
i	=	inlet
a	=	air
s	=	saturation or surface

Appendix I

Specimen Results of Drying Test in the Experimental Through-circulation Dryer.

Series 1 pellets. Test No. 38

Drying Conditions: Air rate 720 lb/h ft^2 dryer area

Inlet air temperature 50°C

" " humidity 0·00737 lb water/lb dry air.

Time min	Weight of bed (lb)	Weight of water in bed (lb)	Moisture content of pellets (lb water/lb B.D.S.)
0	5·035	1·233	0·324
2	4·870	1·068	0·281
3	4·783	0·981	0·258
4	4·693	0·891	0·234
5	4·603	0·801	0·211
6	4·513	0·711	0·187
7	4·426	0·624	0·164
8	4·348	0·546	0·144
10	4·214	0·412	0·108
12	4·091	0·289	0·076
14	3·989	0·187	0·049
16	3·914	0·112	0·029
18	3·861	0·059	0·016

Moisture content of pellets at end of test = 1·53%

Weight of B.D.S. in bed $= 3{\cdot}861 - \frac{1{\cdot}53 \times 3{\cdot}861}{100}$ lb

$= 3{\cdot}802$ lb

Appendix II

Calculation of Transfer Coefficients and Factors.

A specimen calculation of k_g, h_g, j_h, and j_d is presented for test No. 38 of Series 1 pellets.

Experimental Data

Air mass rate	=	720 lb/h
Inlet air dry bulb temperature (t_{ia})	=	50·0°C
Outlet air dry bulb temperature (t_{oa})	=	27·6°C
Outlet air wet bulb temperature (t_{ow})	=	22·6°C
Ambient air dry bulb temperature (t_a)	=	19·0°C
Ambient air wet bulb temperature (t_w)	=	13·7°C
Atmospheric pressure	=	769·8 mm Hg
Constant drying rate	=	5·40 lb water/h
Weight of bone dry solid	=	3·802 lb

Calculation of k_g.

k_g is calculated from the following basic equation:

$$N_c = k_g \, A \, (\Delta H)_{lm} \qquad \text{.....(A.2.1)}$$

$$N_c = 5{\cdot}40 \text{ lb water/h}$$

$$A = 13{\cdot}54 \text{ ft}^2$$

Calculation of $(\Delta H)_{lm}$.

$(\Delta H)_{lm}$ is defined by the equation:

$$(\Delta H)_{lm} = \frac{(H_{is} - H_{ia}) - (H_{os} - H_{oa})}{\log \frac{(H_{is} - H_{ia})}{(H_{os} - H_{oa})}} \qquad \ldots.(A.2.2)$$

The inlet air humidity H_{ia} is calculated from the ambient air conditions using the following pyschrometric equation relating humidity to the wet bulb depression:

$$H_w - H_{ia} = \frac{0.26}{L_h}(t_a - t_w) \qquad \ldots.(A.2.3)$$

where H_w = saturation humidity corresponding to t_w

From a psychrometric chart, the saturation humidity corresponding to a wet bulb temperature of 13.7°C is 0.00970 lb water/lb dry air.

$$\therefore \quad H_{ia} = 0.00970 - \frac{0.26}{590}(19.0 - 13.7)$$

$$= 0.00737 \text{ lb water/lb dry air}$$

The inlet saturation humidity H_{is}, is the saturation humidity corresponding to the inlet air wet bulb temperature. The latter was determined from the inlet air humidity (i.e the ambient air humidity) and the inlet air dry bulb temperature.

In this test, the wet bulb temperature corresponding to a dry bulb temperature of 30.0°C and a humidity of 0.00737 lb water/lb dry air was 24.0°C. From a psychrometric chart,

$$H_{is} = 0.01867 \text{ lb water/lb dry air}$$

The outlet air humidity H_{oa} is computed from equation (A.2.3) using the outlet air conditions of t_{oa} = 27.6 and t_{ow} = 22.6

Whence H_{oa} = 0.01488 lb water/lb dry air

From a pyschrometric chart, the saturation humidity corresponding to a wet bulb temperature of 22·6°C is 0·01711 lb water/lb dry air.

i.e. outlet saturation humidity

$$H_{os} = 0{\cdot}01711 \text{ lb water/lb dry air}$$

Hence

$$(\Delta H)_{lm} = \frac{(0{\cdot}01867-0{\cdot}00737)-(0{\cdot}01711-0{\cdot}01486)}{\log \frac{1130}{223}}$$

$$= 0{\cdot}005589 \text{ lb water/lb dry air}$$

Substituting in equation (A.2.1) and rearranging,

$$k_g = \frac{5{\cdot}40}{0{\cdot}005589 \times 13{\cdot}54}$$

$$= 71{\cdot}36 \text{ lb water/h ft}^2 \text{ unit } \Delta H$$

<u>Calculation of h_g.</u>

h_g is computed from the following general heat transfer equation:

$$q = h_g\, A\, (\Delta t)_{lm} \quad \ldots.(A.2.4)$$

$$q = N_c \times L_h \quad \ldots.(A.2.5)$$

$$= 5{\cdot}40 \times 584{\cdot}8 \text{ Chu/h}$$

$$= 3158 \text{ Chu/h}$$

$$A = 13{\cdot}54 \text{ ft}^2$$

$$(\Delta t)_{lm} = \frac{(t_{ia} - t_{iw}) - (t_{iw} - t_{ow})}{\log \dfrac{t_{ia} - t_{iw}}{t_{oa} - t_{ow}}}$$

where

$$t_{ia} = 50{\cdot}0^{\circ}C$$

$$t_{iw} = 24{\cdot}0^{\circ}C$$

$$t_{ow} = 22{\cdot}6^{\circ}C$$

$$t_{oa} = 27{\cdot}6^{o}C$$

hence $$(\Delta t)_{lm} = \frac{(50{\cdot}0 - 24{\cdot}0) - (27{\cdot}6 - 22{\cdot}6)}{\log \frac{26{\cdot}0}{5{\cdot}0}}$$

$$= 12{\cdot}74^{o}C$$

Substituting in equation (A.2.4) and rearranging it,

$$h_g = \frac{3158}{13{\cdot}54 \times 12{\cdot}74}$$

$$= 18{\cdot}31 \text{ Chu/h ft}^2 \,{}^{o}C$$

Calculation of j_d.

The mass transfer factor j_d, originally derived by Chilton and Colburn, is defined for this system by the equation:

$$j_d = \frac{k_g}{G} Sc^{0{\cdot}67} \qquad \ldots.(A.2.6)$$

where the Schmidt number, Sc, is evaluated at the average film temperature.

Film Temperature.

Mean air temperature $= \frac{50{\cdot}0 + 27{\cdot}6}{2} = 38{\cdot}8^{o}C$

Assuming the surface temperature of the pellets to be at the wet bulb temperature of the air,

Mean pellet temperature $= \frac{24{\cdot}0 + 22{\cdot}6}{2} = 23{\cdot}3^{o}C$

$\therefore$ Mean film temperature $= \frac{38{\cdot}8 + 23{\cdot}3}{2} = 31{\cdot}0^{o}C$

Calculation of Sc.

$$Sc = \frac{\mu}{\rho D_v}$$

From International Critical Tables,

$$D_v = 0.220 \frac{(T)^{1.75}}{(273)} \ ft^2/h$$

$$= 0.220 \frac{(304)^{1.75}}{(273)} = 1.024 \ ft^2/h$$

$$\rho = \frac{0.001293}{(1 + 0.00367t)} \times \frac{P}{76} \ gm/ml$$

$$= \frac{0.001293}{(1 + 0.00367 \times 31)} \frac{77.0}{76} \ gm/ml$$

$$= 0.00116 \ gm/ml$$

$$= 0.0725 \ lb/ft^3$$

From International Critical Tables,

$$\mu = 0.0450 \ lb/ft \ h$$

$$Sc = \frac{0.045}{0.0725 \times 1.024}$$

$$= 0.606$$

Substituting in equation (A.2.6),

$$j_d = \frac{71.36}{720} (0.606)^{0.67}$$

$$= \underline{0.0710}$$

Calculation of j_h.

The heat transfer factor j_h, analogous to j_d, is given by the equation:

$$j_h = \frac{h}{C_p G} Pr^{0.67} \qquad \ldots.(A.2.$$

the Prandtl number Pr being evaluated at the average film temperature of 31·0°C.

Evaluation of Pr.

$$Pr = \frac{C_p \mu}{\lambda}$$

$$C_p = 0{\cdot}24 \text{ Chu/lb}$$

$$\lambda = 0{\cdot}01453 \text{ Chu/h ft } ^\circ C$$

$$\mu = 0{\cdot}0450 \text{ lb/h ft}$$

$$\therefore Pr = \frac{0{\cdot}24 \times 0{\cdot}045}{0{\cdot}0145}$$

$$= 0{\cdot}744$$

Substituting in equation (A.2.7),

$$j_h = \frac{18{\cdot}31}{0{\cdot}24 \times 720} \times (0{\cdot}744)^{0{\cdot}67}$$

$$= \underline{0{\cdot}0870}$$

Appendix III

Correction of Transfer Coefficients for Bed Depth Effect.

As discussed in Section 6.1.2 on page 45, the values of h_g and k_g were modified for the effect of bed depth by multiplying them by a correction factor which was defined as:

$$c.f. \quad = \quad \frac{\text{Area under log. mean curve}}{\text{Area under curve drawn through outlet temp driving forces at intermediate bed depths.}}$$

A description is now given for the derivation of the correction factors used in the modification of the values of h_g obtained in the tests carried out with the 1·5 in and 2 in beds of Series 1 pellets using an air rate of 300 lb/h ft^2 and an inlet temperature of 60^{o}C.

The experimental data required for the calculation of the factors are given below:

Bed depth Inches	Temperatures ^{o}C			
	Inlet		Outlet	
	Dry Bulb	Wet Bulb	Dry Bulb	Wet Bulb
1	60·2	26·7	29·4	25·2
1·5	60·2	25·7	27·7	24·3
2	60·0	26·1	25·9	23·9

Average inlet conditions: dry bulb temperature = 60·1^{o}C

wet bulb temperature = 26·2^{o}C

Hence average inlet temperature differential = 33·9^{o}C

Log. Mean Driving Force.

The log mean curve was constructed for the 2 in bed by plotting the inlet and outlet temperature differentials on semi-log graph paper as shown in Fig. A.3.1. From the curve, values of Δt were interpolated at bed depths of 0·33, 0·67, 1·0, 1·33 and 1·67 inches and substituted with the inlet and outlet values of Δt in Weddle's formula, to determine the area under the curve which is a measure of log mean driving force. Weddle's formula may be expressed as:

$$\text{Area under curve} = x_6 - x_o \; (y_o + 5y_1 + y_2 + 6y_3 + y_4 + 5y_5 + y_6) \qquad \text{....(A.3.1)}$$

where x = bed depth (in)

y = Δt (C deg)

The subscripts 0 to 6 correspond to the range of bed depth. Substituting the values of Δt from the log mean curve in equation (A.3.1),

$$\text{Area under curve} = \frac{2 - 0}{20} (33{\cdot}9 + 5\text{x}21{\cdot}3 + 13{\cdot}2 + 6\text{x}8{\cdot}25 + 5{\cdot}22 + 5\text{x}3{\cdot}21 + 2{\cdot}0)$$

$$= 22{\cdot}64 \text{ in C deg}$$

Actual Driving Force.

A measure of the actual driving force in the 2 in beds was obtained by plotting the outlet temperature differentials, obtained at the 1, 1·5 and 2 in bed depths, against bed depth and determining the area under curve from Weddle's equation. The plot of Δt against Z is shown in Fig. A.3.2.

FIG A.3.1

LOG MEAN TEMPERATURE CURVE

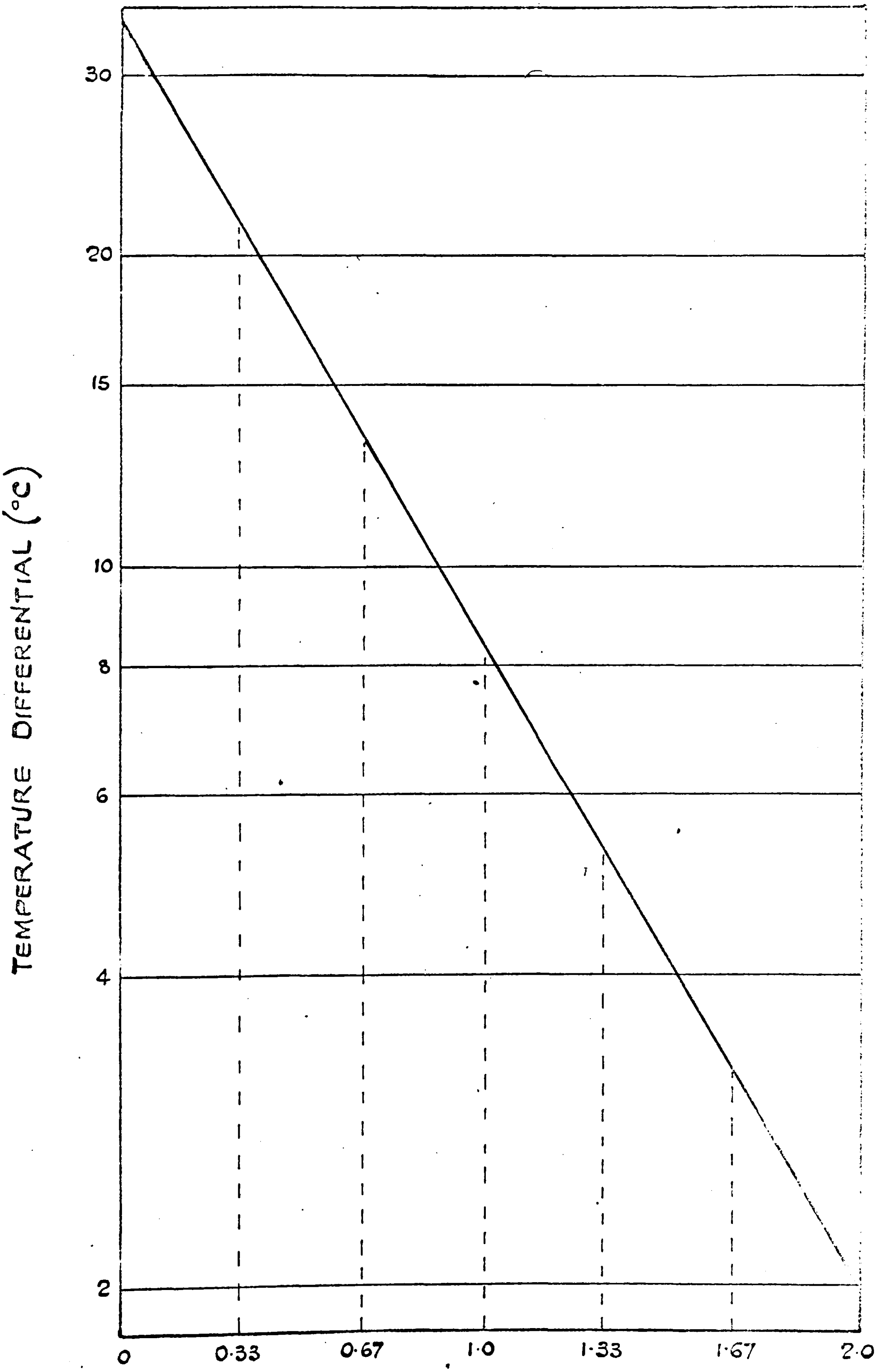

FIG A3.2

ACTUAL TEMPERATURE CURVE

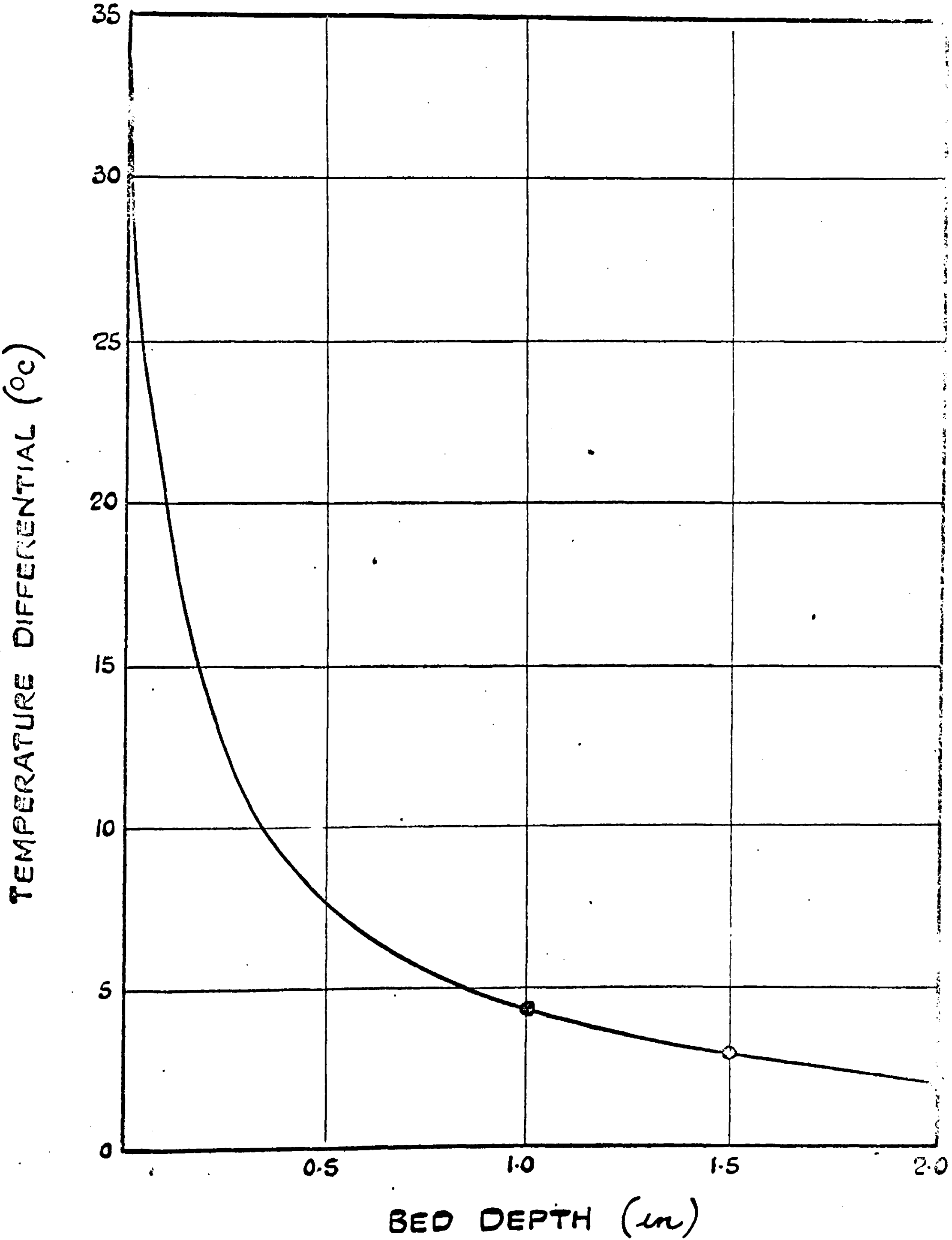

Substituting the values of Δt, interpolated as described above, in equation (A.3.1),

$$\text{Area under curve} = \frac{2-0}{20}\,(33{\cdot}9 + 5\text{x}10{\cdot}1 + 5{\cdot}45 + 6\text{x}4{\cdot}2 + 3{\cdot}6 + 5\text{x}2{\cdot}7 + 2{\cdot}0)$$

$$= 13{\cdot}42 \text{ in, C deg}$$

$$\therefore \text{Correction factor} = \frac{22{\cdot}64}{13{\cdot}42}$$

$$= \underline{1{\cdot}687}$$

From Table 6.6, h_g for 2 in bed = 6·80 Chu/h ft^2 ^{o}C

Hence, modified coefficient,

$$h'_g = 6{\cdot}80 \text{ x } 1{\cdot}687$$

$$= 11{\cdot}5 \text{ Chu/h ft}^2\ {}^o\text{C}$$

By constructing analogous curves for the 1·5 in bed and determining the areas under them, the correction factor for the corresponding heat transfer coefficient is found to be 1·598.

From Table 6.6, h_g = 7·39 Chu/h ft^2 ^{o}C

Hence, h'_g = 7·39 x 1·598

= 11·8 Chu/ft^2 ^{o}C

Appendix IV

Calculation of Reynolds Number Re.

The form of the Reynolds Number used in the heat and mass transfer correlations was introduced by Taecker and Hougen[25] and is given by the equation:

$$Re = \frac{\sqrt{A_p}\,G}{\mu} \qquad \ldots.(A.3.1)$$

For Test No. 38 of the Series 1 pellets,

A_p = 0·00254 ft^2

G = 720 lb/h

μ = 0·0450 lb/h ft

whence Re = 812

Appendix V

Calculation of the Surface Area and Volume of a Tabloid Pellet.

The surface area and volume of a pellet is determined by considering the pellet to consist of two equal spherical segments connected by a cylinder and evaluating the area and volume of each part.

FIG A.5.1

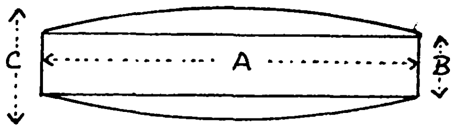

Surface Area of Pellet.

Consider the pellet shown in Fig. A.5.1

Area of spherical segment $= \frac{\pi}{4}\left[(C-B)^2 + A^2\right]$ ....(A.5.1)

and Area of cylindrical body $= \pi AB$ ....(A.5.2)

$\therefore$ total surface area $= \frac{\pi}{2}\left[(C-B)^2 + A^2\right] + \pi AB$ ....(A.5.3)

For a Series 1 pellet from Table 5.1 on page 34

A = 0·406 in

B = 0·075 in

C = 0·161 in

Substituting in equation (A.5.3)

$$\therefore \text{ Surface area of pellet} = \frac{\pi}{2}(0{\cdot}086^2 + 0{\cdot}406^2) + \pi \times 0{\cdot}406 \times 0{\cdot}075$$

$$= \underline{0{\cdot}366 \text{ in}^2}$$

Volume of Pellet.

$$\text{Volume of spherical segment} = \pi \frac{(C-B)}{2}\left[\frac{(C-B)^2}{24} + \frac{A^2}{8}\right] \quad \ldots.(A.5.4)$$

$$\text{and volume of cylindrical body} = \frac{\pi A^2 B}{4} \quad \ldots.(A.5.5)$$

$$\therefore \text{ total volume} = \pi(C-B)\left[\frac{(C-B)^2}{24} + \frac{A^2}{8}\right] + \frac{\pi A^2 B}{4} \quad \ldots.(A.5.6)$$

Substituting the values of A, B and C for a Series 1 pellets in equation (A.5.6)

$$\text{Volume of Series 1 pellet} = \underline{0{\cdot}0154 \text{ in}^3}$$

Voidage of Pellet Bed.

The voidage of a packed bed of pellets was determined by weighing a 4 litre beaker empty, filled with pellets and filled with water. The volume of the beaker was calculated from the weight of water in the beaker. e.g. for the Series 1 pellets:

weight of pellets in beaker = 3410 gm

From the physical properties of a Series 1 pellet given in Table (5.1),

Volume of pellets in beaker = 2640 ml

Volume of beaker = 4730 ml

$\therefore$ voidage of bed = $\dfrac{4730 - 2640}{4730}$

= 0.442

Appendix VI

The Analysis of Variance of a Two-Level Four-Factor Experiment.

Although the theory of the Analysis of Variance is described fully in various textbooks [83, 84], the following outline of the theory may help to clarify the various stages in the arithmetical procedure used in the Analysis.

The total variance V of a number of observations is defined as:

$$V = \frac{\sum(x - \bar{x})^2}{N - 1} \qquad \text{....(A.6.1)}$$

where x = individual observation

$\bar{x}$ = arithmetic mean of all the observations

N = total number of observations

$\sum(x - \bar{x})^2$ is known as the "Sum of Squares" of the deviations of the observations from their mean while the term $N - 1$ refers to the number of independent values of $(x - \bar{x})$ used in obtaining the variance and is known as the degrees of freedom of the variance.

In a factorial experiment, the programme of tests involving various combinations of factor levels produce a range of values in the dependent variable, the total variance of which can be estimated from equation A.6.1. Furthermore, by considering the tests results in groups corresponding to a change in level of one or more factors, smaller variances can be attributed to the effects of various factors and to interactions between factors. Because variance is an additive property, the variance due to the experimental error in the tests can be estimated as the difference between the total variance and the sum of the variances due to the various effects and interactions.

The variance due to the effect of changing a factor A from A_1 to A_2 in a factorial experiment is estimated by considering the results obtained at each level of A in two groups. The variance due to the effect of A is then estimated from the sum of squares of the deviations of the two group means $\bar{x}_i$ from the mean of all the tests $\bar{x}$.

$$\text{i.e.} \quad V_A = \sum n_i \frac{(\bar{x}_i - \bar{x})}{n - 1} \qquad \ldots\ldots(A.6.2)$$

where n_i = number of test results in each group

n = number of groups

Since n = 2 in a two level factorial experiment, the Sums of Squares can be used directly as estimates of the variances.

The theory of the "F test" used to test the significance of the variances attributed to the various effects and interactions has been outlined previously in Section 9.4 on pages 127 to 129

The arithmetical procedure, described in this Appendix for the Analysis of Variance for a two-level four-factor factorial experiment, is that used by Brownlee[80]. The method is illustrated by the analysis of the values of the retention time of the barley in the rotary dryer. The analysis is conducted on the logarithmic values of θ_m given in Table 11.3 on page 141.

The values of $\log_{10} \theta_m$ may be tabulated as:

F_1							
G_1				G_2			
R_1		R_2		R_1		R_2	
T_1	T_2	T_1	T_2	T_1	T_2	T_1	T_2
1·415	1·484	1·090	1·152	1·551	1·588	1·320	1·297
1·464	1·477	1·152	1·207	1·544	1·559	1·196	1·334

F_2							
G_2				G_2			
R_1		R_2		R_1		R_2	
T_1	T_2	T_1	T_2	T_1	T_2	T_1	T_2
1·394	1·394	1·270	1·233	1·415	1·427	1·307	1·332
1·407	1·400	1·301	1·229	1·430	1·401	1·316	1·316

The values from the duplicate tests are now added together

F_1							
G_1				G_2			
R_1		R_2		R_1		R_2	
T_1	T_2	T_1	T_2	T_1	T_2	T_1	T_2
2·879	2·961	2·242	2·359	3·095	3·147	2·516	2·631

F_2							
G_1				G_2			
R_1		R_2		R_1		R_2	
T_1	T_2	T_1	T_2	T_1	T_2	T_1	T_2
2·801	2·794	2·571	2·462	2·845	2·828	2·623	2·648

Four tables are then formed by summing over each of the four factors F, G, R and T.

Summing over F

G_1				G_2			
R_1		R_2		R_1		R_2	
T_1	T_2	T_1	T_2	T_1	T_2	T_1	T_2
5·680	5·755	4·813	4·821	5·940	5·975	5·139	5·279

Summing over G

F_1				F_2			
R_1		R_2		R_1		R_2	
T_1	T_2	T_1	T_2	T_1	T_2	T_1	T_2
5·974	6·108	4·758	4·990	5·646	5·622	5·194	5·110

Summing over R

F_1				F_2			
G_1		G_2		G_1		G_2	
T_1	T_2	T_1	T_2	T_1	T_2	T_1	T_2
5·121	5·320	5·611	5·778	5·372	5·256	5·468	5·476

Summing over T

F_1				F_2			
G_1		G_2		G_1		G_2	
R_1	R_2	R_1	R_2	R_1	R_2	R_1	R_2
5·840	4·601	6·242	5·147	5·959	5·033	5·873	5·271

Six tables are formed by summing over the four variables, F, G, R and T, two at a time.

Summing over F and G

	R_1	R_2	
T_1	11·620	9·952	21·572
T_2	11·730	10·100	21·830
	23·350	20·052	43·402

Summing over F and R

	G_1	G_2	
T_1	10·493	11·079	21·572
T_2	10·576	11·254	21·830
	21·069	22·333	43·402

Summing over F and T

	G_1	G_2	
R_1	11·435	11·915	23·350
R_2	9·634	10·418	20·052
	21·069	22·333	43·402

Summing over G and R

	F_1	F_2	
T_1	10·732	10·840	21·572
T_2	11·098	10·732	21·830
	21·830	21·572	43·402

Summing over G and T

	F_1	F_2	
R_1	12·082	11·268	23·350
R_2	9·748	10·304	20·052
	21·830	21·572	43·402

Summing over R and T

	F_1	F_2	
G_1	10·441	10·628	21·069
G_2	11·389	10·944	22·333
	21·830	21·572	43·402

In order to facilitate the computation of the various sums of squares, the following relationships are used:

$$\sum(x - \bar{x})^2 = \sum x^2 - \frac{S^2}{N} \qquad \text{....(A.6.3)}$$

$$\sum n_i(\bar{x}_i - \bar{x})^2 = \sum\frac{(S_i^{\,2})}{(n_i)} - \frac{S^2}{N} \qquad \text{....(A.6.4)}$$

where S = sum of the individual observations

S_i = sum of group observations

The term S^2/N is known as the "Correction due to the Mean"

(C_1M_1).

Since in this example, $S = 43 \cdot 402$

and $N = 32$

the C_1M_1 is

$$\frac{(43 \cdot 402)^2}{32} = 58 \cdot 866675$$

The Sum of Squares for the main effect of factor F is calculated by squaring the F_1 and F_2 totals, summing the squares, dividing by 16 and subtracting the C_1M_1.

i.e. $(21 \cdot 830^2 + 21 \cdot 572^2)/16 - 58 \cdot 866675 = 0 \cdot 002080$

The Sum of Squares for the other main effects are derived similarly:

For G, $(21 \cdot 069^2 + 22 \cdot 333^2)/16 - 58 \cdot 866675 = 0 \cdot 049928$

For R, $(23 \cdot 350^2 + 20 \cdot 052^2)/16 - 58 \cdot 866675 = 0 \cdot 339900$

For T, $(21 \cdot 572^2 + 21 \cdot 830^2)/16 - 58 \cdot 866675 = 0 \cdot 002080$

The Sum of Squares for the first-order interaction FG, which represents the extent to which the effect of F or G depends on the value of the other, is equal to the difference between the Sum of Squares in the two-way Table for F and G and the sum of F and G Sums of Squares.

i.e. $(10 \cdot 441^2 + 10 \cdot 628^2 + 11 \cdot 389^2 + 10 \cdot 944^2)/8 -$

$58 \cdot 866675 - 0 \cdot 002080 - 0 \cdot 049928 = 0 \cdot 012482$

The Sums of Squares corresponding to the other five first-order interactions are obtained similarly.

The Sum of Squares for the second-order interaction FGR, which measures the extent of the interaction between any two of these factors depends on the level of the third is calculated as the difference between the Sum of Squares for the values in the three-way Table for T, G and R and the total of the Sums of Squares corresponding to main effects of F, G and R and FG, FR and GR interactions.

i.e. $(5{\cdot}840^2 + 6{\cdot}242^2 + 5{\cdot}595^2 + 5{\cdot}673^2 + 4{\cdot}601^2 + 5{\cdot}033^2 + 5{\cdot}271^2) - 58{\cdot}866675 - 0{\cdot}002080 - 0{\cdot}049928 - 0{\cdot}339900 - 0{\cdot}012482 - 0{\cdot}058654 - 0{\cdot}002888 \quad = \quad 0{\cdot}000760$

The Sums of Squares for the other three second-order interactions are determined in a similar fashion.

The Sum of Squares corresponding to the third-order interaction FGRT, which measures the extent any of the second-order interactions depends on the value of the fourth variable is calculated as the difference between the Sum of Squares in the individual values in the Sums of Squares corresponding to the main effects and the first and second-order interactions of the four factors .

i.e. $(2{\cdot}879^2 + 2{\cdot}242^2 + 3{\cdot}095^2 + \qquad + 2{\cdot}462^2 + 2{\cdot}828^2 + 2{\cdot}648^2)/2 - 58{\cdot}866675 - 0{\cdot}002080 - 0{\cdot}049928 - 0{\cdot}339900 - 0{\cdot}002080 - 0{\cdot}000046 - 0{\cdot}000760 - 0{\cdot}000008 - 0{\cdot}000778 - 0{\cdot}000924 \quad = \quad 0{\cdot}00421$

In a factorial experiment in which duplicate tests are not performed, the Sum of Squares of the individual values corresponds to the Total Sum of Squares and the Sum of Squares of the interaction FGRT is used as an estimate of the experimental error.

In this Analysis, the Total Sum of Squares is computed by squaring the 32 original test values, summing the squares and subtracting the C_1M_1

i.e. $(1{\cdot}415^2 + 1{\cdot}464^2 + 1{\cdot}090^2 = 1{\cdot}152^2 + \qquad +$
$1{\cdot}427^2 + 1{\cdot}401^2 + 1{\cdot}332^2 + 1{\cdot}316^2) - 58{\cdot}866675 = 0{\cdot}492923$

The Residual Sum of Squares which corresponds to the experimental error is calculated as the difference between the Total Sum of Squares and the sum of the Sums of Squares of the main effects and first, second and third-order interactions of the four variables.

The Sums of Squares derived for each of the components in the Analysis are divided by the appropriate number of degrees of freedom to give the Mean Sum of Squares or Variance. The results of the Analysis of Variance may be tabulated as:

Source of Variance	Degrees of Freedom	Sum of Squares	Mean Sum of Squares
F	1	0· 002080	0· 002080
G	1	0· 049928	0· 049928
R	1	0· 339900	0· 339900
T	1	0· 002080	0· 002080
FG	1	0·012482	0·012482
FR	1	0·058654	0·058654
FT	1	0·007022	0·007022
GR	1	0·002888	0·002888
GT	1	0·000265	0·000265
RT	1	0·000046	0·000046
FGR	1	0·000008	0·000008
FGT	1	0·000760	0·000760
FRT	1	0·000778	0·000778
GRT	1	0·000924	0·000924
FGRT	1	0·000421	0·000421
Residual	16	0·014687	0·000918
Total	31	0·492923	

The significance of the various main effects and interactions in the Analysis of Variance Table are tested by comparing the Residual Sum of Squares with the Sums of Squares corresponding to (a) the third-order interactions (b) the second-order interactions (c) the first-order interactions and (d) the main effects, in that order. Interactions or effects are significant if the Variance Ratio, F, defined as $\frac{\text{Mean Sum of Squares of interaction}}{\text{Mean Sum of Squares Residual}}$ is greater than the value of F given in mathematical tables[87]. The value of F significant at the 5% level of probability with the appropriate degrees of freedom is 4·5.

It can be seen from the Table that the value of the F ratio for the interactions FGRT, FGR, FGT, FRT, GRT, GR, RT will be less than 4·5 and hence these interactions are not significant. However, the interactions FG, FR and FT will have an F value greater than 4·5, and therefore their interactions are significant at the 5% level of probability.

When an interaction is found to be significant, it is pointless to test the significance of the main effects involved in the interaction as the effect of each factor then depends on the value of the other factor.

Consequently, the Analysis of Variance has indicated that the interactions FG, FR and FT are significant.

Appendix VII

Regression Analysis and Correlation.

Regression

In the analysis of experimental data, it is often desirable to ascertain if a relationship exists between two or more variates and to determine the nature and extent, if any, of this relationship. This Appendix gives an outline of the basic theory used in fitting a regression to a set of experimental data and in determining the extent of the relationship between two variates. A more detailed discussion is given in literature [83, 84].

The method used for fitting a straight line to experimental data is the Method of Least Squares. It is assumed that the value of the independent variate, x, can be measured accurately and that all the errors are in the measurement of the dependent variate, y. The method is designed so that the sum of squares of the vertical deviations form the line is a minimum and thus the error in predicting one property from a knowledge of the other is minimised.

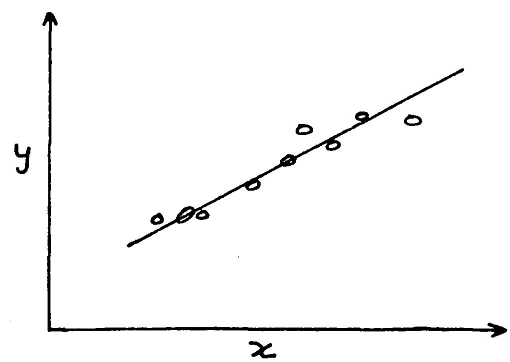

If Y_1 is the predicted value of y, for a given value x_1, then for a linear law:

$$Y_1 = a + bx_1$$

where a and b are constants.

The values of a and b are chosen such that the value of

$$E = \sum_{i=1}^{n} (Y_i - y_i)^2 \text{ is a minimum}$$

n = number of observations in data

i = index

$$E = \sum_{i=1}^{n} (a + bx^{i} - y_i)^2 \qquad \text{.....(A.7.1)}$$

The minimum value of E occurs when $\frac{\partial E}{\partial a} = 0$ and $\frac{\partial E}{\partial b} = 0$

$$\frac{\partial E}{\partial a} = 2\sum_{i=1}^{n} (a + bx_i - y_i) = 0 \qquad \text{...(A.7.2)}$$

$$\frac{\partial E}{\partial b} = 2\sum_{i=1}^{n} x_i(a + bx_i - y_i) = 0 \qquad \text{...(A.7.3)}$$

From equation (A.7.2) it follows that

$$na + nb\bar{x} - n\bar{y} = 0$$

where $\bar{x}$ = mean of x's = $\dfrac{\sum_{i=1}^{n} x_i}{n}$, similarly for $\bar{y}$ ...(A.7.4)

$$\therefore a = \bar{y} - b\bar{x}$$

From equation (A.7.3) it follows that

$$na\bar{x} + \sum_{i=1}^{n} x_i^{\;2} - \sum_{i=1}^{n} x_i y_i = 0 \qquad \text{...(A.7.5)}$$

Substituting for a in equation (A.7.5) and rearranging,

$$b = \frac{\sum_{i=1}^{n} x_i y_i - n\bar{x}\bar{y}}{\sum_{i=1}^{n} x_i^{\;2} - n\bar{x}^2} \qquad \text{...(A.7.6)}$$

$$b = \frac{\sum_{i=1}^{n} (x_i - \bar{x})(y_i - \bar{y})}{\sum_{i=1}^{n} (x_i - \bar{x})^2} \qquad \text{....(A.7.7)}$$

The quantity b is called the Regression Coefficient of y upon x

The precision of the regression equation depends on two factors:

(1) the number of observations

(2) the extent of the scatter about the regression.

The deviation of the observations from the regression line may be regarded as errors. Since the errors in the independent variate, x, are assumed to be negligble, the error about the regression is caused by the deviations of the observations from the regression line in the vertical direction. Therefore, substituting the values of a and b in the expression for E and rearranging, the following relationship is obtained:

$$\text{Sums of Squares} = \sum_{i=1}^{n} (y_i - \bar{y})^2 - b^2 \sum_{i=1}^{n} (x_i - \bar{x})^2 \qquad \text{....(A.7.8)}$$

This is equivalent to:

$$\begin{matrix}\text{Total Sums of Squares} \\ \text{of y about mean}\end{matrix} \qquad \begin{matrix}\text{Sums of Squares} \\ \text{of Errors}\end{matrix} + b^2 \sum_{i=1}^{n} (x_i - \bar{x})^2$$

The quantity $b^2 \sum_{i=1}^{n} (x_i - \bar{x})^2$ is the component of the total variation in y caused by the variations in x and is referred to as the Sum of Squares due to Regression. The regression is significant if the variance or Mean Square due to

Regression is significantly greater than the Mean Square about Regression (or error). The corresponding Analysis of Variance table is given below:

Table A.7.1

Analysis of Variance of Regression.

	Source of Variation	Degrees of Freedom	Sum of Squares
1	Due to Regression	1	$b^2 \sum_{i=1}^{n} (x_i - \bar{x})^2$
2	About Regression	n - 2	$\sum_{i=1}^{n} (y_i - \bar{y})^2 - b^2 \sum_{i=1}^{n} (x_i - \bar{x})^2$
3	Total	n - 1	$\sum_{i=1}^{n} (y_i - \bar{y})^2$

The arithmetical procedure for conducting a regression analysis is now described for the derivation of the equation:

$$N_c' = a_1 G^{b_1}$$

which may be expressed in the form:

$$\log_{10} N_c' = \log_{10} a_1 + b_1 \log_{10} G$$

The values of N_c' and G used in this example are taken from columns 1 and 2 of Table 6.2 on page 39. The analysis is carried out on $\log_{10} 10N_c'$ instead of $\log_{10} N_c'$ which is a negative quantity.

$\log_{10} G$ x	$\log_{10} 10N'_c$ y
2·4771	0·6212
2·5911	0·7235
2·6532	0·7910
2·7204	0·8370
2·7993	0·9058
2·8573	0·9504
2·8943	1·0437
2·9420	1·0115
x = 21·9427	y = 6·8841
$\bar{x}$ = 2·7428	$\bar{y}$ = 0·8605

The arithmetic computations are simplified by using the following relationships:

$$\sum_{i=1}^{n} (x_i - \bar{x})^2 = \sum_{i=1}^{n} x_i^2 - \frac{\left[\sum_{i=1}^{n} x\right]^2}{n}$$

$$\sum_{i=1}^{n} (y_i - \bar{y})^2 = \sum_{i=1}^{n} y_i^2 - \frac{\left[\sum_{i=1}^{n} y\right]^2}{n}$$

$$\sum_{i=1}^{n} (x_i - \bar{x})(y_i - \bar{y}) = \sum_{i=1}^{n} x_i y_i - \frac{\left[\sum_{i=1}^{n} x_i\right]\left[\sum_{i=1}^{n} y_i\right]}{n}$$

Now, $$\sum_{i=1}^{n} x_i^2 = 2·4771^2 + 2·5911^2 + \ldots + 2·8943^2 + 2·9420^2$$

$$= 60·366038$$

And, $$\frac{\sum_{i=1}^{n} x^2}{n} = \frac{21·9427^2}{8}$$

$$= 60 \cdot 185260$$

$$\therefore \sum_{i=1}^{n} (x_i - \bar{x})^2 = 0 \cdot 180778$$

Similarly $\sum_{i=1}^{n} (y_i - \bar{y})^2 = 0 \cdot 147911$

$$\sum_{i=1}^{n} x_i y_i = 2 \cdot 4771 + 0 \cdot 6212 + 2 \cdot 5911 \times 0 \cdot 7235 + \cdots \cdots + 2 \cdot 9420 \times 1 \cdot 0115$$

$$= 19 \cdot 045116$$

$$\frac{\left[\sum_{i=1}^{n} x_i\right]\left[\sum_{i=1}^{n} y_i\right]}{n} = \frac{21 \cdot 9427 \times 6 \cdot 8841}{8}$$

$$= 18 \cdot 881967$$

$$\therefore \sum_{i=1}^{n} (x_i - \bar{x})(y_i - \bar{y}) = 0 \cdot 163149$$

$$\therefore b_1 = 0 \cdot 163149 / 0 \cdot 180778$$

$$= 0 \cdot 902$$

Now $\bar{y} = \log_{10} a_1 + b\bar{x}$

$$\therefore 0 \cdot 8605 = \log_{10} a_1 + 0 \cdot 902 \times 2 \cdot 7428$$

whence $\log_{10} a_1 = -1 \cdot 6135$

$$= \bar{2} \cdot 3865$$

$$a_1 = 0 \cdot 0244$$

As the analysis was carried out on values of $10K_c'$, the true value of a_1 is $0 \cdot 00244$.

Analysis of Variance Table

Source of Variance	Degrees of Freedom	Sum of Squares	Mean Sum of Squares
Due to Regression	1	0·156180	0·156180
Error (About Regression)	6	0·006969	0·001162
Total	7	0·163149	

As the Mean Sum of Squares of the Error is very small compared with the Mean Sum of Squares due to Regression, the regression is highly significant.

Correlation.

The Sum of Squares accounted for by regression is $b^2 \sum_{i=1}^{n} (x_i - \bar{x})^2$. The higher the value of this relation to the total Sum of Squares of y and the closer the relationship between the two variates. In the extreme case when the Sums of Squares are equal, all the points lie on a straight line. On the other hand, when the regression Sum of Squares is zero, there is no linear relationship whatsoever between the variates although a more complex relationship might be obeyed by the data.

Thus when the ratio of the Sum of Squares due to regression over the total Sum of Squares is unity, a perfect relationship exists between the variates; when the ratio is zero, there is no linear relationship between the variates. This ratio is therefore a measure of the correlation between the variates. Its square root is called the Correlation Coefficient and is usually denoted by r.

$$\text{i.e.} \quad r = \sqrt{\frac{b^2 \sum_{i=1}^{n} (x_i - \bar{x})^2}{\sum_{i=1}^{n} (y_i - \bar{y})^2}} \qquad \text{....(A.7.9)}$$

Substituting for b and rearranging, we get

$$r = \frac{\sum_{i=1}^{n} (x_i - \bar{x})(y_i - \bar{y})}{\sqrt{\sum_{i=1}^{n} (x_i - \bar{x})^2 \sum_{i=1}^{n} (y_i - \bar{y})^2}} \qquad \text{....(A.7.10)}$$

The significance of r is tested by comparing the computed value of r with critical values of r given in mathematical tables.

Appendix VIII

Testing of Difference among Regression Coefficients.

In order to determine whether the coefficients of two or more regressions differ significantly a regression combining all the data is derived on the hypothesis that the individual regression coefficients are identical.

If these coefficients are identical, the Sum of Sums of Square due to Regression for each set of data will be the same as the Sum of Squares due to Regression in the combined regression. Hence the difference between the sum of the Regression Sums of Square for each set and the combined Regression Sum of Squares gives a criterion appropriate for an overall test of differences among the individual coefficients.

The method is illustrated by considering the expressions correlating the modified heat transfer coefficients of the Series 1 pellets with the air rate. These expressions, which are given on pages 45 and 47, were:

for the 1 in bed, $h'_g = 0.139\ G^{0.75}$ ....(A.8.1)

for the 1.5 in bed, $h'_g = 0.230\ G^{0.67}$ ....(A.8.2)

and for the 2 in bed, $h'_g = 0.185\ G^{0.69}$ ....(A.8.3)

These correlations, which were derived by conducting a regression analysis on the logarithmic values of h'_g and G may be rewritten respectively as:

$$\log_{10} h'_g = 0{\cdot}75 \quad \log_{10} G - 0{\cdot}8584 \qquad \ldots .(A.8.4)$$

$$\log_{10} h'_g = 0{\cdot}67 \quad \log_{10} G - 0{\cdot}6392 \qquad \ldots .(A.8.5)$$

$$\log_{10} h'_g = 0{\cdot}69 \quad \log_{10} G - 0{\cdot}7320 \qquad \ldots .(A.8.6)$$

where 0·75, 0·67 and 0·69 are the regression coefficients.

From the values of h'_g and G given in Table 6.5, from which equation (A.8.4) was derived, the following sums of squares may be computed:

$$\sum_{i=1}^{n} (x_i - \bar{x})^2 = 0{\cdot}907078$$

$$\sum_{i=1}^{n} (y_i - \bar{y})^2 = 0{\cdot}533145$$

$$\sum_{i=1}^{n} (x_i - \bar{x})(y_i - \bar{y}) = 0{\cdot}673946$$

where $x = \log_{10} G$

and $y = \log_{10} h'_g$

Similar quantities may also be derived for the other sets of values. For the 1·5 in bed,

$$\sum_{i=1}^{n} (x_i - \bar{x})^2 = 0{\cdot}544247$$

$$\sum_{i=1}^{n} (y_i - \bar{y})^2 = 0{\cdot}260451$$

$$\sum_{i=1}^{n} (x_i - \bar{x})(y_i - \bar{y}) = 0{\cdot}364855$$

For the 2 in bed,

$$\sum_{i=1}^{n} (x_i - \bar{x})^2 = 0{\cdot}544247$$

$$\sum_{i=1}^{n} (y_i - \bar{y})^2 = 0{\cdot}296359$$

$$\sum_{i=1}^{n}(x_i - \bar{x})(y_i - \bar{y}) = 0{\cdot}377311$$

Combining the three sets of data, the corresponding Sums of Squares are:

$$\sum_{j=1}^{m}\sum_{i=1}^{n}(x_{i_j} - \bar{x}_j) = 1{\cdot}995572$$

$$m = \text{No. of sets of data}$$

$$\sum_{j=1}^{m}\sum_{i=1}^{n}(y_{i_j} - \bar{y}_j) = 1{\cdot}089955$$

$$\sum_{j=1}^{m}\sum_{i=1}^{n}(x_{i_j} - \bar{x}_j)(y_{i_j} - \bar{y}_j) = 1{\cdot}416112$$

Combined regression coefficient

$$b_c = \frac{1{\cdot}416112}{1{\cdot}995572}$$

$$= 0{\cdot}7096$$

Sum of Squares due to Combined Regression $= 0{\cdot}706 \times 1{\cdot}416112$

$$= 1{\cdot}004794$$

Sum of Regression Sum of Squares for each set $= 0{\cdot}7430 \times 0{\cdot}673946 + 0{\cdot}6704 \times 0{\cdot}364855 + 0{\cdot}6933 \times 0{\cdot}477311$

$$= 1{\cdot}006882$$

Difference $= 1{\cdot}006822 - 1{\cdot}004794 = 0{\cdot}002028$

The Sums of Squares may be tabulated as follows:

Analysis of Variance for Testing Differences of Regression Coefficients.

Source of Variance	Degrees of Freedom	Sum of Squares	Mean Sum of Squares
Combined Regression	1	1·004794	1·004794
Difference of Regression	2	0·002028	0·001014
Combined Residual	82	0·083133	0·001014
Total	85	1·089955	

As the F ratio of $\frac{\text{Mean Sum of Squares of Difference}}{\text{Mean Sum of Squares of Residual}}$ = 1·0 is less than the significant value of 3·1 for F at the 5% level of probability[87], there is no difference in the values of the regression coefficients of the three heat transfer correlations.

Appendix IX

Results of a Rotary Drying Test

Run 15 : $F_1\ G_2\ R_2\ T_1$

Feed rate = 24·0 gm B.D.S./min = 3·17 lb B.D.S./h

Hold-up of barley in dryer = 0·829 lb

$\therefore$ Experimental retention time = $\frac{0{\cdot}829 \times 60}{3{\cdot}17}$ = 15·7 min

Position in dryer from feed end (in)	2·5	6·5	10·5	14·5	18·5	22·5	26·5	30·5	35·5	
wt of dish + sample	29·9310	25·1074	25·5143	27·9858	27·4232	21·9725	21·8134	21·3447	19·9695	
wt of dish + B.D.S. (gm)	18·8940	19·2735	19·0978	20·9432	21·1793	17·5022	17·6017	17·3112	16·167	
wt of dish (gm)	8·6337	8·8192	8·6340	8·6474	9·4340	9·6233	8·7573	8·1668	8·5671	
wt of water lost (gm)	7·0370	6·8339	6·4156	7·0426	6·4156	4·4703	4·2117	4·0335	3·3528	
wt of B.D.S. (gm)	10·2603	10·4543	10·4647	12·1958	11·7453	8·8778	8·8444	9·1444	8·0496	
moisture content (gm water/gm B.D.S.)	0·686	0·654	0·613	0·573	0·532	0·503	0·476	0·441	0·417	
dryer loading (gm B.D.S./in)*	10·263	10·4553	10·4647	12·2958	11·7453	8·8778	8·8444	9·1444	8·0496	
material velocity (in/min)	2·342	2·299	2·296	1·954	2·046	2·706	2·717	2·628	2·985	
average material velocity (in/min)	2·359**	2·321	2·298	2·125	2·000	2·376	2·712	2·673	2·807	
Time per section (min)	1·06	1·72	1·74	1·88	2·00	1·68	1·48	1·50	1·43	1·8
Total time (min)	1·06	2·78	4·52	6·40	8·40	10·08	11·56	13·06	14·49	16·3

* width of each sampling section = 1 inch

** calculated from velocity profile along dryer.